Advances in Energy, Environment and Materials Science

Editors: Yeping Wang & Jianhua Zhao

CRC Press
Taylor & Francis Group
A BALKEMA BOOK

ADVANCES IN ENERGY, ENVIRONMENT AND MATERIALS SCIENCE

This page intentionally left blank

PROCEEDINGS OF THE INTERNATIONAL CONFERENCE ON ENERGY, ENVIRONMENT AND MATERIALS SCIENCE (EEMS 2015), GUANGZHOU, P.R. CHINA, 25–26 AUGUST 2015

Advances in Energy, Environment and Materials Science

Editors

Yeping Wang
School of Mechanical Engineering. Tongji University, Shanghai, China

Jianhua Zhao
College of Materials Science and Engineering, Chongqing University, Chongqing, China

CRC Press
Taylor & Francis Group
Boca Raton London New York Leiden

CRC Press is an imprint of the
Taylor & Francis Group, an **informa** business
A BALKEMA BOOK

CRC Press/Balkema is an imprint of the Taylor & Francis Group, an informa business

Typeset by V Publishing Solutions Pvt Ltd., Chennai, India
Printed and bound in Great Britain and the USA

Published by: CRC Press/Balkema
P.O. Box 11320, 2301 EH Leiden, The Netherlands
e-mail: Pub.NL@taylorandfrancis.com
www.crcpress.com – www.taylorandfrancis.com

ISBN: 978-1-138-02931-6 (Hbk)
ISBN: 978-1-315-64056-3 (eBook PDF)

Advances in Energy, Environment and Materials Science – Wang & Zhao (Eds)
© 2016 Taylor & Francis Group, London, ISBN 978-1-138-02931-6

Table of contents

Environmental analysis and monitoring

Environmental materials

This page intentionally left blank

Advances in Energy, Environment and Materials Science – Wang & Zhao (Eds)
© 2016 Taylor & Francis Group, London, ISBN 978-1-138-02931-6

Preface

This collection of papers from the International Conference on Energy, Environment and Materials Science (EEMS2015, Guangzhou, China, 25–26 August 2015), aims to present novel and fundamental advances in the areas of energy, and environmental and materials sciences. The 161 accepted papers (from 400 submissions) are divided into five chapters:

- Energy Science and Technology
- Environmental Analysis and Monitoring
- Architectural Environment and Equipment Engineering
- Environmental Materials
- Computer Applications

In preparing EEMS2015, we would like to thank the contributors, reviewers, committee members and CRC Press/Balkema (Taylor & Francis Group) for their support of EEMS 2015.

The Organizing Committee of EEMS2015

This page intentionally left blank

Advances in Energy, Environment and Materials Science – Wang & Zhao (Eds)
© 2016 Taylor & Francis Group, London, ISBN 978-1-138-02931-6

EEMS2015 organizing committee

CONFERENCE CHAIRS

Prof. Bachir Achour, *University Mohamed Khider of Biskra, Algeria*
Prof. Li Xie, *Tongji University, China*

TECHNICAL COMMITTEE CO-CHAIRS

Professor L. Hench, *Imperial College London, UK*
Sir C.J. Humphreys, *University of Cambridge, UK*
Professor L. Jiang, *Chinese Academy of Sciences, Beijing, China*

TECHNICAL PROGRAM COMMITTEE

Prof. Yulin Zhong, *South China University of Technology, China*
Prof. Jun Zhang, *Xiangtan University, China*
Prof. Min Xie, *Tongji University, China*
Prof. Peijiang Zhou, *Wuhan University, China*
Prof. Tao Zhu, *China University of Mining and Technology, China*
Prof. Xiaojun Zhou, *Southwest Jiaotong University, China*
Prof. Xiangjun Yu, *Kunming University, P.R. China*
Prof. Tiehong Wu, *Inner Mongolia University, China*
Prof. Haiyun Wang, *China Three Gorges University, China*
Prof. Yonggang Yang, *Beijing Institute of Graphic Communication, China*
Prof. Donglai Xie, *South China University of Technology, China*
Prof. Guangqun Huang, *China Agricultural University, China*
Prof. Johnson Carl, *Portland Community College, US*
Assistant Prof. Miguel Ângelo Dias Azenha, *University of Minho, Portugal*
Dr. Ching Yern Chee, *Faculty of Engineering University of Malaya, Malaysia*
Prof. Chang Li, *University of Science and Technology Liaoning, China*
Prof.Guochang Zhao, *Shenyang Aerospace University, China*
Prof. Hong Liang, *Yunnan University, China*
Prof. Weisheng Shi, *Kunming University of Science and Technology, China*
Prof. Mulan Zhu, *Xiamen University of Technology, China*
Prof. Xinxian Zhai, *Henan Polytechnic University, China*
Prof. Manxia Zhang, *Dalian Maritime University, China*
Prof. Taihua Yang, *Shanghai University of Electric Power, China*
Prof. Hai Fan, *Shandong Normal University, China*
Prof. Shaochun Chen, *Fuzhou University, China*
Prof. Youyuan Wang, *Nanchang Hangkong University, China*
Prof. Ruitao Peng, *Xiangtan University, China*
Prof. Junli Han, *Lnner Mongolia University of Science and Technology, Mongolia*
Prof. Zhonghong Chen, *China University of Petroleum, China*
Prof. Liya Xu, *Liming Vocational University, China*

Energy science and technology

This page intentionally left blank

Advances in Energy, Environment and Materials Science – Wang & Zhao (Eds)
© 2016 Taylor & Francis Group, London, ISBN 978-1-138-02931-6

A reactive power control method of reducing wind farm power loss

Guanfeng Zhang
Electric Power Research Institute of Liaoning Electric Power Company, Shenyang, China

Junjie Sun
School of Electric Engineering, Wuhan University, Wuhan, China

Yangyang Ge, Shenghui Li, Feng Sun & Cijian Xie
Electric Power Research Institute of Liaoning Electric Power Company, Shenyang, China

ABSTRACT: For wind farms consisting of double-fed wind turbines with centralized compensation device SVC, a method was proposed based on a minimum of reactive power compensation, utilization of installed reactive power compensation device SVC and double-fed unit's reactive ability to achieve reactive power optimization. According to actual reactive power generation capability of Double-fed wind turbines and reactive power compensation device SVC, wind Farm automatic voltage control system distributes reactive power with a network Loss minimum of the objective function, this allocation method can play DFIG reactive power regulation capability and can reduce the loss of wind farms. The simulation results show the proposed scheme can effectively reduce the wind farm power losses and improve voltage stability margin.

1 INTRODUCTION

With wind power capacity growing, stabilizing influence of reactive power on the wind farm has become increasingly obvious security, the accident of wind farm voltage collapse was caused due to windfarm reactive configured properly, and caused huge economic losses (Chi, 2007). Currently, most wind turbines use four-quadrant power electronic converters to connect to the grid, achieve decoupling control of active and reactive power by the converters, its own reactive power regulation capability can be applied to wind farm reactive power regulation (Wang, 2011; Jia, 2010). Moreover, wind farms equipped with reactive power compensation equipment, can achieve reactive power control, through cooperative control of DFIG and reactive power compensation device (Zhu, 209).

For wind farm reactive power control strategies, numerous studies have been done at home and abroad. Wind turbine reactive power output sequence was determined to achieve reactive power optimization through reactive power sensitivity different locations outlet buses of wind turbines (Li, 2005), but this method does not consider DFIG reactive power regulation. Literature (Chen, 2009) analyses the reactive power ultimate limit of DFIG, and achieve reactive power optimization control to the losses of the DFIG based on VSCF electrical equivalent circuit, this method only considered reactive loss of wind turbines, not the loss of centralized compensation device, cannot achieve the overall optimization of reactive power.

This article provides a reactive power control method of reducing the power consumption of the wind farm, makes full use of fans nonfunctional force and considers SVC own loss, achieving a coordinated control of wind farm between SVC reactive power compensation equipment and wind turbines, and minimizes the wind farm power loss.

2 DOUBLE-FED WIND TURBINE POWER OPERATING CHARACTERISTICS

In order to obtain wind turbine active and reactive power coupling relationship, mathematical model for wind turbine was analyzed first. DFIG stator side using rotation practices of the generator, rotor side using the motor rotation practices, the equivalent circuit shown in Figure 1.

The following equation was calculated according to the equivalent circuit:

$$\begin{cases} \dot{E}_m = \dot{I}_m \cdot jX_m \\ \dot{U}_s = \dot{E}_m - (R_s + jX_{s\sigma})\dot{I}_s \\ \dfrac{\dot{U}_r}{s} = \dot{E}_m + \left(\dfrac{R_r}{s} + jX_{r\sigma}\right)\dot{I}_r \\ \dot{I}_r = \dot{I}_s + \dot{I}_m \end{cases} \tag{1}$$

where $\dot{E}_m, \dot{U}_s, \dot{U}_r$ was gap magnetic field induced electromotive force, stator and rotor voltage of

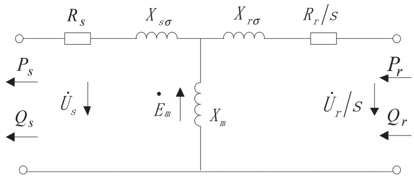

Figure 1. DFIG equivalent circuit.

DFIG respectively, $\dot{I}_m, \dot{I}_s, \dot{I}_r$ was excitation current, the stator and rotor current value respectively, $X_m, X_{s\sigma}, X_{r\sigma}$ was magnetizing inductance and the stator and rotor leakage reactance respectively, X_s, X_r was stator and rotor side reactance value after conversion respectively, s was the slip of DFIG, P_s, P_r, Q_s, Q_r was stator and rotor of active and reactive power respectively; By the formula $X_s = X_{s\sigma} + X_m$, $X_r = X_{r\sigma} + X_m$, rotor side variable have been converted to the stator.

The stator voltage and current RMS is expressed in the form

$$\begin{cases} \dot{U}_s = U_s + j0 \\ \dot{I}_s = I_{sP} + jI_{sQ} \end{cases} \tag{2}$$

where U_s was stator voltage RMS, I_{sP}, I_{sQ} was the active and reactive component of the stator current.

The rotor side current is based on the above formula:

$$\dot{I}_r = \frac{P_s X_s - Q_s R_s}{3X_m U_s} - j\frac{3U_s^2 + P_s R_s + Q_s R_s}{3X_m U_s} \tag{3}$$

Without taking into account reactive power consumes of the system, active and reactive power injected the system are:

$$\begin{cases} P_x = P_s + P_r \\ Q_x = Q_S \end{cases} \tag{4}$$

DFIG rotor maximum current value was set as $I_{r\max}$, which is 150% of the rated current value generally. Stator reactive power can be equivalent to the output of a single wind turbine reactive power. So, a single DFIG reactive power output limit formula is: (Shen, 2003)

$$\begin{cases} -\sqrt{\dfrac{9I_{r\max}^2 U_s^2 X_m^2}{X_s^2} - P_s^2} - \dfrac{3U_s^2}{X_s^2} \le Q_{reg} \\ \quad \le \sqrt{\dfrac{9I_{r\max}^2 U_s^2 X_m^2}{X_s^2} - P_s^2} - \dfrac{3U_s^2}{X_s^2} \\ P_W \dfrac{\sqrt{1-\lambda_L^2}}{\lambda_L} \le Q_{reg} \le P_W \dfrac{\sqrt{1-\lambda_H^2}}{\lambda_H} \end{cases} \tag{5}$$

where λ was the power factor of wind turbine, power factor range of wind turbines under normal working conditions was $\lambda_L \le \lambda \le \lambda_H$, Q_{reg} was each wind turbine maximum output capacity in real time. As can be seen from the formula (5), when wind turbine power factor reaches the maximum, it will lose the ability to regulate reactive power; Under certain wind speed (active issue of the stator certain), the stator reactive and absorptive capacity is asymmetric.

3 REACTIVE POWER COMPENSATION DEVICE SVC OPERATING CHARACTERISTIC ANALYSIS

Typical SVC can be divided into Thyristor Controlled Reactor (TCR), Thyristor Switched Reactor (TSR) and Thyristor Switched Capacitor (TSC). TCR single-phase equivalent circuit shown in Figure 2, Shunt reactor dynamic control reactive from minimum to maximum within the range by

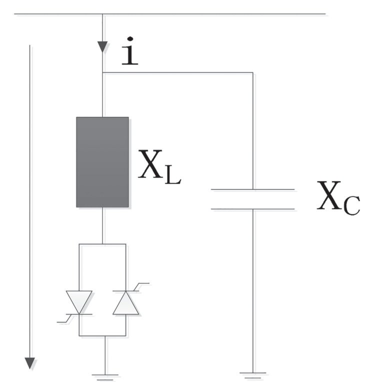

Figure 2. SVC (TCR) single-phase equivalent circuit.

Table 1. The loss results of reactive compensation devices.

No.	Type	Capacity (Mvar)	Loss value (MW)	Losses as a percentage of capacity
1	TCR	−15	0.336	2.24%
2	SVG	±4 Mvar	0.155	3.10%
3	SVG	±5	0.17	3.40%
4	SVG	±5 Mvar	0.18	3.60%
5	SVG	±7 Mvar	0.209	2.98%
6	SVG	±20 Mvar	0.35	3.50%
7	SVG	±5 Mvar	0.299	5.98%
8	SVG	±5 Mvar	0.185	3.70%
9	SVG	±3 Mvar	0.097	3.20%

controlling bidirectional thyristor, SVC is equivalent to a variable shunt reactors, because SVC device also includes transformers, filters, cooling systems, will have a greater power loss during the operation, Table 1 is the loss results of reactive power compensation device SVC and SVG (static synchronous compensator).

4 WIND FARM REACTIVE POWER REGULATION AND OPTIMIZATION

Wind Farm automatic voltage control system features is to ensure wind farms outlets reactive demand for the grid, then sets and distributes wind farm reactive power demand. The entire wind farm reactive power control principle is shown in Figure 3.

This paper implements reactive power control of wind farm level via a layered approach, divided into reactive setting layer and reactive power distribution layer. First, compare the actual voltage and reference voltage given by Power Dispatching Center at control point in the reactive tuning layer, and get the change of reactive power demand for wind farms, then sends reactive demand to reactive distribution layer to determine each wind Turbine and SVC reactive power setpoint.

4.1 *Windfarm reactive power demand value calculation*

The amount of reactive power compensation is calculated via wind farms and outlets voltage and reactive power relations:

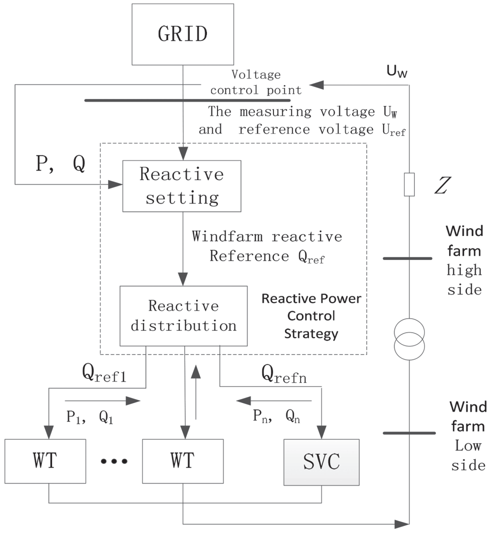

Figure 3. Control diagram of DFIG based wind farm.

$$\Delta U = \Delta Q / S_{sc} \tag{6}$$

$$S_{sc} = \left(U_{now} - U_{last}\right) \Big/ \left(\sum Q_{now} / U_{now} - \sum Q_{last} / U_{last}\right) \tag{7}$$

In Equation (6), (7), ΔQ was reactive power variation, S_{sc} was Short circuit capacity of the system bus side, $\sum Q_{now}$, $\sum Q_{last}$, was last Total Reactive and current total reactive respectively, U_{last}, U_{now} was last bus voltage, current bus voltage.

4.2 *Wind farm level of reactive power optimization*

The entire wind farm reactive power was distributed based on loss minimum, reactive power optimization of the entire wind farm setting program flowchart is shown in Figure 4.

1. When wind turbines generally reactive output capacity Q_{Wref} More than total reactive power demand-ΔQ, at this time SVC reactive power compensation is not required, calculating Q_{ref} though the reactive setting layer, then Distribute Q_{ref} according to the individual wind turbine reactive power capability.

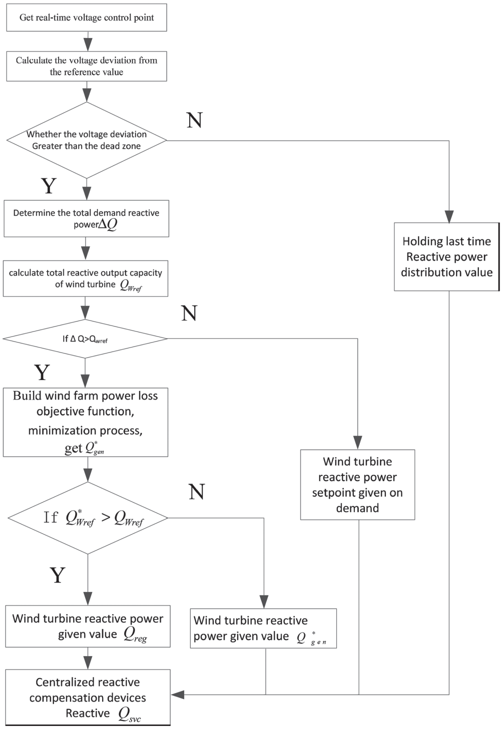

Figure 4. Strategy optimization flowchart of windfarm reactive power control.

2. When $Q_{Wref} < \Delta Q < (Q_{Wref} + Q_{SVC\max})$, Wind turbines and SVC take part in reactive power regulator at the same time, in this paper, in order to achieve the coordination and control between the wind farm reactive power compensation equipment and wind turbines, and wind farm power loss is minimized, the objective function between the wind farm loss and wind turbine reactive is built. Under certain wind speed, wind turbine active power has been set, total power consumption:

$$\begin{aligned}\Delta P_\Sigma(S,V) &= P_0(V) + P_S(S,V) + P_{LL}(S,V) + P_{svc} \\ &= \left(\frac{V}{V_N}\right)^2 \cdot P_{N0} + \left(\frac{S}{S_N}\right)^2 \cdot \left(\frac{V_N}{V}\right) \cdot P_{NS} \\ &\quad + \left(\frac{S}{S_N}\right)^2 \cdot \left(\frac{V_N}{V}\right) \cdot P_{NL} + P_{svc}\end{aligned} \tag{8}$$

where ΔP_Σ was wind farms total power loss, P_0 was transformer load loss, P_S was transformer short-circuit loss, P_{LL} was Line Loss, V was Transformer operating voltage value, V_N was Transformer rated voltage, S was transformer operation apparent power value, S_N was transformer rated apparent power value, P_{N0} was transformer rated load loss, P_{NS} was transformer rated short-circuit loss, P_{NL} was Line Rated power loss, P_{svc} was power loss of reactive power compensation device.

The total power loss ΔP_Σ is set as the objective function, since equipment power consumption of all the series in a set of utility line is:

$$\begin{aligned}P &= I^2 R = \left(S_N/\sqrt{3}U_N\right)^2 \\ R &= \left(P_{gen} \times n/\cos\phi/k/\sqrt{3}U_N\right)^2 R\end{aligned} \tag{9}$$

where $\cos\phi = \lambda$, n is the total number of units of wind turbines, k is the percentage of the rated voltage of the actual voltage.

Power loss of reactive power compensation device P_{svc} is 2%–3% of rated capacity, which is set to a known quantity in accordance with the actual situation of the wind farm referring to Table 1.

So equation (8)–(9) shows that, wind farms total power loss ΔP_Σ only has relation with reactive power of each wind turbine-Q_W, the equation (6) can be transformed to the objective function of wind turbines Reactive Dispatching:

$$\begin{aligned}T &= \Delta P_\Sigma(S,V) = \Delta P_\Sigma(Q_{gen}) \\ &= P_0(V) + P_S(S,V) + P_{LL}(S,V) + P_{svc}\end{aligned} \tag{10}$$

Constraints are equation (5) and $\Delta Q = Q^*_{Wref} + Q_{SVC} - \Delta Q_\Sigma$, where ΔQ_Σ was the total wind farm reactive power loss, it can use wind turbine capacity reactive representation.

The objective function T was made minimum treatment, wind generator reactive power value Q^*_{gen} is obtained when the existence of minimum of the objective function, overall output capacity of wind turbines was $Q^*_{Wref} = \sum_{k=1}^{n} Q^*_{gen}$, then compare overall actual wind turbine reactive power output capability Q_{Wref} with Q^*_{Wref}, if $Q_{Wref} \le Q^*_{Wref}$, wind turbine reactive given was Q_{reg}, Centralized Reactive Power Compensation Device reactive given was $Q_{svc} = \Delta Q - Q_{Wref} - Q_T - Q_{LL}$; if $Q_{Wref} > Q^*_{Wref}$, wind turbine reactive given was Q^*_{gen}, Centralized Reactive Power Compensation Device reactive given was $Q^*_{svc} = \Delta Q - Q^*_{Wref} - Q_T - Q_{LL}$, where Q_T and Q_{LL} was Transformers and reactive power loss, respectively.

3. If $|Q_{SVC\max} + Q_{Wref}| \le |\Delta Q|$, wind Farm automatic voltage regulator control system will give alarm prompt transformer taps.

5 OPERATOR CASES

In this paper, a wind farm in Liaoning was simulated, test and verify the effectiveness of the wind farm reactive control strategy. Wind farm system wiring shown in Figure 5.

The wind farm installed 33 sets of 1.5 MW double-fed induction generator, fan outlet voltage was 690 V, each fan collector through four 35 kV line access in 220 kV substation, and the –10 MVA SVC was installed at the 35 KV bus.

In this paper, to doubly-fed wind farm, take net loss minimum as target to optimize reactive power. Under different wind speeds, wind farm operation as shown in Figure 6–8.

Through simulation calculation shows, when the SVC reactive power compensate alone, there is a network problem of excessive consumption, the

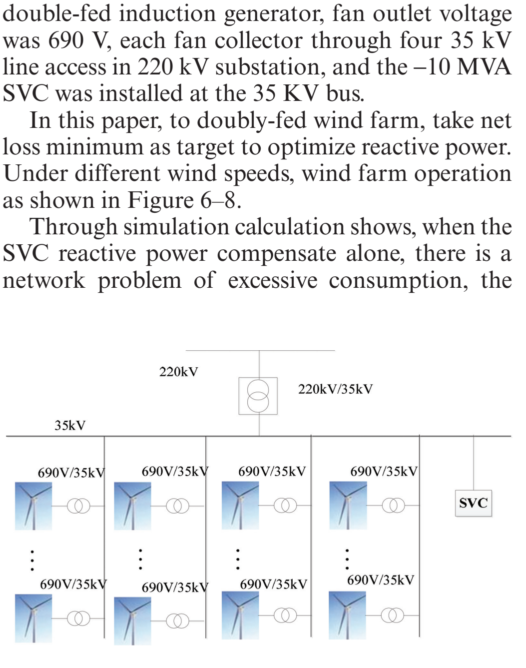

Figure 5. The wiring diagram of sample system.

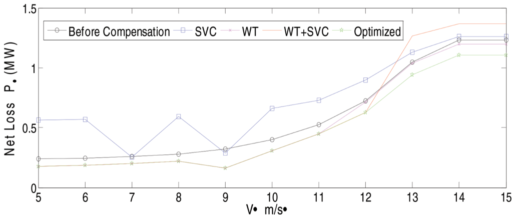

Figure 6. Doubly fed wind farm losses changes under different wind speeds.

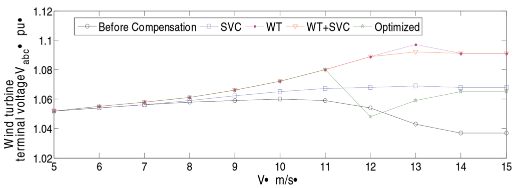

Figure 7. Wind turbine terminal voltage changes under different wind speeds.

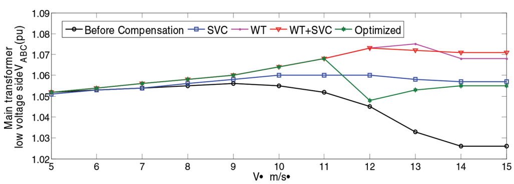

Figure 8. Wind farm main transformer low-side voltage changes under different wind speeds.

largest up 1.369 MW; the wind turbines compensate alone, terminal voltage is too high, especially when the fan is running at high speed, can reach 1.097 pu; After optimization, reducing the wind farm network losses and reduce the 1.369 MW to 1.197 MW, improved voltage stability margin, the maximum terminal voltage decreases from 1.097 pu to 1.08 pu.

6 CONCLUSION

This paper analyzes the wind farm reactive power control principles and reactive power compensation device SVC operating characteristics, proposes a wind farm reactive power control optimization algorithm, which take the wind farm internal power loss as the objective, optimizes the wind farm internal reactive power control strategy on the basis of ensuring the safe and stable operation of wind farms, effectively reduce the wind farm internal reactive loss and improve voltage stability margin.

REFERENCES

Chen Ning, et al. Strategy for reactive power control of wind farm for improving voltage stability in wind power integrated region [J]. Proceedings of the CSEE, 2009, 29(10): 102–106.

Chi Yong-ning, et al. Study on impact of wind power integration on power system [J]. Power System Technology, 2007, 31(3): 77–81.

Jia Jun-chuan, et al. Novel reactive power optimization control strategy for doubly fed induction wind power generation system [J]. Proceedings of the CSEE, 2010, 30(30): 87–92.

Li Jing, et al. Research on subsection and layer control strategy of doubly-fed variable speed wind turbine [J]. Power System Technology, 2005, 29(9): 15–21.

Shen Hong, et al. Variable-speed wind power generation using doubly fed wound rotor induction machine a comparison with alternative schemes [J]. Power System Technology, 2003, 27(11): 60–63.

Wang Cheng-fu, et al. Coordinate var-control during fault of wind power system [J]. Electric Power Automation Equipment, 2011, 31(9): 14–21.

Zhu Xue-ling, et al. Research on the compensation of reactive power for wind farms [J]. Power System Protection and Control, 2009, 37(16): 68–72.

This page intentionally left blank

Advances in Energy, Environment and Materials Science – Wang & Zhao (Eds)

Research on the construction of information service platforms for electricity market large data

Junmei Wang, Ma Chao & Guo Lin
State Grid Chongqing Electric Power Corporation, Chongqing, China

Chuncheng Gao
Nari Group Corporation/State Grid Electric Power Research Institute, Nanjing, Jiangsu Province, China

Dunnan Liu
North China Electric Power University, Beijing, China

ABSTRACT: Electric power large data is an inevitable course for the power industrial technology innovation in energy revolution. Moreover, it is the value form leap of the next generation intelligent power system in the large data era. There are many different kinds of business information of electricity market design, which contains rich information. In order to excavate and apply the biggest value of these information effectively, this paper was based on the information composition of electricity market large data. Besides, construction of information service platforms for electricity market large data was researched on the aspects of application service and consulting service.

1 INTRODUCTION

It is not only a technical progress, but also a great change that involves the development idea, management system and technical route of the whole power system in the large data era. Moreover, it is the value form leap of the next generation intelligent power system in the large data era. The two core lines of power electric power large data are reshaping the core value of electric power and transforming the development mode of electric power (Yan, 2013). The electricity market business involves various kinds of information, such as power transaction data and electrical coal market data. The amount of data is very huge, while the distribution of information is scattered. It is a large amount of work for a single market member to collect and store these data. It needs to put in special and huge manpower and time to obtain effective information related to its business (Jiang, 2007).

Thus, it is responsible for power market organizers to offer just, fair and open information service for intra-regional generation enterprises and companies with large electricity consumption. Also, they have an obligation to build an intra-regional unified information service platform for large data power market, helping market members to find problems, optimize operation and increase benefit (Shi, 2000; Ye, 2009). This paper would design the modes of application service and consulting service to offer application service and consulting service for market members. Consequently, we can help them to get the picture of the market operation situation, grasp market trends, reduce operational costs, participate in trade reasonably and increase the whole benefit.

2 THE INFORMATION COMPOSITION OF ELECTRICITY MARKET LARGE DATA

Electricity market large data contains multi-source heterogeneous information source sets. As the publisher of large data, transaction center offers information service to four objects (power grid, plant, large customers and the public). The data cross association between the above five objects is shown in Figure 1.

There are two main kinds of data in electricity market large data: power grid data sources and public information source for the government and society.

Power grid data sources include the information mastered by transaction center, power grid, plant and large customers. As the information publisher, transaction center masters comprehensive information. And all the data related to trade can be obtained by it. Most of the information mastered by power grid, plant and large customers can

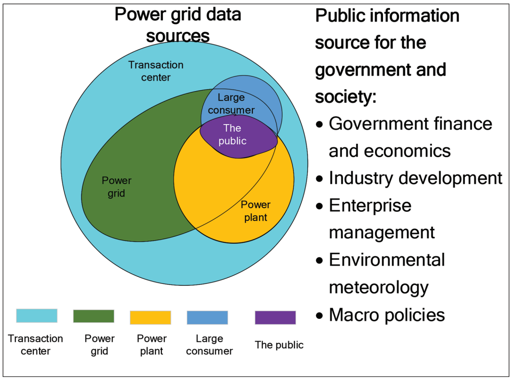

Figure 1. The construction of the information of electricity market large data.

be offered by transaction center. However, some information is private, which is mastered by them respectively. While the information mastered by the public is open.

Outer cataloging data sources are government social public information sources, including government finance and economics, industry development, enterprise management, environmental meteorology, macro policies and so on. This kind of information is obtained from the outside of power grid.

2.1 *Government finance and economics*

Government finance and economics data are reflected by three indexes, which can be expressed by data from direct observation.

1. Regions GDP: It is the total values of goods and services produced in a country or a region during a given period (a quarter or a year)
2. Consumer Price Index (CPI): It is a macroeconomic indicators which reflects the changes of the price level of goods and services purchased by households.
3. Producer Price Index (PPI): It is an index to measure the average changes of ex-factory prices of manufacturers.

2.2 *Industry development*

Industry production total value growth rate: According to the industrial category, industry is divided into the first, second and third industry, to calculate the total ratio of industry production total value with the previous year.

Industrial structure: It is the composition, connection and proportion relations of the industries.

2.3 *Enterprise management*

Profitability: Profitability indicators mainly include the operating profit ratio, the profit margin of costs, earnings cash guarantee multiple, rate of return on total assets, return on net assets and return on capital. In practice. Listed companies often use earnings per share, dividend per share, price-earning ratio and net assets per share to evaluate the profitability.

Debt paying ability: It refers to the ability to repay the long-term debt and short-term debt by enterprises with their assets. Cash payment ability and the ability to repay its debt, it is the key to the healthy survival and development.

Development ability: It is used to analyze development ability mainly considering the following eight indicators: operating income growth rate, hedging and proliferating ratios, rate of capital accumulation, total assets growth rate, business profit growth rate, technology investment ratio, the average growth rate of business income in three years and the average growth rate of assets in three years.

2.4 *Environmental meteorology*

Temperature: The change of temperature has certain effect to the electricity use of users.

Precipitation: Hydro power capacity depends on the amount of precipitation.

Natural disasters: The data of natural disasters (earthquake, frozen) can provide early warning for safe operation of the power system.

2.5 *Macro policies*

Macro policy information service is mainly provided to the user in the form of announcement or web link. It mainly includes the national policies related to energy, low carbon, energy saving and environmental protection policy.

Based on the above various information sources, we can construct information service platform. The platform provides two kinds of services, the mode of application services and consulting services.

3 APPLICATION SERVICE MODE OF INFORMATION SERVICE PLATFORMS FOR ELECTRICITY MARKET LARGE DATA

Three kinds of information service mode are provided.

1. User's free retrieval application service mode
2. Platform information publishing service mode

3. Flexible and interactive self-defined package and intelligent pushing service mode.

3.1 *Platform information publishing service mode*

The information service platform for electricity power large data mainly includes five modules, respectively being introduced as follows:

1. Power market reform
   It mainly sets three topics, which mainly introduces the review of the history of power market reform, the relevant laws and regulations and the situation of current market transactions. At the same time, it can also introduce the situation of foreign power market construction, mainly including California electricity market, the PJM electricity market, the Nordic electricity market, etc.
2. Information publishing
   It mainly sets three topics, including the news broadcasts related with power market transaction, the situation of current electricity trading (trading price and trading electric quantity, etc.), power market annual (quarterly) report, etc. This part is the basic module of the electric power large data information service, which mainly provides the fundamental information of market.
3. Information push
   It mainly sets two topics, including information service subscription and mobile client intelligent information push. The information service subscription is divided into two categories: subscription by keywords and subscription by information type. Mobile client intelligent information push can take the form of Wechat subscription number to push power market information service to users. Push content mainly includes: the power market transaction data of this day, the industry policy, the international electricity market memorabilia and etc.
4. Member service
   Information service platforms for electricity market large data provide paying members customized service, including consulting platform and customized package. By consulting platform, we can achieve real-time online contact with related experts and scholars, the user can also customize the content of package service according to their own preferences.
5. Links to sites
   This part mainly provides convenience for the users to search other relevant information. And links to sites mainly includes grid companies, generation enterprises, emission right transaction platforms such as carbon emission, overseas power market information service platform and etc.

3.2 *Flexible and interactive self-defined package and intelligent pushing service mode*

1. Flexible and interactive self-defined package mode
   Users can only passively accept the type and content of certain packages. Facing to all types of power market users, it develops basic module respectively for the user to choose from. For each type of user, it provides the content customization of fixed module number respectively. And the content of additional customized information belongs to the category of value-added services.

   Government: the trade/industry development analysis prediction module, saving power and electric quantity index statistics module, industry/region energy efficiency analysis module, energy efficiency per unit GDP analysis module, industry load characteristic analysis module and etc.

   Power grid: electric quantity balance analysis module, electricity demand analysis module, purchasing electricity auxiliary decision analysis module and etc.

   Generation: fairness analysis module, power market bidding strategy analysis module and etc.

   Big users: electricity consumption behavior analysis module, power supply security analysis module, the economic benefits of direct electricity purchase analysis module and etc.

   Based on the above modules, users can choose the information type that they want to get freely according to the actual needs. According to user's choice, large data information service center provides unique package information. The main characteristics of flexible and interactive self-defined package mode are:
   1. Set optionally. According to actual needs, the user can choose time limit of package (a month, half a year, a year), type of package information (basic information, transaction data, analysis report, etc.), package delivery time, etc. Information types, information amount is completely decided by the users.
   2. Change optionally. The user can change package content according to the actual demand situation. And the following month would act.
   3. Replace optionally. The user can convert package within different information content which is equivalent to each other according to the actual demand situation.
2. Intelligent pushing service mode
   According to the user's habit of customizing and retrieving, it makes frequency analysis and correlation analysis to recorded data. On the basis

of the analysis results, it pushes the concerned information to users. Learning methods are:

1. Learning directly. It provides operable friendly interface, and allows users to actively put forward suggestion of modification and maintenance of user mode.
2. Feedback learning. They can learn by the all previous feedback suggestion from users' retrieving results.
3. The historical study: Through the analysis of users' historical searching records, after a period of accumulation, we can discover the potential law of user requirements.
4. Observational learning. For client search tools and systems, by making full use of the advantage of combining client tools and environment, we can observe from more aspects and get the characteristics information that is relevant to the user.
5. Reasonable speculation. According to the type of user registration information, we can roughly infer the information that users care about. For example, power grid company customers focus more on power trading information. Power plant customers more concern about the price bidding information. Users concern about peak and valley price and other information which is closely linked with electricity consumption, etc.

4 RESEARCH ON THE MODE OF CONSULTING SERVICE FOR ELECTRICITY MARKET LARGE DATA

4.1 *Intelligence consulting service mode*

First of all, according to the content of power market large data, it build market analysis knowledge

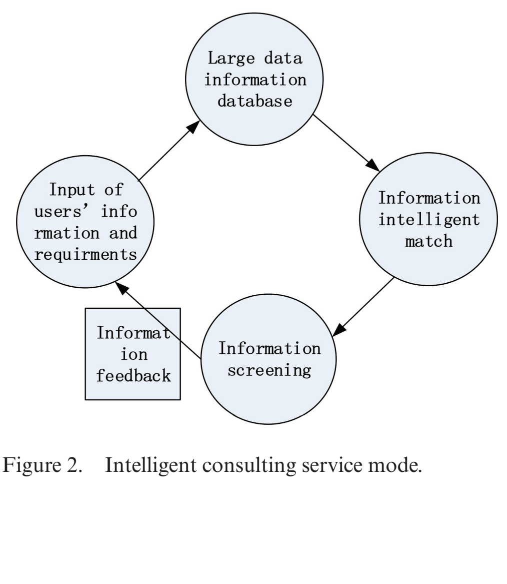

Figure 2. Intelligent consulting service mode.

base of systematization. Or in view of the problems or theme, it builds knowledge base. And then it realizes the fast matching between users' consultation content and knowledge base, to provide users with consulting results.

Intelligence consulting service mode is mainly for the behavior of ordinary users browsing the basic information. This kind of information has large amount but low value, and can be obtained widely. Therefore, all users can search the content of the information they need by the form of intelligent search.

4.2 *Half intelligence consulting service mode*

First of all, according to the content that users need to consult, it retrieves a correlation content from large data platform artificially. And then the professional staffs integrate the content, feedback to the user in the form of the consulting report.

Half intelligence consulting service mode is mainly aimed at the demand for specific information from member users, such as power market development analysis report, power market users' behavior analysis, etc. This kind of consulting reports has high value. They can guide users to make scientific and reasonable management strategies. Therefore, only paying members have privilege to require to provide relevant consulting report. Moreover, different types of membership grade is for different consulting report.

4.3 *Artificial training service mode*

Electricity market large data information service platform builds network training function module, to offer network classroom service for users' consulting.

Artificial training service mode belongs to the highest level of power market large data consulting services, which provides core member of the information service to consulting and training. Users can not only master power market development trends, but also can accept the 'one to one' precise service. Large data information operators can according to customers' actual condition, tailor for customers' behavior strategy to participate in power market transaction, and put forward risk aversion strategies.

5 CONCLUSIONS

This paper built information service module through analyzing the information category composition of electricity market large data and the attention to all kinds of information from each market main body. Moreover, based on the above original information and processed information service module, we built three kinds of power market large data information application service modes and three kinds of consulting service modes. They involved the demand of each main body participating in the power market. Also, they can change along with the demand of the market main body. We can make the most application of the value of power market large data, according to electricity market large data information service platforms achieved by the model in this paper.

REFERENCES

Jiang Jianjian, Kang Chongqing, Xia Qing: Key Information and Rationality Criteria of Electricity Trade. Automation of Electric Power Systems. 2007, 05:34–39.

Shi Yongli: Research of electric power market operation modes. Modern Electric Power. 2000, 04:94–100.

Yan Long-chuan, Li Ya-xi, Li Bin-chen, Zhao Zi-yan: Opportunity and Challenge of Large data for the Power Industry. Electric Power Information Technology. 2013, 04:1–4.

Ye Qing, Tuo Guangzhong, Zhang Yong: Transaction Information Publication System of Power Market and Its Operation Mode. North China Electric Power. 2009, 12:1–4.

This page intentionally left blank

Advances in Energy, Environment and Materials Science – Wang & Zhao (Eds)
© 2016 Taylor & Francis Group, London, ISBN 978-1-138-02931-6

Application of fieldbus control system on AC/DC microgrid

Yunhui Zhang & Jiang Chang
School of Mechanical and Electrical Engineering, Shenzhen Polytechnic, Shenzhen, China

ABSTRACT: Microgrid is becoming a hot spot for the development of world energy system, but also opens up a new direction for the use of renewable energy. When the microgrid control system makes the decision, it depends on acquisition and transmission of the information more than the traditional grid. At the same time, the response characteristics of microgrid equipment have higher requirements on the reliability and real-time communication. In the paper, the advanced FCS technology is used in AC/DC hybrid microgrid, and it makes full use of the advantage of the fieldbus control technology in microgrid communication and data acquisition. It can achieve high precision, high reliability, rapid data acquisition and monitoring for the microgrid, and then improve the operation stability of microgrid.

1 INTRODUCTION

New energy application market is starting in China, concern about the microgrid has been rising. In the 12th five-year plan on renewable energy development, it has been proposed that 30 new energy microgrid demonstration projects will be built in 2015. Although total size of the projects is not big, they are significant. Future development potential of microgrid is huge.

As a new research area, microgrid has some characteristics that are different from the traditional power grid in many aspects (Wang et al. 2005, Wang & Li. 2010, Puttgen et al. 2003). For example, inverter is taken as grid connection interface for the distributed power supply in microgrid, while synchronous generator is often used in traditional power grid, so different operation control and management mode need to be adopted. Because of the existence of distributed power, bidirectional flow of energy becomes possible, so bidirectional flow of information must be realized for corresponding scheduling and protection. These characteristics result in microgrid control system, compared with the traditional power grid, relies more on acquisition and transmission of information when making decisions, while response characteristic of the equipments in microgrid demand for more real-time and reliability of the communication.

Therefore, the establishment of a perfect microgrid communication system is the basic requirement for the microgrid operation control and management. It is advantageous to obtain real-time, accurate and reliable information, can realize the system's centralized monitoring and comprehensive dispatch, and the system optimization control, make the system run more safe, economical, and reliable.

In AC/DC hybrid microgrid, master-slave control mode is the most common, and the data signals from all field equipments are transmitted to control room. However, it will inevitably lead to disadvantages such as low reliability, poor real-time. Since all field nodes are connected with the master control machine, the choice of it determines the configuration of the whole field equipment, the openness is poor. With the development of control, computer, network, module integration technology, Fieldbus Control System (FCS) is appeared in the late 1980's. As the basis of digital communication network, it establishes the communication between the production process and the control equipment, and the connection between the field, the control equipment and the higher control management levels. It is not only a grass-roots network, but also an open, new distributed control system. On the one hand, the solution based on open, standardized, overcomes the defects caused by the closed system; on the other hand, it becomes a new distributed structure, the control function completely into the site.

Open, dispersive, and digital communication are the most obvious advantages of fieldbus system. Because of its advantages, the advanced FCS technique is used in AC/DC hybrid microgrid in this paper, make full use of the advantages of FCS Technology in microgrid control communication and data collection, to enhance stability and economic benefits for the microgrid operation, and more convenient for maintenance, operation, monitoring.

2 FIELDBUS CONTROL SYSTEM (FCS) AND ITS FEATURES

IEC gives the fieldbus definition (Yang. 2010, Li. 2013): Field bus is a technology which applied to the production site, and bidirectional, serial and multi node digital communication is realized between field equipments, and control devices. Fieldbus broke the structure of the traditional control system, and formed a new distributed control system, that is fieldbus control system. It is a new generation control system based on the base type pneumatic instrument control system, the electric unit combined with analog instrument control system, centralized digital control system, distributed control system.

FCS changes single scattered measure and control devices into network nodes, taking the fieldbus control network as the transmission link, each network node can be connected to the network system and control system which can communicate with each other and complete the control task.

The characteristics of FCS are as follows:

1. Bus connection type:
   Each field device is a network node on the bus, and the bus type network connection is used, the connection is simple and can be expanded;
2. Openness of the system:
   Interconnection and information exchange can be realized between different devices. Equipment with similar performance from different manufacturers can replace each other;
3. Digital and intelligent:
   Fieldbus instruments have digital communication capability, and digital communication and network connection are used between the equipments to replace analog signal transmission in the traditional measurement and control system. Digital communication is advantageous to improve the information quantity of communication transmission. Digital calculation can improve control accuracy;
4. Certainty and timeliness of communication:
   FCS provides the communication mechanism for the transmission of data, and provides the time management function to meet the real-time requirements of the control system;
5. Environmental adaptability:
   As the bottom level of the factory network, field bus system works in the front of the production site with bad working environment, and it has environment adaptability for different working conditions.

3 APPLICATION OF FCS IN HYBRID MICROGRID

3.1 *Functional requirements for AC/DC hybrid microgrid system*

The research object in this paper is hybrid microgrid system in Shenzhen Polytechnic, AC bus for three-phase 380 V, DC bus using DC600V. Distributed power (DG) on the AC bus is composed of 10 kW monocrystalline silicon, 10 kW polycrystalline silicon, 3 kW amorphous silicon, 3 kW wind turbine and so on. The DG of the DC bus is made of 4 kW silicon and 4 kW polycrystalline silicon. The energy storage system is composed of 50 kWh lithium iron phosphate battery and 50 kW 10 s super capacitor, and connects the bus and energy storage system to the grid through PCS 50 kW cabinet. There are user loads and adjustable simulation loads on AC bus and DC bus. The system uses the modular design, DC microgrid and AC microgrid, AC/DC hybrid microgrid can be implemented separately. Through flexible combination of modules, the microgrid system can be realized for various functions and occasions, and can meet the needs of many applications.

The main functions of the system are as follows:

1. The information can be real-time interactive among the modules of the system;
2. Real-time parameters and running status information, alarming information of the PV, wind power, AC/DC load and hybrid energy storage subsystem can be acquired in real time. Monitoring comprehensive information of microgrid system, including microgrid system frequency, public connection point voltage, distribution exchange power, statistics and analysis in many aspects, to realize microgrid full control;
3. Predict the DG power generation and load demand, develop an operation plan. According to collected current, voltage, power and other information, real-time adjustment of the operation plan, control the starting and stopping of DG, load and energy storage device, guarantee stability of microgrid voltage and frequency, and provide related protection function for the system;
4. Implement the DG regulation of the microgrid, the charge & discharge control of the hybrid energy storage and load control, and the transient power balance and the low frequency load shedding of the microgrid and the realization of the transient safe operation of the microgrid;
5. Through real-time comprehensive monitoring of the microgrid, achieve the optimal control of DG, energy storage device and load energy according to the power and load characteristics when the microgrid is connected to the grid, from the network operation and state transitions, so to achieve the safe and stable operation of microgrid, it needs to improve the energy utilization of microgrid;
6. From the point of view of the security and economic operation of the microgrid, the microgrid can be coordinating optimal dispatched, and

the microgrid can accept the adjustment control command of the higher power distribution network.

3.2 *System design of microgrid control network*

Because of the distributed characteristic of microgrid, massive amounts of control data and the flexible and changeable control mode, it is difficult to realize flexible and effective dispatch by centralized control method with unified judgment and scheduling by the dispatching center. So the control power is dispersed to the microgrid element, the distributed coordination control method which is based on the microgrid dispatching by the components to change the running state will effectively solve these problems. Thus, FCS technology is the core technology of microgrid control, but also the key to improve energy efficiency, reduce costs and improve the reliability.

In order to meet the functional requirements of the system, the internal information of the microgrid is divided into three layers: Field intelligent node control level, MGCC microgrid center control level and remote monitoring level. Communication structure diagram is as shown in Figure 1.

The fieldbus structure based on Modbus TCP is adopted in the field intelligent node control level. Field intelligent node provides Ethernet interface.

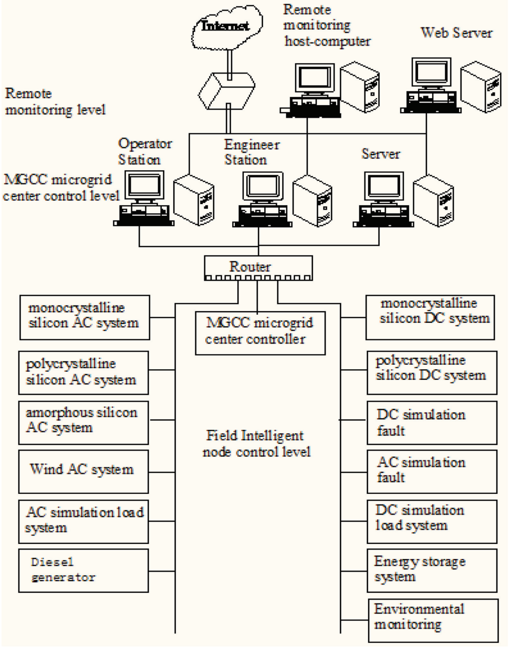

Figure 1. System communication structure diagram.

Modbus TCP industrial ethernet protocol, which has been widely used in industrial field, is used to connect the field equipment network with the central control level of MGCC microgrid, and realize data exchange. MGCC center control level including engineer station, operator station, etc. Modbus TCP protocol is adopted to connect the layer between monitoring computer, and the layer and upper management information network are connected, data exchange is realized, and the monitoring and scheduling is easier. The remote monitoring level includes the monitoring PC and Web server, etc., so as to realize the scheduling between the microgrid and the centralized management of information.

1. Field intelligent node control level

   The microgrid includes many subsystems, scattered in the site, and the whole microgrid control system is divided into distributed power, energy storage unit, load simulation, AC/DC load system. Therefore, multiple field intelligent nodes are respectively used to collect real-time operation parameters, such as PV array output current and voltage, inverter operation state parameters, inverter output grid electricity and electrical energy quality parameters, environmental parameters. In the whole system, intelligent nodes also act as a local controller role.

   The control nodes, the node and the MGCC center control level, are connected by the redundancy ethernet switch, and the field level control network is isolated from the upper level network.

   On the intelligent node control level, the real-time parameters are processed by the arithmetic computation, and form corresponding local transient control strategies, also transfers real-time data through industrial Ethernet to the MGCC microgrid center control level. The overall control strategy of the microgrid is formed, and the feedback information and control commands of the MGCC microgrid center control level are transmitted to the distributed controller to ensure the stable operation of the microgrid. Therefore, the monitoring node should not only have a strong data acquisition and processing power, communication ability, and the stability and real-time requirements are very high.

   Each field intelligent nodes use M44MAD series PLC as the core of Modbus TCP distributed controller. The controller has ethernet communication module, supports the TCP/IP protocol, and has IP address itself. M44MAD series PLC can be remote debugged and redeveloped through Modbus TCP industrial ethernet. The PLC can communicate with PC through many kinds of fieldbus, including CAN and Modbus/TCP.

2. MGCC microgrid center control level
   MGCC microgrid center control level has one or more computer, printer, etc., including the operator station, engineer station, data management station (server) and other equipment. As human-machine interface for the whole microgrid, it mainly completes the monitoring, control and operation of the controlled equipment, responsible for the data collection, verification, and record of the alarm information, and the historical data recording and other functions. This monitoring platform can directly control every single controller of the microgrid and collect the working status of each device through the ethernet. Through the network, MGCC energy management software for microgrid can complete data acquisition, running control, power dispatch, and other functions for the subsystem, and all the controller can realize programming, debugging, download.
3. Remote monitoring level
   Remote monitoring level has one or more computer, printer, etc., including host-computer and Web server, achieve centralized management of the scheduling and information between the microgrid. For remote monitoring level, host-computer monitoring interface is prepared by Kingview, including data acquisition, data display, data storage, data query and alarm prompting modules. Data acquisition module has been listening to the TCP/IP network interface monitoring center; receive the real time data from MGCC transmission through Ethernet. According to received packet identification, data display module display data from each node. Data storage module use Server SQL database to save data. The data query module has the function querying the historical data according to time and equipment number, and can draw the data result into curve shape, and visually identify the changing trend of the data. Alarm module has hierarchical alarm function, when the data exceeds the threshold, pop up device alarm dialog box.

   Web server using the standard Internet browser can read all kinds of information equipment, Modify the configuration of the device and view the history of the fault records, but also the diagnostic function of the system equipment, and it can realize the upgrade of automation system or intelligent device in the Ethernet environment, greatly simplifying the renewal and rebuilding of the control system.

3.3 *Basic communication process*

The basic flow of data communication among different layers is as follows:

Step 1: Collect the operating parameters and equipment operating parameters such as voltage, current, temperature, air pressure, wind speed, wind direction, etc. The above parameters are collected by field intelligent node control level (PLC), then packaged into a Modbus TCP packet which is sent to the engineer station;

Step 2: After the engineer station received TCP Modbus data frame, it sends confirmation message to the intelligent node which sent communication packets, to fulfill a complete Modbus communications;

Step 3: Engineer station will transmit Modbus TCP data frame to the host on the remote monitoring level.

4 SUMMARY

It is inseparable from the data acquisition system to form a correct and real-time control strategy for microgrid system. Microgrid with traditional data acquisition is through the ways such as analog, then its anti-interference ability is weak, the transmission process has the signal attenuation, the data precision is not high. Therefore, the data acquisition characteristics of the microgrid and topological structure of industry ethernet network, which achieves conformance data communication from the field to the control layer until the management level, are used in this paper. Based on FCS, realize microgrid real time numerical data acquisition and monitoring, so as to realize high precision, high reliability, fast data acquisition for microgrid. The system can realize the comprehensive monitoring of information, and is easy to maintain, and has the on-line, real-time function.

REFERENCES

Li Zhengjun. 2013. Fieldbus and industrial Ethernet and its application technology. Beijing: Machinery Industry Press.

Puttgen, H.B., P.R. Macgrego, F.C. Lambert. 2003. Distributed generation: semantic hype or the dawn of a newera. IEEE Power Energy Magazine 1:22–29.

Wang Cheng-shan, Li Peng. 2010. Development and Challenge of Distributed Generation, Microgrid and Smart Distribution System. Automation of Electric Power Systems 2(34):10–14.

Wang Jian, Li Xing-yuan, Qiu Xiao-yan. 2005. Power System Research on Distributed Generation Penetration. Automation of Electric Power Systems 9(24):90–97.

Yang Xian-hui. 2009. Network control system-Field Bus Technology (Second Edition). Beijing: Tsinghua University Press.

Advances in Energy, Environment and Materials Science – Wang & Zhao (Eds)
© 2016 Taylor & Francis Group, London, ISBN 978-1-138-02931-6

The regulate and control method research of wind acceptance regarding power peak adjustment

Tao Zhang
Electrical Power Research Institute of Liaoning Electric Power Co. Ltd., Shenyang, China

Junjie Sun
School of Electric Engineering, Wuhan University, Wuhan, China

Chao Wang, Qiang Zhang & Gang Wang
Electrical Power Research Institute of Liaoning Electric Power Co. Ltd., Shenyang, China

ABSTRACT: Traditional calculation method of the ability to wind acceptance, without considering the scheduling operation mode of actual power grid, is lack of common practicability. Under the premise of considering peak regulation constraints, sensitivity analysis on the important boundary conditions which affect the ability to wind acceptance, relying on the D5000 technical support system, reading operation data of the generator mode in power grid. The theory and method are proposed, by which wind acceptance index of provincial grid can be calculated, and then optimization scheduling model which coordinate power grid scheduling plan with accept ability of wind power is constructed, thus realizing the coordinated operation of the conventional power and wind power is realized, reducing the impact of wind power to the grid, and making the calculated results more accurately reflect the actual acceptance of wind power. The run data proves the calculation method of the ability to wind acceptance is effective.

1 INTRODUCTION

In the state supports the renewable energy industry policy regulation and encouraged, wind power in China got rapid development (Feng, 2011; Xie, 2011; Zhang, 2011). China has reached 60 of 830 MW wind power grid capacity, capacity of 1, 00.4 billion kWh in 2012. New wind power installed capacity of up to 14 000 MW, wind power has been over nuclear power become the third largest after coal and hydropower main power supply (Xie, 2012; Hou, 2012; Geng, 2011; Liu, 2011; Zhang, 2012; Huang, 2010). With the rapid growth of wind power installed capacity, large-scale wind power grid given problem more and more prominent, all regions have appeared different degree of wind power brownouts phenomenon, research on the acceptance ability of power grid wind power in the industry. The traditional calculation method of wind power acceptance ability, mainly according to the factors that may influence the system load, combined with the wind load characteristics to define (Zhang, 2012; Wang, 2011; Wang, 2010; Yao, 2010; Sun, 2011; Li, 2011). The calculation method is very adaptive to the theoretical analysis, but in determining the actual power grid wind power acceptance, without considering the actual operation mode of the power grid, so lack of common utility. At present, the method of calculating the acceptance ability of wind power has been studied: The literature (Li, 2010) was established to accommodate wind power capacity for peak objective function model, in the calculation of the capacity of the wind power, the uncertainty of the intermittent energy is considered, but the influence of the power side is not considered; The literature (Han, 2010) proposed a method for calculating wind power acceptance capacity constraints to the peak load capacity of power network, quantitatively researching on the impact of wind power on power peaking, but not related to the actual power grid dispatching operation mode; The literature (Zheng, 2010) studied the optimal dispatching method of wind power to improve the acceptance of wind power, what basis on considering grid security and stability constraints, but this method is only applicable to optimization of wind power operation strategy, and does not apply to other units in the arrangement of grid short boot mode; The literature (Zha, 2012) built the simulation platform which based on the timing analysis of Delphi, under the condition of the transmission power of the tie line, the load curve is adjusted, the improvement of wind power acceptance ability in the new load time series curve, however, due to not considering the scheduling scheme in the unit on the boot mode, the calculation accuracy is affected. Therefore, in order to meet the requirements of the rapid development of wind power, in strengthening the power grid construction, the method of calculating the wind power acceptance ability of the actual operation mode of the power network and the power grid is needed, not only can meet the peak power constraint, but also can maximize reflect the wind power acceptance ability of the actual power grid.

On the basis of the above research, this paper presents a method of calculating the acceptance of wind power based on the operation mode of scheduling. This method is based on the D5000 intelligent power grid dispatching technology support system, and the operation data of the short time power mode of the power grid is read, considering power balance equations and contact line adjustment coefficient, the peaking capability of the unit comprehensive constrained, on an actual power system boot way to properly adjust, achieving the coordinated operation of conventional power and wind power, reduce the impact of wind power on power grid operation, so that the results can more accurately reflect the actual acceptance of wind power grid.

2 PRINCIPLE ANALYSIS OF WIND POWER ACCEPTANCE

2.1 *Wind power acceptance space under the constraint of peaking*

In the analysis of power system active power balance, on the one hand to satisfy the peak load capacity of power demand, on the other hand also consider valley load time grid unit can reach the minimum output. In consideration of the valley period of load peak power constraint based, the difference between the value of load and the system in all the units minimum output electricity can be supplied by wind power, the difference of power is the wind power of the receiving space. Under the constraint of power peaking wind power maximum acceptance space and load forecasting value, tie line, minimum unit output and reserve capacity, calculation formula is:

$$P_{\max} = P_{\text{pre}} + P_{\text{line}} - P_{\text{G}\min} - P_{\text{R}} \tag{1}$$

In the formula: represents the peaking capacity under the constraint of maximum wind power acceptance space; represents the maximum load; represents contact line plan represents minimum output of conventional units; represents spinning reserve capacity.

By formula (1) can be seen, when the ability of the conventional unit clipping small and power load demand is also very hour, the smaller the force and the load demand is also very small, the smaller the wind power acceptance space, when the peak wind receiving space constraint is negative, it should limit the output of wind power to meet peak constraint.

This article mainly concerns about the peak load restraint multi variable correlation, put forward the formation principle of wind power acceptance space. Highlight the peak load restraint the lowest margin, the selected month peak to valley difference, as a typical, launches the analysis, program and the time scale in typical day in 96 time node as a benchmark. Taking the provincial power grid for a typical day operation of the power grid as an example, as shown in Figure 1 the principle of peak under the constraint of wind power accommodation space.

Figure 1 is the provincial power grid a typical day, the maximum adjustable output, full bore power supply load and the province of the minimum adjustable output curve. In Figure 1, A curve is the maximum adjustable output curve, the C curve is the province's minimum adjustable output curve, and the B curve is the full diameter of the load curve.

Where: the maximum adjustable output curve by the plan of the maximum direct water, fire, nuclear power units, the tie line is received by the electric power (both are converted to the power supply side) and the maximum power station is added to the power and the spinning reserve; Provincial minimum adjustable output curve by the plan of the minimum of direct regulating water, fire and nuclear power unit output, tie line by electric power were converted to the supply side) and the smallest local power plant Internet power can be obtained by adding; full bore power load curve by the full aperture load statistics obtained.

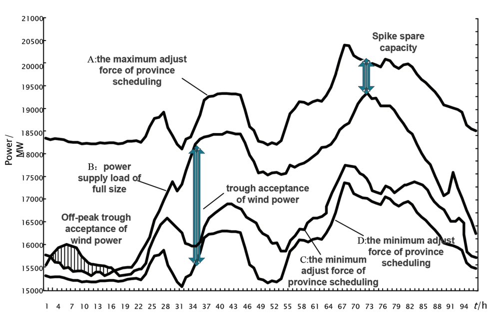

Figure 1. Schematic diagram of wind power acceptance under peak regulating constraint.

From the angle of the operation of the power grid, wind power with the change of the wind speed is changeable. However, such stochastic variations can be grid accepted depending on current grid peak shaving means wind Internet space size, including with conventional power supply, load minimum output power difference. The accurate index value of the wind power is the target of this article. In Figure 1, B curve and C curve of the space for the wind power. The maximum/minimum output of the unit and the load peak and valley changes are reflected by the formula (1). What can be seen from Figure 1, the time period of the load is the smallest of the power grid acceptance of the wind power, which the main time of wind power.

2.2 *Beyond the peak wind power dispatching constraint*

Actual power grid wind power to accept ability essentially reflects to abandon the wind amount of wind power. When the wind power forecasting power exceeds the maximum wind power, the measures to limit the wind power output are required. Two typical wind power wind conditions are listed below.

1. Off-peak load of wind power
   When the thermal power units because of the heating or the stability of the system operation constraints lead to valley period of load output large, in order to ensure the system active power balance must be removal unit minimum adjustable output curve (including wind turbine output) was higher than that of low load curve to ensure the safe and stable operation of the system. In Figure 2, the shadow part is the output of the power grid during the load and the low period.
2. Peak load of the wind power
   When the wind power output is very large, there is a possibility that the minimum adjustable output curve (including wind turbine output)

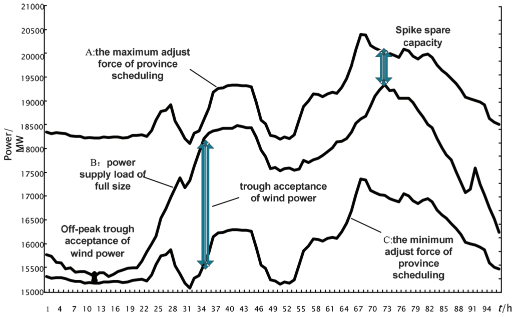

Figure 2. Curves of abandon wind power and others during low load period.

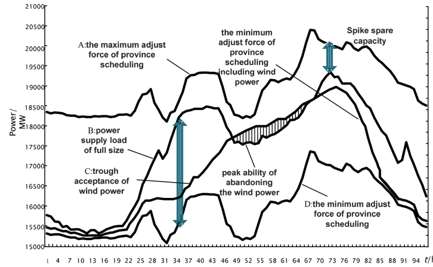

Figure 3. Curves of abandon wind power and others during peak load period.

is higher than that of the load peak curve. As shown in Figure 3 if the unit minimum adjustable output higher than this moment full bore load, in order to ensure the system active power balance must be removal unit minimum adjustable output curve (including wind turbine output) is higher than that of the peak load curve of parts to ensure the safe and stable operation of the system. In Figure 3, the shadow part is the output of the power grid of the load peak period.

3 CALCULATION METHOD OF WIND POWER ACCEPTANCE CAPACITY BASED ON THE OPERATION MODE OF DISPATCHING

3.1 *Calculation process design*

Based on the operation modes of the acceptance of wind power capacity calculation method is considering the unit output, contact line adjustment factor, system spinning production capacity, local hydro thermal power electric power to the Internet. According to the operation mode of the power network, the reasonable peak mode is determined by the peak load forecasting. Then in the peak load time of electricity under the premise of network loss and the Internet power plant, the network loss rate based on industry standard selection. Determining the load low moment smallest boot mode that on the basis of participate in all kinds of power peaking capacity analysis and meet the Electricity Regulatory Bureau approved the minimum start-up mode, in order to obtain the minimum power supply network, combined with the low load, and peak earning power. Based on the study of wind farm cluster effect, conclude the power grid safety electric capacity, so as to provide technical support for the reasonable arrangement of wind power planning and scheduling strategy.

The calculation process of the capacity of wind power based on the operation mode of scheduling is shown in Figure 4.

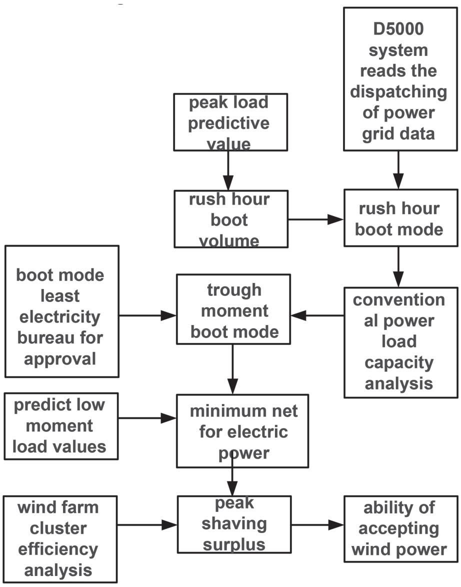

Figure 4. Design drawing of calculation process.

3.2 *Calculation method*

1. Calculation principle
   1. According to the maximum load of the month, the minimum load, the minimum power of the power plant, the power of the power plant and the power to start the power, the power of the wind power is calculated on a monthly basis;
   2. According to the power balance of the power grid, during the low load time peak pressure, prone to abandon wind phenomenon, so adopt the principle of load low peak shaving, calculate the wind power acceptance;
   3. In the peak load period, according to the actual power grid dispatch load statistics, the power to participate in the power balance;
   4. In the off-peak load, Directing thermal power, nuclear power, hydropower, wind power, ting line transmission power and local Internet power in peak shaving;
   5. According to the peak time of power grid peaking capacity calculate the acceptance capacity of wind power in the month.
2. Calculation steps
   1. The calculation of peak output of the unit
   The power to turn on the Internet is the sum of the power, nuclear power and hydropower calculate by formula (2).

$$p'_{\text{Gpower max}} = p'_{\text{Gf max}}(1-\beta_{\text{f}}) + p_{\text{Gnmax}}(1-\beta_n) + p_{\text{Gwmax}}(1-\beta_w) \quad (2)$$

In the formula: represents direct power grid power combined (not considering the rotation of the spare capacity and the limited capacity of the unit); represents direct power to adjust the total power (not considering the spinning reserve and the unit output is limited); represents coal-fired power plant auxiliary power rate; represents straight nuclear power boot combined; represents the rate of nuclear power plant auxiliary power; represents direct the waterworks boot combined; represents the rate of power plant auxiliary power.

According to the sum of the contact line output and the power of the Internet power is power of the network, conclude formula (3).

$$p_{\text{power max}} = (p_{\text{line max}} + p_{\text{Gpower max}})(1-\alpha) \quad (3)$$

In the formula: represents peak grid for power; represents tie line output; represents the loss rate of Net.

According to power balance, Full bore loads in rush hour is the sum of Network for power and local electric power grid power, conclude formula (4).

$$p_{\text{L max}} = p_{\text{power max}} + p_{\text{G max}} \quad (4)$$

In the formula: represents peak load; represents the local fire power grid peak power.

Considering the spinning reserve and the limited capacity of the unit, use formula (5) to calculate the capacity of the direct adjustment.

$$p_{\text{Gf max}} = p'_{\text{Gf max}} + p_{\text{G}} + p_{\text{Glim}} \quad (5)$$

In the formula: represents spinning reserve; represents unit output capacity.

Formula (2)–formula (5) can be adjusted directly to the power of the starting capacity, as shown in formula (6).

$$p_{\text{Gf max}} = \frac{p_{\text{L max}} - p_{\text{Gpower max}} - (p_{\text{line max}} + p_{\text{Gn max}}(1-\beta_n) + p_{\text{Gw max}}(1-\beta_w))(1-\alpha)}{(1-\alpha)(1-\beta_{\text{h}})} + p_{\text{G}} + p_{\text{Glim}} \quad (6)$$

2. Calculation of the low output power of the unit
According to the minimum starting mode of the thermal power unit, determine the power generating capacity on the peak time and starting capacity of thermal power units in the trough.

According to formula (7) calculate other boot capacity thermal power unit on the peak time.

$$p_{\mathrm{Gf\,max}} = p_{\mathrm{G\,max}} - p_{\mathrm{Gh\,max}} \tag{7}$$

According to other boot capacity thermal power unit and peak rate, use formula (8) to calculate other starting capacity of thermal power units in the trough p_{Gfmin}.

$$p_{\mathrm{Gfe\,min}} = p_{\mathrm{Gfe\,max}}(1-\delta) \tag{8}$$

In the formula, represents the other peak power unit rate.

Therefore, total capacity of thermal power generating units at low point $p_{\mathrm{Gh\,min}}$ is:

$$\begin{aligned} p_{\mathrm{Gf\,min}} &= p_{\mathrm{Gh\,min}} + p_{\mathrm{Gf\ else\ min}} \\ &= p_{\mathrm{Gh\,min}} + p_{\mathrm{Gf\ else\ max}}(1-\delta) \end{aligned} \tag{9}$$

3. Calculation of peak load capacity of power network
   Direct power on the Internet is the sum of thermal power, nuclear power and hydro power of the Internet in the trough, use formula (10) to calculate.

$$\begin{aligned} p_{\mathrm{Gpower\,min}} &= p_{\mathrm{Gf\,min}}(1-\beta_{\mathrm{f}}) \\ &\quad + p_{\mathrm{Gn\,min}}(1-\beta_{\mathrm{n}}) + p_{\mathrm{Gw\,min}}(1-\beta_{\mathrm{w}}) \end{aligned} \tag{10}$$

In the formula: represents direct power grid power combined; represents direct power to adjust the total power; represents straight nuclear power boot combined; represents direct the waterworks boot combined.

According to Network for power is the sum of tie line output and direct power on the Internet, conclude formula (8).

$$p_{\mathrm{power\,min}} = (p_{\mathrm{line\,min}} + p_{\mathrm{Gpower\,min}})(1-\alpha) \tag{11}$$

In the formula: represents trough for electric power network; represents tie line output.

Using formula (12) to calculate peak load capacity when the load is low.

$$\begin{aligned} p_{\mathrm{peak}} &= p_{\mathrm{L\,min}} - p_{\mathrm{power\,min}} - p_{\mathrm{else\,min}} \\ &= p_{\mathrm{L\,min}} - p_{\mathrm{else\,min}} - (p_{\mathrm{line\,min}} \\ &\quad + p_{\mathrm{Gf\,min}}(1-\beta_{\mathrm{f}}) + p_{\mathrm{Gn\,min}}(1-\beta_{\mathrm{n}}) \\ &\quad + p_{\mathrm{Gw\,min}}(1-\beta_{\mathrm{w}}))(1-\alpha) \end{aligned} \tag{12}$$

4. Calculation of wind power acceptance
   According to the wind power installed to provide network for power equal to the load capacity, conclude formula (13).

$$p_{\mathrm{Gwind}}(1-\beta_{\mathrm{wind}})(1-\alpha)\varepsilon = p_{\mathrm{peak}} \tag{13}$$

4 ANALYSIS OF WIND POWER ACCEPTANCE CAPABILITY OF LIAONING POWER GRID

4.1 *Liaoning power grid load status*

Liaoning power grid is the main power grid, which has less power than the coal, and no gas, fuel and other power generating units fast peak load capacity of power network is relatively weak. At the same time, Liaoning power grid thermal power units due to poor coal quality and equipment defects will always exist, put great pressure on grid trough peak shaving. In addition, grid heating unit of Liaoning is more, in the winter heating period, heating units need to heat, the output can be adjusted range limited, therefore, Winter is the most difficult period of peak of Liaoning power grid, and the reverse peak winter wind power output has a greater difficulty of power peaking.

4.2 *Computational boundary conditions*

In the case of the system power supply structure, the whole network of wind power accommodation affected by load size, water seasons and dry seasons, the heating period and non heating period and other multiple factors, the ability of the wind power system has obvious seasonal characteristics. Therefore, in this paper, we consider the factors such as the starting mode and load characteristics of different months, 2013~2015 in Liaoning power grid is the monthly peak load balance, According peak earnings to calculate the ability of wind power consumptive each month. In the process of load balance, considering the full aperture load, local hydrothermal Internet power, and tie line by electric capacity, system spinning reserve capacity and additional units to participate in peaking factors.

4.3 *Analysis of wind power acceptance capability of Liaoning power grid*

Based on the 2.2 section, the method of calculating the wind power acceptance capability based on the operation mode of the scheduling is proposed, the principle of scheduling the daily scheduling of unit output, on the basis of meeting the minimum boot mode, combined with the annual load forecasting and peak and valley difference of each level, concluded Liaoning wind power accommodation. The results are shown in Table 1.

1. From the installed wind power seasonal average consumption perspective, 2013~2015 annual average wind power installed capacity for consumption were 2 810 MW, 2 750 MW and 2 290 MW.
2. From the balance results can be seen, 2013~2015 Liaoning power grid wind power installed in winter the lack of absorptive

capacity, summer can consume large amount of wind power, which installed wind power consumptive capacity is almost 0 on January and February, to force acceptance of wind power, it is necessary to break the minimum starting unit; Power grid acceptance of wind power reached the maximum on September and October.

5 CONCLUSION

To accommodate wind power dispatching accurate guidance and planning under the constraints of power peaking, this article mainly considers the global change of operation parameters, given power grid peak shaving methods of wind power capacity calculation principle of the accepted, and the establishment of the corresponding wind power scheduling index calculation model and method of acceptance. The solving process of peaking in the parameter of conventional thermal power units, output and standby, the same month the typical daily load peak and valley value and wind power admissible capacity is a key parameter modeling and computing, an accurate analysis of the peak load and wind power to accept the numerical relationship between amount of dispatch. Through the analysis of a provincial power grid actual examples, using this model to analyze and calculate that wind power acceptance ability index value of the peak load capacity of power network, example, and the results verify the index for the rationality of the evaluation of the power grid peak shaving means, and guide the intermittent wind power access mode of power grid dispatching safe and stable operation.

REFERENCES

Feng Li-min, FAN Guo-ying, Zheng Tai-yi, et al. Design of wind power dispatch automation system in Jilin power grid [J]. Automation of Electric Power Systems, 2011, 35(11): 39–42.

Geng Jing, Yan Zheng, Jiang Chuan-wen, et al. The studies of peak regulation transaction considering environment costs [J]. Power System Protection and Control, 2011, 39(20): 111–114.

Han Zi-fen, Chen Qi-juan. Wind power dispatch model based on constraints [J]. Automation of Electric Power Systems, 2010, 34(2): 89–92.

Hou Ting-ting, Lou Su-hua, Zhang Zi-hua, et al. Capacity optimization of corollary thermal sources transmitted with large-scale clustering wind power [J]. Transactions of China Electrotechnical Society, 2012, 27(10): 255–260.

Huang Xue-liang, Liu Zhi-ren, Zhu Rui-jin, et al. Impact of power system integrated with large capacity of variable speed constant frequency wind turbines [J]. Transactions of China Electrotechnical Society, 2010, 25(4): 142–150.

Li Xiao-ming, Rong Shi-yang, Li Xiao-long, et al. Analysis on maximum wind power penetration into power grid [J]. Hebei Electric Power, 2011, 30(1): 31–35.

Li Zhi, Han Xue-shan, Yang Ming, et al. Power system dispatch considering wind power grid integration [J]. Automation of Electric Power Systems, 2010, 34(19): 15–18.

Liu Yang-yang, Jiang Chuan-wen, Li Lei, et al. Peak regulation right trading model considering DSM [J]. Power System Protection and Control, 2011, 39(9): 38–43.

Lu Shun, Quan Cheng-hao, Liu Jian, et al. The analysis of wind dissolve technical support system [C] // The third paper of power quality and flexible transmission.

Sun Rong-fu, Zhang Tao, Liang Ji. Evaluation and application of wind power integration capacity in power grid [J]. Automation of Electric Power Systems, 2011, 35(4): 70–74.

Wang Rui, Gu Wei, Sun Rong, et al. Analysis on wind power penetration limit based on probabilistically optimal power flow [J]. Power System Technology, 2011, 35(12): 214–217.

Wang Zhi-ming, Su An-long, Lu Shun. Analysis on capacity of wind power integrated into Liaoning power grid based on power balance [J]. Automation of Electric Power Systems, 2010, 34(3): 86–88.

Xie Guo-hui, Li Qiong-hui, Gao Chang-zheng. The research of wind dissolve ability based on Balmorel model [J]. Energy Technology and Economics, 2011, 23(5): 29–33.

Xie Jun, Zhang Xiao-hua, Wu Fu-xia, et al. Peaking cost allocation using cooperative game theory and engineering concept [J]. Power System Protection and Control, 2012, 40(11): 16–22.

Yao Jin-xiong, Zhang Shi-qiang. Analysis on capacity of wind power integration into grid based on peak load regulation [J]. Power System and Clean Energy, 2010, 27(7): 25–28.

Zha Hao, Shi Wen-hui. The research of probability optimization coordinating wind dissolve ability [J]. Power System Protection and Control, 2012, 40(22): 14–17.

Zhang Kun, Wu Jian-dong, Mao Cheng-xiong, et al. Optimal control of energy storage system for wind power generation based on fuzzy algorithm [J]. Transactions of China Electrotechnical Society, 2012, 27(10): 236–240.

Zhang Li-zi, Fan Peng-fei, Ma Xiu-fan, et al. Timing planning method for investment of clustering wind farms considering risk of peak load regulation [J]. Proceedings of the CSEE, 2012, 32(7): 14–18.

Zhang Ming-li, Li Qing-chun, Zhang Nan. The evaluation method research of wind dissolve ability based on multi-objective economics peak shaving model [J]. Northeast Electric Power Technology, 2011, 22(9): 23–25.

Zheng Tai-yi, Feng Li-min, Wang Shao-ran, et al. An optimized wind power dispatching method considering security constraints in the power grid [J]. Automation of Electric Power Systems, 2010, 34(15): 71–75.

Advances in Energy, Environment and Materials Science – Wang & Zhao (Eds)
© 2016 Taylor & Francis Group, London, ISBN 978-1-138-02931-6

A research on wind and thermal power joint ancillary service market behaviors

Ang Li
School of Economics and Management, North China Electric Power University, Huilongguan Changping District, Beijing, China

Ling Wang
State Grid Liaoning Electric Power Co. Ltd., Benxi Power Supply Company, Benxi, China

Xingang Zhao
School of Economics and Management, North China Electric Power University, Huilongguan Changping District, Beijing, China

ABSTRACT: Wind and thermal power joint ancillary service is an effective and efficient way to guarantee the safe and stable operation of electricity systems, to reduce service cost and improve the integration of wind power. In order to make a further research on wind and thermal power joint ancillary service market behaviors, this paper, based on the evolutionary game theory, and in the condition of bounded rationality and incomplete information, simulates the transaction behaviors to reach equilibrium of wind and thermal power vendors in the ancillary service market and the process of their gaming. Thereby, the market behaviors of both wind and thermal power vendors in ancillary service market in different conditions are analyzed. The findings are expected to provide a basis for the macro-control of wind and thermal power joint ancillary service market.

1 INTRODUCTION

1.1 *Background*

China's current ancillary service work by starting up/shutting down thermal power or hydropower units, controlling the power and load of traditional generation to ensure the safety of grid operating and stability of electricity supply. With the rapid development of wind power in China, the problem of wind power integration has received widespread attention from the society and power dispatch departments, but serious problems of wind curtailment still exist in some areas especially in valley periods. The increasing installed capacity of wind power has made it more difficult to solve the problem of wind power integration. Simultaneously, the startup/shutdown cost of wind power units is much lower than traditional thermal power units. Renewable energy connection to the gird makes it more difficult for traditional thermal power units to provide ancillary services. In some places, problems began to arise that traditional ancillary services only cannot ensure the safety and stability of electricity supply. Therefore, wind and thermal power joint ancillary service is an efficient and effective way to resolve and adjust overcapacity to provide a good market and institutional environment.

1.2 *Literature review*

Because of the features: volatility, uncertainty and not being able to be peak-regulated (Tu 2009), wind power connected to the grid mainly affects the peak-regulation and the standbys of ancillary services, with little effect on other ancillary services (Hannele 2008). With the increase of wind power installed capacity, the effect caused by the instability of wind power load is more and more significant. It is more difficult for thermal power units to provide corresponding ancillary services. This will surely affect the fairness of generating vendors (Li 2013). Zhang (2010) through the simulation of chronological load curve and wind power output sequence curves in planning years analyzed the influence of large-scale wind power system on peak-regulation from a new perspective. Bai (2009) brought out a framework of promoting efficient wind power integration ancillary services. He (2013) proposed several sharing and compensation systems of ancillary service costs caused by wind power accessed. Zhang (2005) compared different ancillary service models and conducted extensive research on pricing and market system problems.

In addition, current researches on renewable energy storage and prediction technologies have made it possible for wind power vendors to join the ancillary service market. To be close to the actual operating situation of the system in the future, Wang (2011) introduced the interval value estimate of maximum wind power units' capacity under a certain confidence probability. Liu (2009) conducted a weighted average combined forecasting model of wind power farm output. Liu (2013) introduced the integrated learning method and conducted a dynamic adjustment of weight distribution integrated learning method for wind power prediction.

This paper, based on the evolutionary game theory, simulates the behaviors of wind and thermal power vendors in the joint ancillary service market, studies on the strategies wind and thermal power vendors choose to reach the equilibrium under the assumption of bounded rationality and incomplete information and on how to achieve the optimum benefit.

2 ASSUMPTIONS AND PARAMETERS DEFINITIONS

2.1 *Model assumptions*

This model has 4 assumptions:

Assumption 1: Both thermal and wind power vendors are bounded rationality.
Assumption 2: Assumptions are restricted by incomplete information.
Assumption 3: Wind power vendors are able to provide ancillary services themselves.
Assumption 4: In the wind and thermal power joint ancillary service market, the capacity can be completely integrated.

2.2 *Parameters definitions*

Parameters used in modeling and their economic definitions are given as follows:

Q_1-Conventional generating capacity of thermal power vendors
Q_2-Conventional generating capacity of wind power vendors
P-Electricity price
C-Generating cost of thermal power vendors and cost of providing ancillary services for themselves
C'-Unit cost of thermal power units to provide ancillary services
C''-Costs of wind power units to provide ancillary services
α-Capacity of thermal power units corresponding to ancillary services needed by wind power vendors.
β-Capacity of wind power units corresponding to ancillary services needed by wind power vendors.
a-Compensation of thermal power vendors for providing unit ancillary service.
Of which: $C' \geq C''$, $\beta \geq \alpha$.

3 BASIC MODEL

Replicator dynamics actually describe the dynamic differential equations that the frequency of a particular strategy used in a population. According to the principle of evolution, if the adaptive value and payment of a strategy is higher than the average, this strategy will develop in the population. That is, the survival of the fittest is reflected that the growth rate $\frac{1}{X_k}\frac{dx_k}{dt}$ of this strategy is greater than zero, which can be calculated as follows:

$$\frac{1}{X_k}\frac{dx_k}{dt} = [u(k,s) - u(s,s)],\ k = 1, 2 \ldots K \tag{1}$$

In which, x represents the ratio using strategy k in one population; $u(k,s)$ represents the adaptive value using strategy k; $u(s,s)$ represents average adaptive value; k stands for a different strategy.

Table 1 is the payoff matrix of thermal and wind power vendors in the ancillary services market strategy gaming.

In this 2 × 2 asymmetric game payoff matrix, π and $\prod$ represent profits of thermal power vendors and wind power vendors. The payoffs of wind and thermal power vendors are:

$$\{\pi_1, \Pi_1\} = \{Q_1P + \alpha a - C - \alpha C', Q_2P - \alpha a\}$$
$$\{\pi_2, \Pi_2\} = \{Q_1P - C, (Q_2 - \beta)P - \beta C''\}$$
$$\{\pi_3, \Pi_3\} = \{(Q_1 + \alpha)P - C, 0\}$$
$$\{\pi_4, \Pi_4\} = \{(Q_1 + \alpha)P - C, (Q_2 - \beta)P - \beta C''\}$$

If the proportion of ancillary services thermal power vendors choose to sell is x, the proportion they choose not to sell will be $1-x$. Similarly, when the proportion of ancillary services wind power vendors buy from thermal power vendors is y, the proportion they choose not to buy is $1-y$.

Then, the fitness thermal power vendors choose to sell their ancillary services is:

Table 1. Payoff matrix.

	Wind power vendors	
	Buying ancillary services	Not buying ancillary services
Thermal power vendors		
Selling ancillary services	π_1, Π_1	π_2, Π_2
Not selling ancillary services	π_3, Π_3	π_4, Π_4

$$\mu_T(S,J) = y(Q_1P + \alpha a - C - \alpha C') + (1-y)(Q_1P - C) \quad (2)$$

The fitness thermal power vendors choose not to sell their ancillary services is:

$$\mu_T(NS,J) = y(Q_1P + \alpha P - C) + (1-y)(Q_1P + \alpha P - C) \quad (3)$$

The average fitness of thermal power vendors is:

$$\overline{\mu}_T = x \cdot \mu_T(S,J) + (1-x)\cdot \mu_T(NS,J) \quad (4)$$

Therefore, the dynamic replication thermal power vendors choose to sell their ancillary services is:

$$\frac{dx}{dt} = x[u_T(S,J) - \bar{u}_s] = x(1-x)[y(\alpha a - \alpha C') - \alpha P] \quad (5)$$

Similarly, the dynamic replication wind power vendors choose to buy ancillary services is:

$$\frac{dy}{dt} = y[\mu_W(B,J) - \bar{u}_b] = y(1-y)[x(Q_2P - \alpha a) + \beta C'' + \beta P - Q_2P] \quad (6)$$

Differential equations (5) and (6) describe the group dynamic of evolution system, and represent the adjusting speed of thermal and wind power vendors towards different trading strategies. If and only if the replicated dynamic equation is 0, the game will come to a relatively stable equalization. Making $dx/dt = 0$ and $dy/dt = 0$, four equilibrium results are obtained: O(0,0), A(1,0), B(1,0), C(1,1). If and only if $P + C' < a < \frac{\beta}{\alpha}(P + C'')$, D is the fifth equilibrium. The equation is:

$$D\left(\frac{Q_2P - \beta P - \beta C''}{Q_2P - \alpha a}, \frac{P}{a - C'}\right)$$

The Jacobian of the replication dynamic process is:

$$J = \begin{vmatrix} (1-2x)[y(\alpha a - \alpha c') - \alpha P] & x(1-x)(\alpha a - \alpha c') \\ y(1-y)(Q_2P - \alpha a) & \begin{matrix}(1-2y)[x(Q_2P - \alpha a) \\ +\beta C'' + \beta P - Q_2P]\end{matrix} \end{vmatrix}$$

In Table 2, for different equilibrium, if the sign of Jacobian is positive but the symbol of the trace is negative, the corresponding equilibrium will be stable. If the sign of Jacobian is positive and the symbol of the trace is positive too, the corresponding equilibrium will be unstable. Besides, if the sign of Jacobian is negative, the equilibrium will be a saddle point.

Table 2. Local stability of evolutionary game.

Sign of Jacobian	Sign of the trace	Stability of corresponding equilibrium
+	–	Stable equilibrium
+	+	Unstable equilibrium
–		Saddle point

1. If the parameters do not meet $P + C' < a < \frac{\beta}{\alpha}(P + C'')$, O(0,0) is the only stable equilibrium, A and B are saddle points, C is unstable equilibrium. In this condition, the vendors' market strategy will be stable that thermal power vendors do not sell and wind power vendors do not buy ancillary services.
2. If $P + C' < a < \frac{\beta}{\alpha}(P + C'')$, the corresponding Jacobian of equilibrium D is:

$$J = \begin{vmatrix} 0 & \dfrac{(Q_2P - \beta P - \beta C'')(\beta P + \beta C'' - \alpha a)(\alpha a - \alpha C')}{(Q_2P - \alpha a)^2} \\ \dfrac{P(a - C' - P)(Q_2P - \alpha a)}{(a - C')^2} & 0 \end{vmatrix}$$

In this case, equilibrium $D\left(\frac{Q_2P - \beta P - \beta C''}{Q_2P - \alpha a}, \frac{P}{a - C'}\right)$ is a saddle point; O(0,0) and C(1,1) are stable equilibriums; A and B are unstable equilibriums. The strategy of thermal and wind power vendors premising on bounded rationality will be stable in the circumstances that thermal power vendors sell while wind power vendors buy ancillary services and thermal power vendors do not sell while wind power vendors do not buy according to their long-time learning and experience. The dynamic evolution game process of thermal and wind power vendors is shown in Figure 1.

In the dynamic evolution game process of thermal and wind power vendors, the area of quadrilateral OADB stands for the probability that thermal power vendors do not sell and wind power vendors do not buy ancillary services. The larger the area OADB is, the greater possibility that thermal and wind power vendors will choose this strategy. The area of quadrilateral OADB is shown as follows:

$$S_{OADB} = \frac{1}{2}\left(\frac{Q_2P - \beta P - \beta C''}{Q_2P - \alpha a} + \frac{P}{a - C'}\right)$$

With other parameters constant, the greater the capacity of thermal power vendors providing ancillary services, (i.e. the smaller α or C' and S_{OADB} is), the greater preference thermal

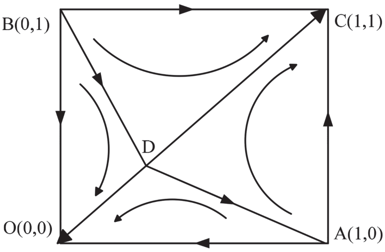

Figure 1. The dynamic evolution game process of thermal and wind power vendors.

and wind power vendors will have to cooperative market strategies. Analogously, the smaller the capacity of wind power vendors providing ancillary services (i.e. the greater β or C'' and S_{OADB} is), the more willing thermal and wind power vendors will be to choose cooperative market strategies. According to $\frac{\partial S_{OADB}}{\partial Q_2}$, S_{OADB} is decreasing with the increase of Q_2. That is, under the condition of $P + C' < a < \frac{\beta}{\alpha}(P + C'')$, the possibility of wind and thermal power vendors' cooperation is decreasing with the increase of the wind power generating capacity. According to $\frac{\partial S_{OADB}}{\partial a}$, in the case of $P + C' < a < \frac{\beta}{\alpha}(P + C'')$ and $a \geq C' + \frac{Q_2 P\sqrt{P} - \alpha C'\sqrt{P}}{\alpha\sqrt{P} + \sqrt{\alpha(Q_2 P - \beta P - \beta C'')}}$, if other parameters are constant, S_{OADB} is increasing with the increasing of parameter α. That is, the increase of compensation will lead to an increasing possibility of thermal and wind power vendors' cooperation. According to $\frac{\partial S_{OADB}}{\partial P}$, when $P > \frac{\alpha a}{Q_2} + \frac{\sqrt{(Q_2 - \beta)(a - C')\alpha a - (a - C')\beta C'' Q_2}}{Q_2}$, if other parameters are constant, S_{OADB} is decreasing with the increasing of parameter P. That is, with the rising of electricity prices, the possibility of thermal and wind power vendors' cooperation in ancillary service market is decreased.

4 RESULTS

When the parameters meet the condition of $P + C' > a$, which means the compensation thermal power vendors received from providing ancillary services for wind power vendors is lower than the opportunity and operating cost of units providing ancillary services, the thermal power vendors will not volunteer to provide ancillary services for wind power vendors. When the parameters meet $a > \frac{\beta}{\alpha}(P + C'')$ that is when wind power vendors buy ancillary services from thermal power vendors, if the compensation paid to thermal power vendors is higher than the cost wind power vendors providing ancillary services themselves, the wind power vendors will not buy ancillary services from thermal power vendors voluntarily. Only in the condition that $P + C' < a < \frac{\beta}{\alpha}(P + C'')$, will it be possible that transactions between wind and thermal power vendors happen in the joint ancillary service market. In that case, their business possibility is related to the generating capacity of wind power, the compensation level of ancillary services, current prices of electricity and the capability of wind and thermal power vendors have to provide ancillary services.

ACKNOWLEDGMENT

This article is supported by "Science and technology projects funding by State Grid Liaoning electric power co., LTD. Benxi Power Supply Company" (Grant NoFZJS1400824, FZJS1400825), "Science and technology project funding by State Grid Liaoning electric power co., LTD" (Grant No.5222 JJ14001F) and "Science and technology project funding by State Grid Corporation".

REFERENCES

Bai Jianhua, Xin Songxu et al. 2009. Analysis on the Planning and Operation Problems of Large-scale Wind Power Development in China. *Electric Power Technologic Economics*, 2: 004.

He Yang, Hu Junfeng, Yan Zhitao, et al. 2013. Compensation Mechanism for Ancillary Service Cost of Grid-Integration of Large-Scale Wind Farms. *Power System Technology*, 37(12): 3552–3557.

Hannele H., Michael M., Brendan K. et al. 2008. Using standard deviation as a measure of increased operational reserve requirement for wind power. *Wind Engineering*, 32(4): 355–378.

Li Yu. 2013. A Discussion on the Transaction Systems of Wind and Thermal Power Units' Startup/shutdown Peak-regulated Ancillary Services Based on a Large-scale Wind Power Grid. *Inner Mongolia Science Technology & Economics*, (16): 75–77.

Liu Chun, Fan Gaofeng, Wang Weisheng et al. 2009. A combination forecasting model for wind farm output power. *Power System Technology*, 33(13): 74–79.

Liu Kewen, Pu Tianjiao, Zhou Haiming, et al. 2013. A Short Term Wind Power Forecasting Model Based on Combination Algorithms. *Proceedings of the CSEE*, (34).

Qian W., Lizi Z., Guohui X. 2011. Probabilistic Calculation and Confidence Interval Estimation of Several Wind Farm Penetration Limit. *Acta Energiae Solaris Sinica*, 4: 020.

Tu Qiang. Existing applications of wind power forecasting technology and relevant suggestions. 2009. *Power System and Clean Energy*, 25(10): 4–9.

Zhang N., Zhou T., Duan C., et al. 2010. Impact of Large-Scale Wind Farm Connecting With Power Grid on Peak Load Regulation Demand. *Power System Technology.*

Zhang Baohui, Wang Yongli, Tan Lunnong et al. 2005. A new transaction mechanism for ancillary service market based on bilateral reliability bidding of both power supply and demand. *Power System Technology*, 29(23): 50–55.

Advances in Energy, Environment and Materials Science – Wang & Zhao (Eds)
© 2016 Taylor & Francis Group, London, ISBN 978-1-138-02931-6

Research on peak-regulation pricing and compensation mechanism of wind power in China

Di Zhao
School of Economics and Management, North China Electric Power University, Huilongguan Changping District, Beijing, China

Ling Wang
State Grid Liaoning Electric Power Co. Ltd., Benxi Power Supply Company, Benxi, China

Xingang Zhao
School of Economics and Management, North China Electric Power University, Huilongguan Changping District, Beijing, China

ABSTRACT: Wind power is an important renewable energy. However, wind curtailment occurs occasionally due to the large volatility of wind. Peak-regulation ancillary service is the most important way to adjust load balance, promote grid-connected of wind power generation, and reduce wind curtailment. This paper analyzes the recent status quo of wind power and ancillary services in China. So the study of peak-regulation is crucial. And also proposes the model which can price and compensate the peak-regulation ancillary services of wind power generation in China, in accordance with the principle of "compensation for costs and reasonable revenues". Then calculate the price and compensation of peak-regulation in the four different types of wind resource areas in China.

1 INTRODUCTION

1.1 *Background*

Recent years, wind energy as a kind of clean, renewable energy, gradually became an important strategic choice for countries to develop clean energy. With the increasing attention Chinese government pays to renewable energy development, as the fastest-growing and most promising way of renewable energy generation, the degree of concern about wind power development also increases [Wang Ruogu, 2011]. Wind power generation has the advantages of energy-saving and lower cost. However, due to the active output of wind power is volatile, intermittent and random, in order to maintain the balance of power in real time and to ensure the safe and stable operation of power system, hydropower, thermal power and other conventional power need to provide for integration of wind power with a lot of auxiliary services, such as peak-regulation, frequency-modulation, voltage-regulation and standby, and others. This increases the burden of ancillary services of thermal power and hydropower generation and results in the increasing of energy consume and generation cost for conventional units involve in power system ancillary services. The phenomenon of wind curtailment occurs occasionally. Therefore, the study of peak-regulation pricing and compensation mechanism of wind power generation is crucial for promoting integration of wind power, as well as ensuring safe and stable operation of the power system.

1.2 *Literature review*

Actually, there were many scholars who had analyzed related issues about peak-regulation pricing and compensation mechanism. Shen Shuangjing (2003) studied the pricing and correlative economic compensation for peak adjustment of ancillary services in power market. The models, with the goal of the max sum of power energy income and peak capacity income, are presented to optimize combination of units. He mainly introduced the cost of deep peak-regulation, but it did not analyze the cost of start and stop peak-regulation. Hu Jianjun, Hu Feixiong (2009) introduced the idea of peak-regulation capacity liability regime and proposed a new method based on equivalent available load rate indicators to compensate for the peak-regulation capacity. Wang Ruogu et al. (2011) proposed an estimate method of hydropower peak-regulation compensation. This method analyzed the water loss due to the hydropower output below the low-bound of the fee peaking internal, and then the water loss can be converted to profit loss, which can serve as the hydropower peaking compensation. Xie Jun, Li Zhenkun et al. (2013) according to the peaking value of generators which is quantified by using the proposed economic dispatch model, based on Shapley value and peaking mileage concepts, two peaking cost compensation methods are proposed. Wang Mei (2013) adopts K-means cluster analysis to classify the units based on the unit capacity and the highest peaking rate indicators, and then puts forward a new auxiliary service compensation model. Cui Qiang et al. (2015) proposed a stagger peak-valley Time-of-Use (TOU) price mechanism, in which heavy energy-consuming enterprises are impelled to participate in the peak load regulation under the Demand Side Management (DSM). Lv Quan et al. (2013) introduced the operation mechanism, technical characteristics and available scopes of peak regulation by cogeneration units. Moreover, the application and economic efficiency of this peak regulation mode are forecasted. Zhu Zhiling et al. (2011) summarizes the key factors which impact on wind power integration, including system regulation capacity, transmission capacity, technical performance of wind power, wind power dispatch levels, etc. Then some measures are proposed to improve wind power integration in China. Poul Alberg Østergaard (2006) analyses the possibilities for integrating even more wind power using new power balancing strategies that exploit the possibilities given by the existence of CHP plants, as well as the potential impact of heat pumps used for district heating and installed for integration purposes.

This paper analyzes the recent status quo of wind power and ancillary services in China. And also proposes the model which can price and compensate the peak-regulation ancillary services of wind power generation in China, in accordance with the principle of "compensation for costs and reasonable revenues".

2 MODEL OF PRICING AND COMPENSATING ON PEAK-REGULATION

In the electricity market, all main participants in the power system is to achieve the objective of maximizing benefits, in the premise of ensuring the safe and stable operation of the power system. For example, when the load is low, generator units need to reduce output in order to achieve load balance. This would reduce the generating efficiency of generator units, if the power plants' economy is affected due to providing the peak-regulation ancillary services. Therefore, to ensure the enthusiasm of providing peak-regulation ancillary services, it is crucial to provide some compensation for the wind power plants which provide peak-regulation ancillary services, to ensure that their cost is covered or even get a reasonable profit.

Currently, peak-regulation ancillary services can be divided to paid peak-regulation and free peak-regulation, which is called basic peak-regulation. Unlike basic peak-regulation, paid peak-regulation can be divided into deep peak-regulation and start and stop peak-regulation. The way of peak-regulation, which active output of the generator set accounts for less than 50% of the rated capacity is called deep peak-regulation. The way of peak-regulation, which needs to achieve stopping the generator units according to the peak-regulation needs of power grid and starting the generator units in 24 hours, is called start and stop peak-regulation. So, the compensation of peak-regulation can also be divided into deep peak-regulation compensation and start and stop peak-regulation compensation.

The installed capacity of wind turbines is generally about 2 MW, so it is generally to use the wind farm as a unit to provide peak regulation ancillary services for the power grid. The cost of running peak regulation capacity may be replaced by its equivalent opportunity cost. The generation capacity of wind farm reduces since it provides peak regulation ancillary services. Then reducing amount of generation capacity can decrease the revenue of electric energy, the decreased revenue is just the opportunity cost, which the wind farm provide running peak regulation capacity. The paid peak regulation can be made up of the deep peak regulation and start and stop peak regulation.

2.1 *Deep peak-regulation*

A certain wind farm *i* losses a part of capacity due to providing peak regulation ancillary services in a certain time Δt. Thus, we can use the revenue difference before and after peak regulation as the opportunity cost loss of deep peak regulation. In another words, it is the compensation of deep peak regulation.

1. When it provides maximum output $P_{i,\max}$, its revenue is $G_{Tp_{i,\max}}$

$$G_{Tp_{i,\max}} = P_{i,\max}\Delta t\left(\rho_E - C_i\right)\left(1 - P_{i,FOR}\right) \tag{1}$$

ρ_E—Electricity price in Δt
C_i—Cost of generation at the output level
$P_{i,FOR}$—Short-term forced outage rate of the wind farm.

2. When it provides output P_i, its revenue is G_{Tp_i}

$$G_{Tp_i} = P_i\Delta t\left(\rho_E - C_i\right)\left(1 - P_{i,FOR}\right) \tag{2}$$

3. So, there is a revenue difference ΔG_i before and after the peak regulation in a certain wind farm i in a certain time Δt.

$$\Delta G_i = G_{Tp_{i,\max}} - G_{Tp_i} = \left(P_{i,\max} - P_i\right)\Delta t\left(\rho_E - C_i\right)\left(1 - P_{i,FOR}\right) \quad (3)$$

2.2 *Start and stop peak-regulation*

A certain wind farm i losses all the capacity due to providing start and stop peak regulation ancillary services in a certain time Δt. Thus, the loss of electricity during this period multiplied by the corresponding price is the opportunity cost of start and stop peak regulation. The calculating method is equal to the revenue before the deep peak regulation in the maximum output case. It can be shown as follows:

$$G_{Tp_{i,\max}} = P_{i,\max}\Delta t\left(\rho_E - C_i\right)\left(1 - P_{i,FOR}\right) \quad (4)$$

ρ_E—Electricity price in Δt
C_i—Cost of generation at the output level
$P_{i,FOR}$—Short-term forced outage rate of the wind farm.

3 EMPIRICAL ANALYSIS

By July 2009, the NDRC (National Development and Reform Commission) announce "A notice on improving the wind power feed-in tariff policy". According to the announcement, NDRC established the principle of regional benchmarking feed-in tariff. As seen from the Table 1, the whole nation was divided into four types of wind resource areas. The wind power in-grid prices in the four areas were formulated based on the situation of wind energy resources and wind power projects construction.

Therefore, this article will be based on the four types of wind resource areas, calculates their different peak regulation price and compensation of wind power.

3.1 *Peak-regulation price of wind power*

First, we can calculate the peak-regulation price of wind power in Category I. We can see that in Category I, $\rho_E = 83.57$ \$/MWh. Assuming profit rate is 8%. So, we can conclude that $\rho_E - C_i =$ 6.6856 \$/MWh. In China, the Short-term forced outage rate of the wind farm is usually equal to 0.05. So, the peak-regulation price of wind power can be calculated:

$$P_{\mathrm{tf}} = 6.6856 \times (1 - 0.05) = 6.3513 \text{ \$/MWh}$$

Table 1. Benchmark feed-in tariffs for China's onshore wind power.

Resource zone	Benchmark feed-in tariff	Area coverage
Category I	83.57 \$/MWh	Inner Mongolia autonomous except: Tongliao, Chifeng, xing'anmeng, Hulunbeier; Xinjiang uygur autonomous: Urumqi, Yale, Changing hui autonomous prefecture, Karamay, Shihezi
Category II	88.49 \$/MWh	Hebei province: Zhangjiakou, Chengde; Inner Mongolia autonomous: Tongliao, Chifeng, xing'anmeng, Hulunbeier; Gansu province: Zhangye, Jiayuguan, Jiuquan
Category III	95.04 \$/MWh	Jilin province: Baicheng, Songyuan; Heilongjiang province: Jixi, Shuangyashan, Qitaihe, Suihua, Yichun, Daxinganling region, Gansu province except: Zhangye, Jiayuguan, Jiuquan, Xinjiang autonomous region except: Urumqi, Yale, Changing, Karamay, Shihezi, Ningxia Hui autonomous region
Category IV	99.96 \$/MWh	Other areas of China not mentioned above

Sources: Yuanxin Liu et al. 2015 [11]

Table 2. Peak-regulation price of wind power in China.

	Category I	Category II	Category III	Category IV
Peak-regulation price	6.3513 \$/MWh	6.7252 \$/MWh	7.223 \$/MWh	7.597 \$/MWh

We can also calculate the peak-regulation price of wind power in the other three wind resource areas using the same method. The result is shown in Table 2.

3.2 *Peak-regulation compensation of wind power*

Based on the last part, we can conclude that a certain wind farm i can get compensation ΔG_i if it is providing deep peak-regulation.

$$\Delta G_i = 6.3513\left(P_{i,\max} - P_i\right)\Delta t \quad (5)$$

Table 3. Compensation of peak-regulation in China.

	Compensation of peak-regulation	
	Deep peak-regulation	Start and stop peak-regulation
Category I	$6.3513\ (P_{i,\max} - P_i)\ \Delta t$	$6.3513\ P_{i,\max}\ \Delta t$
Category II	$6.7252\ (P_{i,\max} - P_i)\ \Delta t$	$6.7252\ P_{i,\max}\ \Delta t$
Category III	$7.233\ (P_{i,\max} - P_i)\ \Delta t$	$7.233\ P_{i,\max}\ \Delta t$
Category IV	$7.597\ (P_{i,\max} - P_i)\ \Delta t$	$7.597\ P_{i,\max}\ \Delta t$

And a certain wind farm i can get compensation ΔG_i if it providing strat and stop peak-regulation.

$$\Delta G_i = 6.3513 P_{i,\max} \Delta t \tag{6}$$

So according to the four types of wind resource areas in China, we can calculate the compensation of deep, start and stop peak regulation in the different wind resource areas in China. The result is shown in Table 3.

4 CONCLUSION

Ancillary service is the most important way to ensure the balance of electricity supply and demand, protect the safe and stable operation of power system and improve quality of power. With the expanding scale of the grid-connected of wind power, peak-regulation pricing and compensation mechanism as an important way to adjust load balance, promote grid-connected of wind power generation and reduce wind curtailment, whether it can be fully provided is a decisive factor to the capacity that system can accept wind power. This paper analyzes the recent status quo of wind power and ancillary services in China. And also proposes the model which can price and compensate the peak-regulation ancillary services of wind power generation in China, in accordance with the principle of "compensation for costs and reasonable revenues". Then calculate the price and compensation of peak-regulation in the four different types of wind resource areas in China. The prices of peak-regulation are 6.3513 \$/MWh, 6.7252 \$/MWh, 7.223 \$/MWh, 7.597 \$/MWh. China's wind power is still under development, in order to achieve safe and economic operation of wind power, it is necessary to carry out the reform of the electricity market, and improve peak-regulation pricing and compensation mechanism of wind power generation. However, measures to implement still need further study.

ACKNOWLEDGMENT

This article is supported by "Science and technology project funding by State Grid Liaoning electric power co., LTD. Benxi Power Supply Company" (Grant NoFZJS1400824, FZJS1400825), "Science and technology project funding by State Grid Liaoning electric power co., LTD" (Grant No. 5222 JJ14001F) and "Science and technology project funding by State Grid Corporation".

REFERENCES

Cui Qaing, Wang Xiuli, Wang Weizhou. 2015. Stagger Peak Electricity Price for Heavy Energy-Consuming Enterprises Considering Improvement of Wind Power Accommodation. *Power System Technology*, 39(4): 946–951.

Hu Jianjun, Hu Feixiong. 2009. A novel compensation mechanism of remunerative peak load regulation under energy-saving dispatch framework. *Automation of Electric Power Systems*, 33(10): 16–18.

Jin Dan, Ding Kun, He Shien. 2011. Discussion on active power regulation mechanism of wind power generation in Denmark and its enlightment to China. *Electric Power Environmental Protection*, 27(4): 50–53.

Lv Quan, Chen Tianyou. 2013. Review and Perspective if Integrating Wind Power into CHP Power System for Peak Regulation. *Electric Power*, 46(11): 129–136.

Poul Alberg Østergaard. 2006. Ancillary services and the integration of substantial quantities of wind power. *Applied Energy*, (83): 451–463.

Shen Shuangjing. 2003. Pricing and correlative economic compensation for peak adjustment of ancillary services in power market. Shanghai Jiao Tong University: Shanghai Jiao Tong University. 1–72.

Wang Ruogu, Wang Jianxue et al. 2011. A cost analysis and practical compensation method for hydropower units peaking service. *Automation of Electric Power Systems,* 35(23): 41–46.

Wang Mei. 2013. Research on Peak-regulation Ancillary Service Compensation and Trade Mechanism for Promoting Wind Power Utilization. North China Electric Power University: North China Electric Power University. 1–70.

Xie Jun, Li Zhenkun. 2013. Peaking Value Quantification and Cost Compensation for Generators. *Transaction of China Electrotechnical Society*, 28(1): 271–276.

Yuanxin Liu et al. 2015. The industrial performance of wind power industry in China. *Renewable and Sustainable Energy Reviews* 43: 644–655.

Zhu Lingzhi, Chen Ning, Han Hualing. 2011. Key Problems and Solutions of Wind Power Accommodation. *Automation of Electric Power Systems*, 35(22): 29–34.

Advances in Energy, Environment and Materials Science – Wang & Zhao (Eds)
© 2016 Taylor & Francis Group, London, ISBN 978-1-138-02931-6

A method to extend fast charging lead-acid battery cycle life for electric vehicles

Yuzhuo Zhang
School of Economics and Management, North China Electric Power University, Beijing, China

Haojun Wang
Yancheng Power Supply Bureau, Jiangsu Yancheng, China

Ling Wang
State Grid Liaoning Electric Power Co. Ltd., Benxi Power Supply Company, Benxi, China

Xingang Zhao
School of Economics and Management, North China Electric Power University, Huilongguan Changping District, Beijing, China

ABSTRACT: Study of making electric vehicles becomes the focus of scholars as the development of new energy. The study of lead-acid batteries is an important factor, which affects the development of electric vehicles. In order to increase the lead-acid battery charging efficiency, the lead-acid battery charging and discharging mechanism is based on a fast charge mode. The experiment proved that this method could effectively improve the charging efficiency, shortened the charging time and increased battery cycle life. This paper provides a new method for greatly improving future electric vehicle fast charging life.

1 INTRODUCTION

Due to the shortage of fuel consumption resulting in energy, environment increasingly destroyed. Environmentally friendly and energy-efficient electric vehicles will be better solutions to solve these problems [Genchang Wu, 2009]. As the core of electric vehicles, how to extend battery cycle life becomes a problem to overcome for scholars. Now the main types of battery, which are acid batteries, nickel cadmium batteries, nickel metal hydride batteries, and lithium-ion batteries, have advantages and disadvantages. Lead-acid batteries with its low cost, large capacity, no memory effect and mature technology advantages become the first choice of electric vehicle batteries [Abudura A, 2001] [Jinghong Zhong, 2006] [Yonghua Song] [Chaowei Duan, 2013]. Meanwhile, the main reason for affecting the life of lead-acid battery is power supply, thus the use of reasonable charging method has important practical significance [Jingjin Chen, 2004].

Juan Hao (2010) mentioned two traditional charging methods in the constant current charging and constant voltage charging. Although the control circuit methods are simple and easy to implement, but the charge cycle is too long, technical tend to a single charge, and the battery would cause unnecessary harm due to which battery life is affected, thus there are inevitable limitations. Based on the principle stage constant current battery charge, the battery depth of discharge cannot be distinguished and it is difficult to control, so it affects the battery life. According to the law proposed by Maas, fast charging method is of complexity structure and high cost. Several techniques above are developing relatively mature, but the lead-acid battery itself nonlinear dispersion and complexity of the various methods are not well satisfied the rapid development of modern electric vehicle charging requirements. It is not ideal. Therefore, on the basis of conventional charging methods, this paper further proposes new charging model. The results of using the charging circuit PSCAD simulation show that the new method can greatly improve fast charging rate and shorten the charging time.

2 LEAD-ACID BATTERY WORKS

Lead-acid battery is a secondary power supply. The positive plate active material is lead dioxide (Pb), through the water in the sulfur acid molecules, unstable material lead hydroxide (PbOH) is produced by the combination of water and a small amount of lead dioxide. Because lead ions are on the anode, hydroxide ions is present in the solution, so the positive lack of electrons. A chemical reaction occurs, when lead-acid battery charges, the negative plate of lead and sulfuric acid electrolyte. It can get lead ions. Due to the transfer of lead ions in the electrolyte, the negative plate excess of two electrons can be seen. When opening, after a series of chemical reactions, the excess electrons of the negative electrode plate and the positive electrode plate *e* deletion with a potential difference between the two plates. According to the theory above, the reaction obtained positive and negative electrodes of lead-acid batteries and the total reaction is as follows:

Negative reactions:

$$Pb + HSO_4^- \rightleftharpoons PbSO_4 + H^+ + 2e$$

Cathode reaction:

$$PbO_2 + 3H^+ + HSO_4^- + 2e \rightleftharpoons PbSO_4 + 2H_2O$$

Battery overall reaction:

$$Pb + PbO_2 + 2H^+ + HSO_4^- \rightleftharpoons 2PbSO_4 + 2H_2O$$

Lead-acid battery charging process, in a nutshell, is to produce electrical energy into chemical energy and stored. When charging, at the negative electrode, the formation of metallic lead is due to the reduction of lead sulfate of metallic lead, and its speed is far greater than the speed of lead sulfate to form. At the positive electrode, speed of lead sulfate oxidized to lead dioxide is also accelerated and turns into lead dioxide. In order to avoid loss of water, when to maintain, ionized water needs to be added on a regular basis.

Internal battery reaction is as follows:

Positive:

$$PbSO_4 - 2e + 2H_2O = PbO_2 + H_2SO_4 + 2H^+$$
$$H_2O - 2e = 2H^+ + \frac{1}{2}O_2$$

Negative:

$$PbSO_4 + 2e + 2H^+ = Pb + H_2SO_4$$
$$2H^+ + 2e = H_2$$

The charging process can be divided into three stages, namely efficient phase, mixed phase, and gas phase precipitation. The main role of the high-stage is to convert Pb to $PbSO_4$ and PbO_2. The charge acceptance rate, which is the ratio of the electrical energy converted to electrochemical for reserve and charging from the electromechanical, is about 100%. In the mixing stage, charge acceptance rate gradually decreases as a result of water electrolysis and the main reactions occur at the same time. We can know when the battery voltage and the acid concentration is no longer growing, the battery is considered is full. Gas precipitation stage, the battery is already full, then will self-discharge and water electrolysis reaction.

In summary, there are many factors that can influence the battery fast charge, such as the different levels of activity of the active substance plate, the electrolyte concentration and temperature, thus the charge will make a big difference. Different put some state, using and saving time will affect the battery charging. Since the charge current curve of the nonlinear characteristic, the charging time with the charging process decreases exponentially.

3 THE BASIC PRINCIPLE OF BATTERY CHARGE AND DISCHARGE

Rapid charging technology is based on three basic laws of the battery charge, namely, three laws by Maas made. These three laws are as follows.

The first Law: A battery can be in any given current discharge, and then its charge acceptance rate and discharge capacity of C is inversely proportional to the square root, namely:

$$a = \frac{K}{\sqrt{C}} \tag{1}$$

Formula k is a proportional constant.

And because:

$$a = \frac{I_o}{C} \tag{2}$$

Therefore,

$$I_o = K\sqrt{C} \tag{3}$$

It can be seen that for the same discharge current, power and charge acceptance is proportional. To release more power, the stronger charge is acceptance.

The second law: In any depth of discharge, battery charge acceptance ratio and the logarithm of discharge current for both linear relationship. Available:

$$a = \frac{K}{\sqrt{C}}\log(KI_d) \tag{4}$$

The formula shows that the discharge rate and depth of discharge affect battery charge acceptance rate. According to the second law, Charge acceptance rate will decrease as the battery long time of discharge in small current.

The third Law: The battery charging acceptance current is the sum of each discharge rate under current. That is:

$$I_t = I_1 + I_2 + I_3 + \dots \tag{5}$$

$$a_t = \frac{I_t}{C_t} \tag{6}$$

where I_t is the total for the current; C_t is total power emitted; a_t is total charge acceptance rate.

Release by the battery discharge can make all the battery and the charging acceptance current increases. Thus, to discharge before and after the battery in charging can increase the charge acceptance rate.

Charging technology has a big breakthrough for ever because of Mass three laws as the theory basis of quick charge technology. In the process of quick charge battery, a short stop charging and join the discharge pulse in it.

4 NEW FAST CHARGE MODE

4.1 *Lead-acid battery model*

Based on the understanding of current various kinds of charging model and on the basis of summing up predecessors' experience, we propose the circuit model shown in Figure 1 and Figure 2. The charging circuit comprises two main parts, the main one is the charging circuit was shown in the Figure 1, and the charging control circuit was shown in the Figure 2.

Charge controls the main route back three components:

1. Lead-acid battery equivalent model circuit.

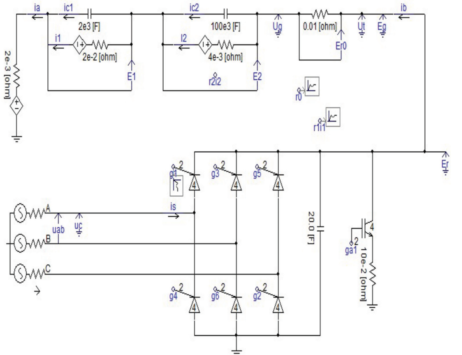

Figure 1. Charge and discharge of the main circuit.

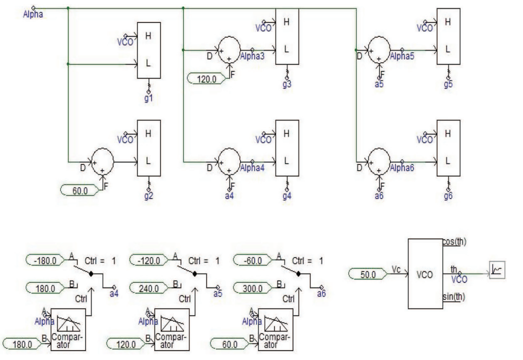

Figure 2. Pulse control loop.

2. Figure 3 is a three-phase bridge rectifier circuit: It is composed of six sent 60 degrees each pulse and it makes six thyristor conduction of the circuit, so as to control and regulate output voltage value.
3. IGBT control circuit is shown in Figure 4: This circuit controls the stop and reverses the lead-acid battery charging and discharging process.

4.2 *Select new rapid charge mode data*

1. The choice of the negative pulse amplitude has a very important significance.
   Negative pulse is mainly used to remove the polarization effect. If the amplitude value choice is very small, it does not remove the polarization effect. If the amplitude of choice is very big, it will shorten the life of the battery plate. Therefore, we will set multiple sets of parameters in the process of testing and the amplitude can vary widely.
2. Select the pulse width
   1. Before the stop time: Whenever the battery after a period of time to stop, polarization effect weakened gradually, ohm polarization immediately disappear, concentration polarization will gradually diminish over time. The longer the intermittent time, depolarization effect is more obvious. But because this is a quick charge, the interval time should not be too long, so we should choose the right down time.
   2. Negative pulse of time: Because the dynamic characteristic of the rechargeable battery, according to the different types of batteries, they need the negative pulse time is not the same. Specific analysis requires specific circumstances. Generally, select between 100 ms to 600 ms. If the time is too short, the depolarization will not achieve the effect, but if the time is too long, it will increase the amount of discharge, the battery charge is negative.

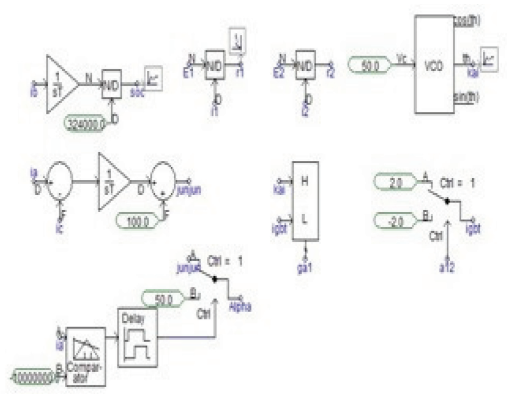

Figure 3. Controlled three-phase bridge rectifier circuit.

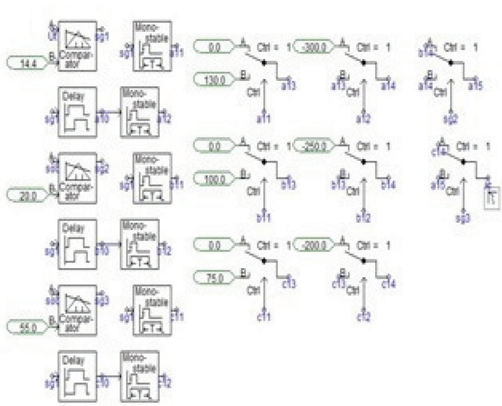

Figure 4. IGBT control circuit.

3. The stop time: this time is not appropriate for too long, the longer the terminal voltage will increase more time.

   Depolarization pulse charging method has been developed into several kinds of modes. Such as constant current, constant periodic pulse fast charging method, constant current, set gas rate pulse charging, constant current, constant voltage pulse fast charging.

3. Determine the size of the charge current

   The first stage takes 1–2 times the rated capacity of the battery as a large current during charging current value. Various stages of the selection of current required to charge according to each stage in the electricity into the battery SOC decision.

5 CONCLUSIONS

This paper focuses on the technology fast charging electric vehicles. The charging process parameters, such as the charge level among the variation width of the positive pulse amplitude, the amplitude of the positive pulse, the negative pulse duration, the amplitude of the negative pulse, etc. We explore the theoretical and experimentally study these parameters and propose a new fast—charge mode. This paper presents the design studies for its fast charge mode efficient, rapid, non-destructive, and so on. It can be as the quick charger to provide a reliable reference and theoretical basis for the research on electric vehicles.

ACKNOWLEDGMENT

This article is supported by "Science and technology project funding by State Grid Liaoning electric power co., LTD. Benxi Power Supply Company" (Grant No. FZJS1400823 and FZJS1400824), and "Science and technology project funding by State Grid Liaoning electric power Co, Ltd.," (Grant No. 5222JJ14001F).

REFERENCES

Abudura A., Kenichi S. 2001. Present status and future prospects of electric vehicles. Advanced Technology of Electrical Engineering and Energy 20(1):49–53.

Chaowei Duan, Lei Zhang et al. 2013. Design of the pulse-type fast speed charging system of lead-acid battery for electric car. Process Automation Instrumentation 34(7):75–77.

Genchang Wu. 2009. Study on selection of the electric vehicle batteries and the charging methods. *China Science and Technology Information* 23:144–155.

Jinghong Zhong, Chengning Zhang et al. 2006. The research about quick pulse charge system of lead-acid battery for electric vehicle. Power Supply Technology 30(6):504–506.

Jingjin Chen, Ningmei Yu. 2004. Study on the multi-stage constant current charging method for VRLA battery system. Power Supply Technology 28(1):32–33.

Juan Hao, Qiang Li, Jianhua Yue. 2010. Discussion on charge pattern for electric vehicle charging station. *Inner Mongolia Electric Power* 28(6):7–9.

Yonghua Song, Yuexi Yang et al. 2011. Present Status and Development Trend of Batteries for Electric Vehicles. Power System Technology 35(4):1–7.

Advances in Energy, Environment and Materials Science – Wang & Zhao (Eds)
© 2016 Taylor & Francis Group, London, ISBN 978-1-138-02931-6

Study of solar energy technology applied in oil fields

W. Qiu, H. Huang, X. Xu & R. Wang
Petroleum Exploration and Production Research Institute, SINOPEC, Beijing, China

ABSTRACT: Solar energy is a clear renewable energy. It is applied in oilfields exploration, production, storage, and transportation to reduce cost and carbon emissions. Solar energy used for generation and low-temperature heat supply is widely used in auxiliary facility in oil fields. Besides, solar energy plays an important part in large projects in exploration, storage, and transportation. Through collectors for vapor generation is used in heavy oil development instead of vapor generated by fuel. Solar energy as single heater source or auxiliary heater system has been widely used in petroleum transportation. Combined solar energy with other energy to solve the influence of radiation change will help to increase the application of solar energy in petroleum engineering.

1 INTRODUCTION

Solar energy is an important clean renewable energy. It has been one of good choices to solve lack of resource problem, environmental pollution, and climate change. Wide use of solar energy can reduce the pollution effectively and the reliance of traditional resources (Yan, Y.F. et al. 2012, Li, K. & He, F.N. 2009). Recently, the application of solar energy is mostly focused on power generation and heating (Arif, H. & Zeyad, A. 2011, Shi, J.L. 2013). According to the prediction of global resource structure from Europe United Research Centre, solar electrical energy generation technology will develop faster after 2030, and replace traditional resource step by step (Hu, Z.P. 2008).

Low voltage electrical technology has been applied in petroleum exploration and development as logistic support and auxiliary measures. In 2001, a solar electrical energy station was put into operation in the offshore platform in Shengli oilfields to supply power for navigation lights, fog horn, and living facilities (Lang, X.C. & Wang, M.X. 2001). Amoco Company used solar battery for casing anti-corrosion by catholic protection (Ralph, S.Jr. & Horkondee, J. 1979). Solar energy is also fully used in Jidong oilfield offshore artificial island of petroleum exploration to supply light and heat (Cao, X.C. et al. 2009). Solar energy is also widely used in heavy oil thermal recovery and oil storage and transportation.

2 GETTING STARTED SOLAR ENERGY APPLICATION ON HEAVY OIL THERMAL RECOVERY

Underground viscosity of heavy oil is over 50 mPa.s or relative density is higher than 0.92 at room temperature. The worldwide proved reserves of heavy oil is more than 2100×10^8 m^3 and the production is over 900×10^4 m^3/d. Thermal enhanced oil recovery such as steam injection is a common way for heavy oil recovery. Steam injection concludes cyclic steam stimulation and steam flooding. The steam stimulation technology is the most popular method in developing the heavy oil and also the main method for thermal production of heavy oil in our country. Inject amount of steam into the well first, then shut-in the well for a period of time. When the vapor expands to the oil column, open the well for production. Steam flooding heats oil formation by continuous steam injection of high dryness to reduce oil viscosity and the injected steam turns to hot fluid driving oil to productive wells where oil is to be developed.

Both these two methods need amounts of steam. According to some research results, the best injection rate of these two methods is usually higher than 100 t/d, even to 400 t/d for some special oilfields (Wu, X.D. et al. 2007, Ling, J.J. et al. 1996). The vapor temperature is at 100–250°C (Yang, B. et al. 2012, Mozaffari, S. et al. 2013). Steam is usually generated by steam generators, which will cost a lot and release greenhouse gases such as CO_2, causing pollution to the environment (Zhang, X.K. et al. 2007). The solar steam generator can figure out these problems.

Figure 1 shows the structure of common trough solar vapor generator. Water absorbs the solar energy from vacuum tube collector array mirror field and generates steam at the outlet. After separation of steam and water, water will flow to the recycle pump again and steam will be used in the petroleum production. The scale of the mirror field is depended on the steam temperature and rate that is required. For example, a vacuum tube

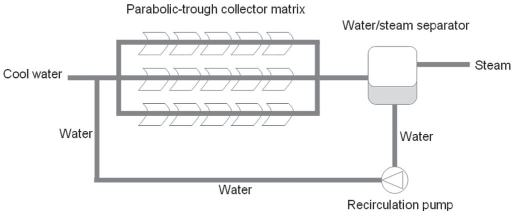

Figure 1. Schematic of direct steam generation using solar power.

collector array mirror field has 7 columns with total collector length 980 m (including pre-heated length 294 m, evaporation length 490 m and superheat section length 196 m). The steam generated by the field can reach 290°C and the superheat section 411°C (Fraidenraich, N. et al. 2013).

The solar steam generator applied in the industry includes DC type, intermediate filler type and recirculation type (Du, J.L. et al. 2013). Among these, DC type has simplest structure with lowest initial cost, but the parameters are hard to control. The recirculation type costs less with easy control of parameters (Liao, W.C. & Ke X.F. 2008).

It is analyzed that steam generated trough solar vapor generator can meet the demand of heavy oil thermal recovery. However, the oilfield needs to fit the following requirements. The sunlight is sufficient and the climate is suitable with stronger solar radiation and lower wind speed. The dust content is low. And an enough plain space is also needed for solar collectors.

Glass Point Solar Company fixed the first solar recovery device in California in 2011. At the same year, Bright Source Energy Company and Shevron Corporation built a 29 MW solar steam generator at Coalinga oilfield in California (Palmer, D. & O'Donnell, J. 2014). Oman Amal West oilfields used solar thermal recovery technology to get stream 50 t per day. After one year operation, it was shown that using solar thermal recovery in the desert in Mid-east is feasible. The system operated time was 98.6% and it can operate in the desert. Heavy oil resource in China is distributed in Xinjiang, Liaohe, Shengli and so on, which has good conditions for using solar energy for thermal recovery.

3 SOLAR ENERGY IN OIL STORAGE AND TRANSPORTATION

Produced oil needs to be stored nearby and then transported to plants by long pipelines, oil truck, or ship. Pipelines are the main way of crude oil transportation with large volume and low cost. However, due to high viscosity of heavy oil it is hard to transport at room temperature. As a result, it needs to take measures such as heating, adding light oil or drag reducer and so on to reduce viscosity and friction loss, and save the power consumption (Guo, J.L. & Han, Q.S. 2011).

Heavy oil transported by heating pipeline is an important way, including heat treated and preheated transportation (Sun, W.M. 2003.). The former way is to heat oil before transportation and then cool it down to transportation temperature at same rate in steady state or cool it at low rate in the pipelines. How to control heating and cooling temperature is the key point of this technology. The latter way pre-heats the pipe by electric heating belts, thermal station, or hot fluid and takes measure for insulation to maintain crude oil flowing at high temperature. Steam-hot water heating and electric heating are two main methods for heating crude oil.

Traditional heating methods use fuel and electricity causing high cost. Since 1990s, solar energy heating technology has been developed fast and put into practice. Use of solar energy to heat crude oil for transportation includes directly and indirectly heating (Jia, Z.W. & Song C.M. 2009). Directly heating is to heat the crude oil in the solar collectors with high effectiveness. However, the collector is hard to wash due to high viscosity of crude oil. And temperature difference is too high to control, causing crude oil burning in serious conditions. The heat from solar energy of the indirectly heating method is transferred by media. Then the media enters the heat exchanger and heats the crude oil. It improves the safety and stability of the system. The common solar energy heating process is shown in Figure 2 (Jia, Z.W. & Yang Q.M. 2009).

At normal radiation, the recycle pump starts, and hot water from the tank flows to the heat exchanger. Crude oil heated in the exchanger flows to the pipeline. Before entering to the pipeline net, a heating furnace turns on automatically according to crude oil temperature. If the temperature is lower than the required value, crude oil will enter into the furnace to be heated.

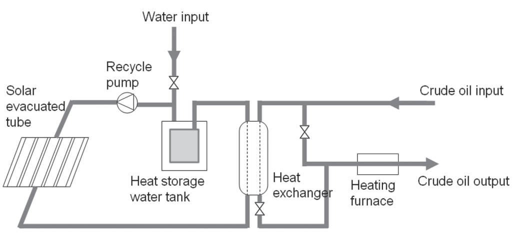

Figure 2. Process flow diagram of crude oil heating using solar power.

The temperature of crude oil needs to be heated to 50°C~55°C from 25°C~30°C before entering the next test station. It is required that the temperature of collector outlet has to reach 70°C~80°C. So, solar collectors must have high thermal efficiency, stable operation, and high resistance to pressure and freeze resistance in winter. There are three kinds of solar collectors including flat plate solar collector, all-glass solar vacuum tubular collector, and heat-pipe type vacuum collector. The flat plate solar has a higher thermal efficiency with smaller temperature difference between water inlet temperature and ambient temperature. As the difference gets larger, the efficiency gets lower fast. Vacuum collectors are influenced by temperature and have a high thermal efficiency even when the temperature is higher than 90°C (Yang, X.F. et al. 1997). Flat plate collectors have strong pressure resistance, stable operation, and bad freezing resistance, which are just the contrary to the all-glass solar vacuum tubular collectors. Heat-pipe type vacuum collectors are characterized with strong pressure and freezing resistance and stable operation (Zhu, M. et al. 2006). Each kind of collector has its own characters. And the choice of collectors should depend on the detailed conditions in the field.

At present, solar energy to heat oil has been widely used in oil fields, especially, for the areas with long-time sunshine and large solar radiation. The average daylight hour for Jiangsu oilfields every year is about 2200 h and the solar radiation is 6000 MJ/m^2. Liaohe oilfields are 2750 h sunshine and 7000 MJ/m^2 solar radiation. Both of these two fields have good conditions for using solar energy (Hu, J.Y. & Hua, X.P. 2009 & Wang, X.S. et al. 2004). In 2006, Wanglongzhuang oilfield in Jiangsu applied 30 sets heat-pipe type vacuum collectors with the total area 60 m^2 to assist the electricity heat system for heating. Good results were shown. Between July and September with enough solar radiation, electricity heat system may be stopped and the other time the solar system and electricity system can be used in turns. It saved 4×10^4 kWh after using the system in one year. Libao oilfield built 262 m^2 solar collectors in 2008 for heating oil in a 25 m^3 storage tank with an electricity heater inside (Wu, M.J. & Wang, C.L. 2010). It changed the traditional heating mode and reduced a lot of cost.

Liaohe oilfields built a heating system with solar collection 392 m^2. It occupied 792 m^2. And the heat exchanging area reached 55 m^2 due to promotion of exchanging tube structure. When it has good sunshine condition, solar energy can be used separately to heat the circulated fluid and the rest of the energy will be stored in the heat accumulator. When the sunshine is not good enough, the water jacket heater can be used. Since using the system, it saves 30% gas consumption every day (He, Z.N. 2014).

4 DISCUSSION

With the development of technology and high requirement of environment protection, solar energy has applied in petroleum industry more and more. However, there are two challenges. One is that solar radiation periodic changes by time and season. And the second challenge is that when it's cloudy or rainy or foggy and so on, the solar radiation will be affected.

Periodical or temporary changes of solar radiation have influence on steam production. However, it was studied that the ultimate recovery is not sensitive for the changes of steam rejection rate. These changes only affects seasonal recovery (Heel A.V. et al 2010). It is also recommended that solar system combined with coal units for steam generation (Chen H.P. 2013). If the solar radiation is weak, coal units are used only for heavy oil recovery.

For crude oil storage and transportation, the widely used methods are combination of solar energy and electricity for heating and combination solar energy and heat pump for heating (Peng Z. 2008, Wang X.S. et al. 2010). At good conditions for solar radiation, electricity heaters or heat pumps don't start up. And when it gets worse, electricity heaters or heat pumps will supply energy to make up the weakness of slow start-up and un-stability of the solar energy system. So, solar energy fluctuation has little influence for the production if proper measures are taken.

5 CONCLUSION

1. Solar energy is clean and regenerative, which can save energy and protect environment. Solar energy for power generation and low-temperature heating has been widely used in the oilfield production and life, such as office warming, lights and low-voltage power supply for equipments, and so on.
2. Steam injection is one of those important methods for heavy oil production. Trough solar vapor generator can replace some of coal and fuel for steam generation. Application of the technology has just been started.
3. Solar energy as a sole heat resource or auxiliary heat resource is used for crude oil storage and transportation. There are many types of solar collectors and mature pipeline design methods. This technology has been popularized and applied in many oilfields.
4. Solar radiation changes by time and season and reduces a lot at bad weather, which effects heating performance. As a result, solar energy

should be applied in areas with enough sunlight and strong annual average solar radiation and combined with other heating methods to keep the heat supply stable.

REFERENCES

Arif, H. & Zeyad, A. 2011. A key review on present status and future directions of solar energy studies and applications in Saudi Arabia[J]. *Renewable and Sustainable Energy Reviews*, 15: 5021–5050.

Cao, X.C. et al. 2009. Application on solor energy in Jidong oilfield exploration and development[J]. *Energy Conservation Technology*, 27(3): 281–283.

Chen, H.P. 2013. Optimal design of a solar aided coal-fired thermal power generation system[J]. Thermal Power Generation, 42(8): 13–16, 33.

Du, J.L. et al. 2013. Experimental study of trough type solar thermal technology used in heavy oil production[J]. *Solar Energy*, 1: 27–32.

Fraidenraich, N. et al. 2013. Analytical modeling of direct steam generation solar power plants[J]. *Solar Energy*, 98: 511–522.

Guo, J.L. & Han, Q.S. 2011. Research and application of energy-saving technology for viscous crude pipeline transportation[J]. *Sino-global Energy*, 16(4): 101–103.

He, Z.N. 2014. Application of solar heating system for raw petroleum during its piping transport[J]. *Energy Procedia*, 48: 1173–1180.

Heel, A.V. et al. 2010. The impact of daily and seasonal cycles in solar-generated steam on oil recovery[C]. SPE 129225.

Hu, J.Y. & Hua, X.P. 2009. Application of solar energy auxiliary electric heating technology in crude oil storage and transportation[J]. *Petroleum Engineering Construction*, 12: 24–25.

Hu, Z.P. 2008. Energy structure variation and alternative energy development prospect at home and abroad[J]. *China Electical Equipment Industry*, (10): 29–38.

Jia, Z.W. & Song C.M. 2009. Discussion on solar energy-saving system used for crude oil transmissing[J]. *Petroleum Engineering Construction*, 35(4): 57–59.

Jia, Z.W. & Yang Q.M. 2009. Discussion on energy conservation of crude oil conveying system using solar power[J]. *Oil-Gasfield Surface Engineering*, 28(3): 5–7.

Lang, X.C & Wang, M.X. 2001. Application of solar energy in offshore production platform[J]. *Ocean Technology*, 20(4): 73–75.

Li, K. & He, F.N. 2009. Analysis on mainland China's solar energy distribution and potential to utilize solar energy as an alternative energy source[J]. Progress in Geography, 29(9): 1049–1054.

Liao, W.C. & Ke X.F. 2008. Application of solar energy in medium & high temperature steam generation[J]. *Energy Conservation Technology*, 26(4): 328–331.

Ling, J.J. et al. 1996. The effect of steam injection rate on the performance of steam drive[J]. *Petroleum Exploration and Development*, 23(1): 66–68.

Mozaffari, S. et al. 2013. Numerical modeling of steam injection in heavy oil reservoirs[J]. *Fuel*, 112: 185–192.

Palmer, D. & O'Donnell, J. 2014. Construction, Operations and Performance of the First Enclosed Trough Solar Steam Generation Pilot for EOR Applications[C]. *SPE*-169745-MS.

Peng Z. 2008. Crude oil storage and transportation system using solar-electrical heating[J]. Oil-Gasfield Surface Engineering, 27(6): 58–59.

Ralph, S.Jr. & Horkondee, J. 1979. Application of solar energy to producing operations of oil and gas field [J]. *Journal of Petroleum Technology*, 2: 151–154.

Shi, J.L. 2013. Review of renewable energy development in China[J]. *Automation Panorama*, 6: 28–32.

Sun, W.M. 2003. Review of heavy oil pipeline technology[J]. *Oil-Gasfield Surface Engineering*, 22(5): 23–24.

Wang, X.S. et al. 2004. Applied research of solar energy for heating crude oil of transportation[J]. *Oil & Gas Storage and Transportation*, 23(7): 41–45.

Wang X.S. et al. 2010. New crude oil transportation system using solar energy and heat pump heating[J]. Oil-Gasfield Surface Engineering, 29(3): 55–56.

Wu, M.J. & Wang, C.L. 2010. Research and application of energy conservation technique of surface technology in Libao Oilfield[J]. *Complex Hydrocarbon Reservoirs*, 3(4): 82–84.

Wu, X.D. et al. 2007. Steam stimulated wells gas injection orthogonal optimization design[J]. *Petroleum Drilling Techniques*, 35(3): 1–4.

Yan, Y.F. et al. 2012. Application and utilization technology of solar energy[J]. Acta Energiae Solaris Sinica, 33(S): 37–56.

Yang, B. et al. 2012. Research on optimized multiple thermal fluids stimulation of offshore heavy oil reservoirs[J]. *Petroleum Geology and Engineering*, 26(1): 54–56.

Yang, X.F. et al. 1997. Performance computation of a few kinds of solar collectors and comparison among them[J]. *Journal of Chongqing Jianzhu University*, 19(5): 98–100.

Zhang, X.K. et al. 2007. Study of modification for thermal recovery steam generator for oil fields[J]. *Industrial Boiler*, 27(3): 8–10.

Zhu, M. et al. 2006. Collectors of solar heating system for crude oil transportation[J]. *Energy Technology*, 27(1): 10–12.

Advances in Energy, Environment and Materials Science – Wang & Zhao (Eds)
© 2016 Taylor & Francis Group, London, ISBN 978-1-138-02931-6

Research on energy storage optimal configuration of renewable energy generation under different control objectives

B. Liu & Y. Meng
Shanghai Electric Power Design Institute Co. Ltd., Shanghai, China

S.Y. Zhou & T. Lin
School of Electrical Engineering Wuhan University, Wuhan, China

ABSTRACT: The output power of renewable energy power plants (wind farms and solar power plants) fluctuates. In order to smooth power fluctuation or tracking power generation schedule, energy storage devices are often configured in power system. In this paper, charging and discharging characteristics of battery is analyzed as representative of energy storage devices and an energy storage system model is established. For different operation modes, an optimal configuration model is studied under two different control objectives, which mean tracking power generation schedule and smoothing the output fluctuations. The optimization objective is the minimization of energy storage devices investment costs, and the decision variables are the rated power and rated capacity of energy storage devices. For a practical case, Matlab is used to calculate the optimal solution.

1 INTRODUCTION

In recent years, fossil energy shortages and environmental pollution have become increasingly serious. To relieve the stress of the energy and environmental problems, countries all over the world are developing clean renewable energy. Among all sorts of renewable energy, wind power and solar photovoltaic power develop most rapidly. At present, China leads the world in capacity of all installed wind turbines.

Although wind power generation and solar photovoltaic power generation help to save energy and protect the environment, the output power will change with weather conditions such as the wind speed, and the output cannot maintain stability like that of traditional power generation to operate precisely according to generation schedule. In addition, wind power farms and photovoltaic power plants in large scale accessing to power grid may affect the stability and security of the system, and bring inconvenience to users.

In order to smooth the power fluctuations of wind farms and photovoltaic plants, energy storage devices can be installed on the outlet side of wind farms and photovoltaic plants. Energy storage devices can limit the renewable energy power fluctuations to some degree, and reduce the impact on power system and users. However, the installation of energy storage devices will increase the costs, so the research on the configuration of energy storage devices in new energy power generation system is significant.

In (Hu, 2012), the annual energy balance method is proposed for the independent wind power generation system, using batteries to balance the power difference between the power generating system and the power consumption for capacity configuration. This method is also applied to wind power and solar power hybrid generation systems with simple algorithm, and it applies well to engineering. In (Wang, 2008), peak integration method is proposed, taking the maximum absolute value of the integration of batteries charging and discharging on the entire time axis as the capacity of batteries. In (Liu, 2008), maximum negative integration method is proposed, taking the maximum value of integration in the interval of batteries discharging as the capacity of the battery.

However, the methods mentioned above fail to take an account of the internal characteristics of the battery, such as the state of charge. The capacity of batteries determined by methods above may not supply smooth power in wind power and photovoltaic power generation system, due to restriction of the operating conditions of batteries.

In this paper, a model is established with the internal characteristics of batteries taken into account for certain amount of wind power and photovoltaic power generation. There are two control objectives: (1) tracking generation schedule; (2) smoothing output power fluctuations to the predetermined range. The decision variables are the rated power and rated capacity of energy storage devices, and the optimization objective is the minimization of energy storage devices investment. Sequential enumeration method is used to get the optimal solution.

2 WIND POWER AND PHOTOVOLTAIC POWER GENERATION SYSTEM

Wind power and photovoltaic power generation system usually consist of wind turbines, solar photovoltaic cells, energy storage devices, inverters and the load. When wind power and photovoltaic power supply the load sufficiently, the energy storage devices charges to store the excess energy, otherwise the energy storage devices discharges to ensure smooth and continuous power supply.

2.1 *Model of wind power generation*

The output power of wind power generation is influenced by a number of factors, whereas it can be attributed to wind speed only with secondary factors ignored, as shown below (Bowden, 1983).

$$P_W = \begin{cases} 0, \; v \le v_i, \; v \ge v_o \\ \dfrac{v^3 - v_i^3}{v_R^3 - v_i^3} P_R, \; v_i \le v \le v_o \\ P_R, \; v_R \le v \le v_o \end{cases} \tag{1}$$

In equation 1, P_W is the output power, v_i is the cut-in wind speed, v_o is the cut-out wind speed, v_r is the rated wind speed, P_R is the rated output power.

2.2 *Model of solar photovoltaic generation*

In practical engineering, the output power of photovoltaic cells can be described in simplified model, namely, that the output power of the photovoltaic cells is only related with solar radiation and ambient temperature values. The equation is shown as below (Niu, 2010).

$$P_{PV} = P_{std} G_{AC} \frac{1 + k(T_c - T_r)}{G_{std}} \tag{2}$$

where P_{PV} is the output power of photovoltaic cells, G_{AC} is the light intensity; P_{std} is the maximum test power under standard test conditions; G_{std} is the light intensity under standard test conditions; k is the power temperature coefficient; T_c is the working temperature of photovoltaic cell; T_r is the reference temperature.

2.3 *Model of energy storage devices*

The remaining energy of batteries at moment t is related with that at moment t–1, charging and discharging during interval [t–1, t] and its own energy attenuation. The charging and discharging process of it can be described as follows (Ding, 2012; Ding, 2011; Ding, 2011):

When charging, there is:

$$P_S(t) \ge 0 \tag{3}$$

$$E(t) = (1 - \sigma)E(t-1) + \eta P_S(t)\Delta t \tag{4}$$

When discharging, there is:

$$P_S(t) \le 0 \tag{5}$$

$$E(t) = (1 - \sigma)E(t) + P_S(t)\Delta t / \eta \tag{6}$$

where $E(t)$ is the remaining energy of batteries at moment t; $P_S(t)$ is the charging/discharging power of batteries during interval [t–1, t]; σ is its self-discharging rate; η is the efficiency of its charging and discharging process; Δt is the time window for calculation. To simplify the problem, ideal case is taken into consideration, i.e. self-discharging rate σ is taken as 0, the charging and discharging efficiency η is taken as 100%. Therefore, the charging and discharging process can be unified expressed as:

$$E(t) = E(t-1) + P_S(t)\Delta t. \tag{7}$$

3 MODEL OF OPTIMAL CONFIGURATION OF ENERGY STORAGE DEVICES

In order to record the remaining energy during the process of charging and discharging, and calculate the charging and discharging power value of power stations at different time, annual data of wind farms and photovoltaic power plants is needed as known condition. In this paper, energy storage devices are assumed to be installed on the outlet side of wind farms and photovoltaic power plants to meet the specific requirements of control objectives. And there are two control objectives: a. tracking generation schedule; b. smoothing power fluctuation to predetermined range.

3.1 *The decision variables and objective function*

Economic and rational allocation of power and capacity of batteries are very necessary. The decision variables are the rated power and rated capacity of energy storage devices (Ma, 2015; Xie, 2012), and the optimization objective is the minimization of energy storage devices investment, i.e.

$$\min f = aP_R + bE_R \tag{8}$$

where a and b respectively represent the unit price of battery power and battery capacity, and the corresponding units are Yuan (¥)/(kW) and Yuan (¥)/(MWh); P_R is the rated power of batteries, and

E_R is the rated capacity of batteries, f is the investment cost of energy storage devices. In the objective function contains, both the rated power and the rated capacity are taken into consideration.

3.2 *Constraints*

Constraints include the self constraints of the energy storage devices and constraints under different control objectives. Self constraints of the energy storage devices constraints:

1. limit of the charging and discharging power,

$$-P_R \le P_S(t) \le P_R \tag{9}$$

2. limits of the State of Charge (SOC) of energy storage devices. State of Charge (SOC) represents the ratio of the remaining capacity of the energy storage devices and its rated capacity, and SOC can be expressed in percentage, ranging from (Bowden, 1981). Expressions of SOC can be written as:

$$SOC = (E_{ini} + \sum P_S(t)\Delta t)/E_R \tag{10}$$

where E_{ini} is the initial capacity of energy storage devices. The SOC limit is:

$$SOC_{\min} \le SOC \le SOC_{\max} \tag{11}$$

For different control objectives, there are different constraints. Tracking generation schedule is required to meet the constraints of power balance, so the sum of wind power, photovoltaic power, and the power of the energy storage devices should keep equal with the power generation schedule, namely:

$$P_W(t) + P_{PV}(t) - P_{GS}(t) = P_S(t) \tag{12}$$

where $P_{GS}(t)$ is the scheduled power; and smoothing power fluctuations to the predetermined range has to satisfy the constraints below:

$$|(P_W(t) + P_{PV}(t) - P_S(t)) - (P_W(t-1) + P_{PV}(t-1) - P_S(t-1))| \le \delta \tag{13}$$

where δ is the range of power fluctuation during period Δt.

3.3 *Optimization method*

In this paper, sequential enumeration method is adopted to solve the model. For example, under control objective a, first the power differences between wind power, photovoltaic power, and scheduled power generation need to be calculated. The rated power of batteries equals to the maximum absolute value of the power difference. Then charging and discharging power of batteries during each time window needs to sum up to get the maximum positive value and negative absolute value. And then rated capacity can be calculated according to limits of SOC. Finally, the minimization of investment cost can be calculated. The method is analogous under objective b. When the power difference is within the limit, power of batteries equals 0, otherwise it equals the maximum of the absolute value of the power difference plus or minus δ.

4 CASE ANALYSIS

In this paper, data of the case is from annual data of wind farms and solar photovoltaic plants in a certain area. The rated wind power is 90 MW, and the rated photovoltaic power is 50 MW. After computing, the annual wind power generation curve are shown in Figure 1.

The generation schedules of wind power generation, photovoltaic power generation and wind power and photovoltaic power hybrid generation are not the same. Due to space limitations, only wind power and its generation schedule are shown below as examples in Figure 1 and Figure 2. The limit range of power fluctuations is shown in Table 1.

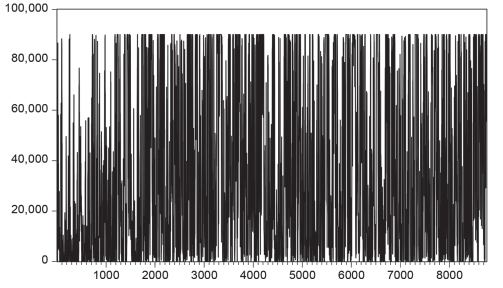

Figure 1. Annual wind power curve.

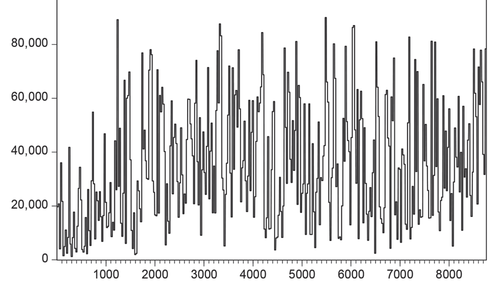

Figure 2. Annual wind power GS curve.

Table 1. Limit range of power fluctuations.

Operation mode	ΔP in 1 hour
Wind power generation	Rated power/3
Photovoltaic power generation	Rated power
Wind power and photovoltaic power hybrid generation	Rated power/3

Table 2. Parameters of lithium iron phosphate battery.

Power unit cost a	1500 Yuan/kW
Capacity unit cost b	3500 Yuan/(MWh)
SOC range	[0.2,1]
σ	0
η	100%
Δt	1 h
E_{ini}	0.5 E_R

Table 3. Results of optimal configuration.

	Control objective a			Control objective b		
Operation mode	Rated power/kW	Rated capacity/MWh	Investment/ 10^7 Yuan	Rated power/kW	Rated capacity/MWh	Investment/ 10^7 Yuan
Wind + battery	8.2773×10^4	1.4076×10^3	12.9086	5.5292×10^4	1.0971×10^3	8.6778
PV + battery	2.3769×10^4	1.1295×10^2	3.6049	1.5521×10^4	2.2435×10^2	2.4067
Wind + PV + battery	8.8453×10^4	1.6011×10^3	13.8283	3.4792×10^4	1.0461×10^3	5.5849

In this paper, lithium iron phosphate battery is taken as an example, and its parameters are shown in Table 2.

According to the acquired data of wind power and photovoltaic power, as well as generation schedule and the predetermined power fluctuation range, the rated power, rated capacity and investment are calculated under different operation modes for different control objectives. By use of Matlab, results of optimal configuration are shown in Table 3.

According to the results, conclusion can be drawn that: under control objective a, photovoltaic power generation costs least, while wind power and photovoltaic power hybrid generation costs most; under control objective b, photovoltaic power generation costs least, while wind power generation costs most.

5 CONCLUSION

In this paper, method of energy storage devices configuration is studied for wind power and photovoltaic power generation system. Energy storage devices model is established with the internal characteristics of battery taken into account. The optimization objective is the minimization of energy storage devices investment costs, and the decision variables are the rated power and rated capacity of energy storage devices. For different control objectives, Matlab is used to get the optimal solution under different operating modes for the practical case.

REFERENCES

Bowden, G.J. & Barker, P.R. 1983. Weibull distribution function and wind power statistics. *Wind Engineering*, 7(2): 85–98.

Ding, Min & Zhang, Yingyuan 2011. Economic operation optimization for microgrids including na/S battery storage. proceedings of the CSEE, 31(4): 7–14 (in Chinese).

Ding, Ming & Lin, Gende 2012. A Control strategy for hybrid energy storage systems. *Proceedings of the CSEE*, 32(7): 1–6 (in Chinese).

Ding, Ming & Xu, Ningzhou 2011. Modeling of BESS for smoothing renewable energy output fluctuation. *Automation of Electric Power Systems*, 35(2): 66–72 (in Chinese).

Hu, Guozhen & Duan, Shanxu 2012. Sizing and cost analysis of photovoltaic generation system based on vanadium redox battery. *Transactions of China Electrotechnical Society*, 35(5): 260–267 (in Chinese).

Liu, Zhihuang & Yang, Yimin 2008. Model of optimal design for wind/photovoltaic hybrid power system. *Computer Engineering and Design*, 29(18): 4836–4838 (in Chinese).

Ma, Suliang & Ma, Huimeng 2015. Capacity configuration of the hybrid energy storage system based on bloch spherical quantum genetic algorithm. *Proceedings of the CSEE*, 35(3): 592–596 (in Chinese).

Niu, Ming & Huang, Wei 2010. Research on economic operation of grid-connected microgrid. *Power System Technology*, 34(11): 38–42 (in Chinese).

Wang, X.Y. 2008. Determination of battery storage capacity in energy buffer for wind farm. *IEEE Trans on Energy Conversion*, 123(3): 868–878.

Xie, Shixiao 2012. A chance constrained programming based optimal configuration method of hybrid energy storage system. *Power System Technology*, 36(5): 79–83 (in Chinese).

Advances in Energy, Environment and Materials Science – Wang & Zhao (Eds)
© 2016 Taylor & Francis Group, London, ISBN 978-1-138-02931-6

A new electric power emergency command system for electric grid

Xiaoming Jin, Xiaodong Chen & Tie Li
Liaoning Electric Power Co. Ltd., State Grid Corporation of China, Shenyang, Liaoning, China

Shan Jiang & Yuhang Cui
Tellhow Software Co. Ltd., Nanchang, Jiangxi, China

Wentao Sun & Jian Zhang
Liaoning Electric Power Co. Ltd., State Grid Corporation of China, Shenyang, Liaoning, China

ABSTRACT: The modern power system is growing rapidly in the context of constant social development and economic growth, as a result, power grid tends to run in more complex modes. To resolve the problems, such as lack of effective prejudgment for power accidents, and unablility to effectively and quickly define the power equipment state, a new electric power emergency command system is proposed. The system has been designed based on "One Center, Two Host Lines, Three Links and Multiple Platforms". It cores the unified command for system security, realizes the closed-loop control for emergency disposal of risks and failures, ensures a well analyzed put-in-place control, and achieves the linkage of overall system. Depending on this system, the operating staff in charge of grid control can be of great capacity in control of volume growth and accidents handling, besides on-time disposal capacity against grid accidents.

1 INTRODUCTION

Electric Power Emergency Command System constitutes a new need with higher demands for the power management, which is mainly applicable for aid supports to commanders when a vital accident occurs. The said aid supports can be divided into three parts: first, collect and display various information associated with the system; second, make data summary and statistics; third, provide an assistant decision-making via an intelligent method based on those above. Until now, most of power emergency commanding systems have been at Phase I or Phase II, that is, data collection and demonstration phase, which can only help decision-makers to produce some statements and statistical reports. In details, decision-making still relies on commander's past experiences.

At present, the grid system applies single servers in provinces and local areas which work for accidents monitoring and multiple-departments, so there exist a quantity of problems related to data sharing. Upon the above analysis, the shortcomings are as follows: one lies at wide application and uncompleted functions. The reason is that the system used in a variety of departments can only summarize common characteristics of dispatching departments and take less consideration on their actual status. The other lies at poor extensibility and difficult post-maintenance. First, the system serves a variety of departments, so it features for weak data access and poor data security, which may bring great difficulty for second functional use. Second, such weak data access and high data sharing rate may result in re-development difficulties, even risks of high development cost and maintenance cost.

In electric power system, the factors that may affect grid's safe and stable operation cover many aspects, such as grid's running mode, flow status, equipment status, etc. In addition, how a personnel can obtain these data timely and accurately is vital important. The secure and stable operation of Liaoning Power Grid lies at a mass of scattered system platforms and unsatisfied data interactivity. To change this status, a new method herein, according to power grid emergency standards, has been proposed to realize system's centralized management, data integration and smooth communications, besides on-time monitoring of sudden accidents, prediction and modeling, failure forecasting, and accident handling. The final is for integrated, intellectual, and optimized control.

2 TECHNICAL REQUIREMENTS

2.1 *Technical problems that need to be solved*

The problem needed to be solved lies in how to transform and upgrade the traditional mode to a modern one, namely, from the extensive mode to an intelligentized mode (Liu, 2010). Depending on this system, the operating staff in charge of grid control can be of great capacity in control of volume growth and accidents handling, besides on-time disposal capacity against grid accidents.

Modern power system is growing rapidly in the context of constant social development and economic growth, as a result, power grid tends to run in more complex modes (Gantz, 2011). System's stable operation is subject to a variety of factors, such as current distribution, equipment state, weather situation, etc. The result is that the system can only play a supporting role in conclusion of power flow and decision-making of power supports and has defects of longer response time, strong subjective and poor systematicness. Besides those, it is lack of the effective prejudgment for power accidents, and unable to effectively and quickly define the power equipment state, accident influence scope and flow control mode especially in the case of cascading faults.

2.2 *The situation in Liaoning electric grid*

The new proposed method has been designed in Liaoning electric grid in the northeast part of China, with more than ten sets of different intelligent grid distribution systems, such as real time data monitoring, equipment management, online system analysis, failure data collection, etc (Zhao, 2013; Demchenko, 2012). Hence, the data that has been collected and managed can be synthetically computed, matched, and analyzed for the purpose of intelligent and all-round comprehensive analysis made available for grid accidents. Meanwhile, the real time failure data system can help the personnel in charge of control and regulation to obtain and understand completed and accurate key data within the shortest time and accidents trend, besides in favor of aid decision making as well. Such an upgrading from the traditional extensive mode to a modern intelligent system can highly help the personnel in charge of grid control and regulation to boost their capacities in grid control and accidents disposal, furthermore, help power system boost its capacity in real time emergency processing against grid accidents.

3 SYSTEM STRUCTURE AND FUNCTIONS

One importance against blackouts becomes vital to improve grid service quality other than daily operation, particularly, in special periods such as earthquake, thunderstorms, lingering high temperatures in summers, and yearly seasonal typhoons. The present system that specializes in grid management and control is unable to service as an information platform in case of meeting blackouts. Hence a new system has been proposed that features for technical countermeasures against grid (emergency) operation and platform building via a variety of analysis of recently major blackouts at home and abroad, sudden-onset disaster and its characteristics, as well as the theoretical foundation and the existing problems.

3.1 *System structure*

The system has been designed based on "One Center, Two Host Lines, Three Links and Multiple Platforms". Concretely to say, it cores the unified command for system security, realizes the closed-loop control for emergency disposal of risks and failures, ensures a well analyzed put-in-place control, and achieves the linkage of overall system. The system targets at leveling up the operation, focuses at the running and equipment situation, seizes two hosts including risk control and default disposal, implements the risk management, keeps the linkage efficiency under control. The purpose is to establish a uniform platform for the whole system. The work-flow of the system is shown in Figure 1.

3.2 *System functions*

1. Mass data acquisition in system provides a search function of leap-type data query (Wigan, 2013). A centralized control mode system is established without switching different systems for data query and information retrieval, which depends on multi-format, mass data acquisition, and message-switching technique.
2. Comprehensive analysis can be made on problems related to grid security. This system is considered as a comprehensive information-based forecast system against risks and disasters, which depends on Java's SOA (service-oriented platform building

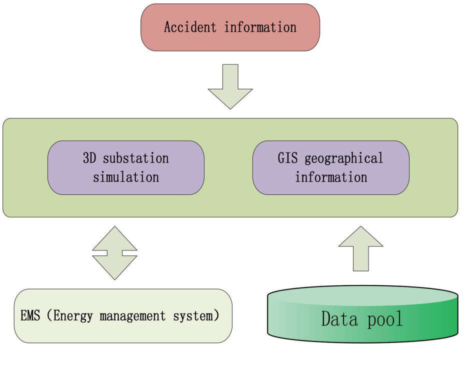

Figure 1. The work-flow of the system.

technology) to perform grid's security analysis. Grid security is an organic integrity, which can be divided into information security, operation security and infrastructure security, whereas only more research on operation security and infrastructure security in the past. Figure 2 shows 3D simulation of transformer substation picture in Liaoning electric grid.

3. A leap-type and accessible data exchange platform can be established to realize integration. XML-based data exchange platform is built across different regional networks, departments, platforms, and databases. This platform automatically extracts system-required data across heterogeneous platforms and databases as the standard XML-format data exchange protocol. And data is stored in power dispatching III area's center public resource database based on XML-standard unloading format and compression transmission technology to conduct data flow, data exchange between different systems to realize integration.
4. Instant information can be transmitted safely, quickly, and stably in combination with mobile information technology. System's automatically distributing work, sending message to look for someone and sending message to phones can be realized by comprehensively using database JOB technology, GSM/MODEM, SOCKET SMS technology.

Figure 2. 3D simulation of transformer substation picture in Liaoning electric grid.

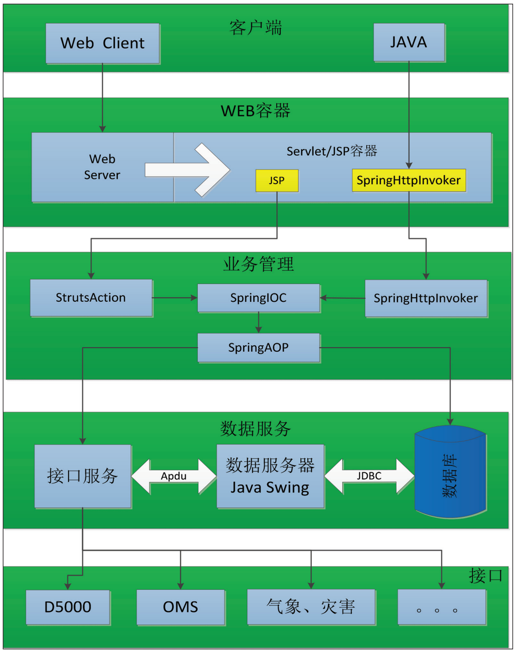

Figure 3. Emergency Command Project mechanism.

Emergency Command Project is a web-based approach besides with Java client-side and IOS client-side. Concrete thinking shown in Figure 3.

4 SYSTEM SOFTWARE

4.1 *Introduction to spring*

Spring, an open-source framework is created to decrease complexity of enterprises' application development. One of framework's main advantages lies in its layered architecture which can give you prior option of components, meanwhile provide integrated framework for J2EE application development. Spring Framework's functions can be applied to any J2EE servers, mostly of which also can be used to non-managed environment. Spring Framework's core lies in supporting reusable business and data access objects which not tied to specific J2EE service. Such objects can be reusable among different J2EE environments (Web or EJB), standalone applications and test environments. Here is mainly to introduce Spring's technologies AOP and IOC.

Spring AOP: Spring AOP (Aspect-Oriented Programming) module directly integrates aspect-oriented programming function into Spring Framework upon configuration management characteristic. As a result, it is easy to make any object in Spring Framework support AOP. And transaction management service is provided for objects in Spring's applications by Spring AOP module. Using Spring AOP can integrate declarative transaction management into applications without depending on EJB (Enterprise Java Bean).

4.2 *Introduction to web container*

WEB container: helps the application components herein (such as JSP, SERVLET) achieve interactive

Table 1. Advantages of the new method.

	Analysis and calculation of grid's security and stability	Grid mode adjustment, output of power plant and load adjustment, etc
Traditional operation mode	15 minutes, off-line computation in technical support rooms	10 minutes, decision-making upon operating experience after operators' querying procedures
New method	Auto starting on-line computation to obtain a consequence and auto prompting grid's weakness	Auto generation assistant decision-making

at environment variable interface without any interference. All these can be realized by WEB server such as TOMCAT, WEBLOGIC, WEBSPHERE, etc. Interfaces provided herein strictly abide by the WEB APPLICATION standards in J2EE specification. WEB server in accordance with the above standard is considered as the WEB container in J2EE.

4.3 *Introduction to spring HTTP invoke*

Spring HTTP invoker is a remote invocation model in Spring Framework, performing HTTP-based remote invocation (it can penetrate a firewall), and use JAVA's serialization for data transfer. It is a bit similar to but different from WebService that client-sides can easily invoke objects on remote servers just as invoking local objects.

4.4 *Introduction to struts*

Struts architecture respectively maps Model, View and Controller to components in Web to implement MVC design pattern's concept. Model is composed by Action represented system state and business logic, and definition labels provided by struts and JSP realize View, besides, Controller is in charge of control flow, completed by Action Servlet and Action Mapping.

Beneficial effects that the system brings to Power Grids are listed on tables below for contrast of dispatching emergency command system between before and after using this method when accidents occur.

5 CONCLUSIONS

In modern electric power system, the factors that may affect grid's safe and stable operation cover many aspects. For example, the grid's running mode, flow status, equipment status, etc. In particular, how a personnel can obtain these data timely and accurately is vital important. The secure and stable operation of Liaoning Power Grid lies at a mass of scattered system platforms and unsatisfied data interactivity. To solve these problems, a new power emergency command system is proposed-according to power grid emergency standards-to realize system's centralized management, data integration and smooth communications. Furthermore, on-time monitoring of sudden accidents, prediction and modeling, failure forecasting and accident handling. The final function is for integrated, intellectual, and optimized control.

REFERENCES

Demchenko Y., Zhao Zhiming, Grosso P., et al. Addressing big data challenges for scientific data infrastructure [C]//2012 IEEE 4th International Conference on Cloud Computing Technology and Science. Taipei, Taiwan: IEEE, 2012: 614–617.

Gantz J., Reinsel D. Extracting value from chaos [J]. Proceedings of IDC iView, 2011: 1–12.

Liu Zhenya. Smart grid technology [M]. Beijing: Chinese Electric Power Press, 2010 (in Chinese).

Wigan M.R., Clarke R. Big data's big unintended consequences [J]. IEEE, 2013, 46(6): 46–53.

Zhao Guodong, Yi Huanhuan, Mi Wanjun, et al. Historic opportunity in the era of big data [M]. Beijing: Tsinghua University Press, 2013 (in Chinese).

Advances in Energy, Environment and Materials Science – Wang & Zhao (Eds)
 ISBN 978-1-138-02931-6

Experimental study on the performance of 15 kW OTEC system

Fengyun Chen
Harbin Engineering University, Harbin, China
First Institute of Oceanography State Oceanic Administration, Qingdao, China

Liang Zhang
Harbin Engineering University, Harbin, China

Weimin Liu, Lei Liu & Jingping Peng
First Institute of Oceanography State Oceanic Administration, Qingdao, China

ABSTRACT: The cycle efficiency calculation method for the Ocean Thermal Energy Conversion (OTEC) is obtained through the theoretical analysis and model establishment of the equipment in the OTEC system. A 15 kW OTEC plant is built using Rankine cycle and ammonia as working medium to research the performance of the OTEC plant under different operating conditions. Then the relationship between cycle efficiency, turbine efficiency and seawater temperature difference are obtained through the analysis of the experimental data, and the heat transfer performance of the evaporator and condenser is obtained. The results show that within the scope of the test conditions, the system achieves 15 kW power rating system, and the maximum efficiency of turbine about 73% when the temperature difference is 19.7°C.

1 INTRODUCTION

An Ocean Thermal Energy Conversion (OTEC) plant is basically a heat engine that utilizes the temperature difference between the warm surface seawater and deep cold seawater to drive a turbine to produce electricity (Lavi, 1980). In Rankine cycle the low boiling point working fluid is vaporized by the warm surface seawater in the evaporator. The vaporized fluid expands to do work in a turbine and generate electricity. Then the low pressure exhaust is condensed in the condenser by cold deep seawater. The condensed working fluid is pumped back to the evaporator and the cycle is repeated. Figure 1 shows a schematic diagram of a closed cycle OTEC plant (Uehara, 1990).

Ocean thermal conversion energy is abundant in south China sea. The theory reserves of ocean thermal conversion energy close to China's offshore is about $14.4\times10^{21} \sim 15.9\times10^{21}$ J and the total installed capacity which could be utilized is $17.47 \times 10^8 \sim 18.22 \times 10^8$ kW, and 90% of the reserves distribute in the south China sea (Wang, 2009). In the face of environmental pollution and gradually reduce of fossil fuel, the utilization of the OTEC can not only promote the development of the marine economy and coastal defense construction, but also solve the power shortage of coastal and island area. The construction of the OTEC plant could supply power and fresh water for the oil production in offshore engineering, and achieve the purpose of energy conservation and emission reduction.

The development of OTEC will contribute to alleviating the pressure of the energy, improving our country's industrial structure, and also environmental protection. As a result, the ocean thermal energy as a kind of clean and renewable energy, the development and utilization of the ocean thermal energy has important practical significance to the sustainable development of national economy and the improvement of people's living standard.

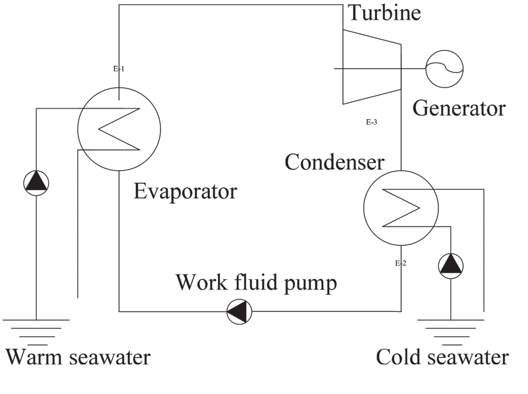

Figure 1. Schematic diagram of a Rankine cycle OTEC plant.

2 SYSTEM DESCRIPTION

2.1 *Principle of Rankine's cycle*

In this paper the OTEC system uses Rankine cycle and ammonia as working medium in this system. The system is composed of evaporator, turbine, generator, condenser, pump etc. The liquid ammonia evaporates in the evaporator where it gains heat from the warm surface seawater. Ammonia vapor enters into the turbine and expands thereby delivering mechanical work. The working fluid at the exit of the turbine is condensed in the condenser by cold deep seawater. The working fluid is saturated liquid at the exit of the condenser, it is then pumped into the evaporator, in this way the cycle is continued. The experimental system is showed in Figure 2.

The T-S diagram of Rankine cycle is showed in Figure 3. In the T-S diagram 1–2 means the progress of conversion of heat into power in turbine, 2–3 means the exothermic process from the working fluid at the exit of the turbine to cold deep seawater. 3–4 is the process of working medium through the pump, 4–1 is the evaporation of working medium in the evaporator.

Figure 2. Diagram of the experimental system.

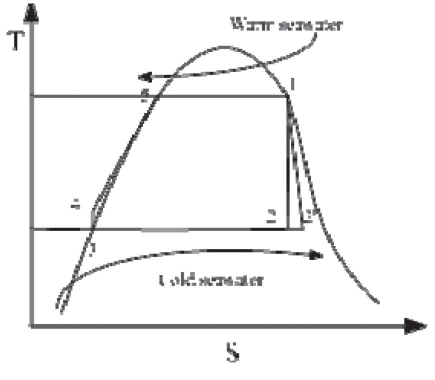

Figure 3. The T-S diagram of Rankine cycle.

2.2 *Thermodynamic analysis*

Thermodynamic analysis in each component is conducted in this study. For the cycle performance simulation, the following assumption are made: pressure drop in pipes and heat losses to the environment in the condenser, evaporator, generator, turbine and pump are neglected; The system remains uniform flow condition.

Evaporator: under this process, the liquid ammonia is heated at constant pressure. Equation of heat balance is:

$$Q_{\mathrm{E}} = m\ (h_1 - h_4) \tag{1}$$

Condenser: The working fluid at the exit of the turbine is condensed by cold deep seawater. Equation of heat balance of condenser is:

$$Q_{\mathrm{C}} = m\ (h_2 - h_3) \tag{2}$$

Turbine: the turbine converts thermal energy of ammonia vapor into mechanical work. The work produced by turbine is:

$$W_t = m\ (h_1 - h_2) \tag{3}$$

Pump: The process is assumed as isentropic process. The work consumed by the pump is:

$$W_{\mathrm{P}} = m\ (h_4 - h_3) \tag{4}$$

Thermal efficiency of the cycle is defined on the basis of the first law of thermodynamic as the ratio of net power output to the heat transferred from the warm surface seawater to the working fluid in the evaporator.

$$\eta_{\mathrm{t}} = \frac{(h_1 - h_2) - (h_5 - h_4)}{h_1 - h_4} \tag{5}$$

where Q_E = heat exchange amount through evaporator; m = system mass flow rate; and h = specific enthalpy; Q_C = heat exchange amount through condenser; W_t = work produced by turbine; W_p = work consumed by pump; η = thermal efficiency.

3 SELECTION AND CALCULATION OF SYSTEM COMPONENTS

3.1 *Selection of heat exchanger*

Due to the temperature difference between warm surface seawater and cold deep seawater is small, so the area of heat exchanger needs to be larger. Heat exchanger is an important equipment in thermal conversion process, so choosing a heat exchanger which has high performance can improve system efficiency, and greatly reduce the cost of investment. Commonly used form of heat exchangers include shell-and-tube heat exchanger, plate heat exchanger, plate-fin heat exchanger etc. Whereby the shell-and-tube heat exchanger is widely used and the technology has been perfected. However coefficient of shell-and-tube heat exchanger is small, result in increasing of the temperature difference, the volume of the heat exchanger, and then additional cost. Design of the ocean thermal energy conversion system is based on two factors: high heat transfer efficiency and low cost (compact size).

At present the structure of plate heat exchanger includes dismountable-mountable type and brazed plate heat exchangers, the compression capability of the dismountable-mountable plate is strong, however it is expensive. Currently heat exchangers adopt brazed plate heat exchanger in case of operating pressure greater than 1.0 MPa. Considering the. But considering the cost of brazed plate heat exchanger is large, in the developed OTEC plant, dismountable-mountable plate heat exchangers are chose. In order to increase the compression capability, use silicone rubber gasket and coated pressure tight sealant. In pressure testing experiment could be 2.0 MPa. Considering the corrosive performance of seawater, SOS316L is chose as plate heat exchanger material, material of E as gasket.

3.2 *Calculation model of heat exchanger*

The heat transfer coefficient is calculated and compared with the experimental data.

Calculation equation of heat transfer coefficient of the evaporator is:

$$Q = c_p m \Delta t = KA\Delta t_m \tag{6}$$

Thus the heat transfer coefficient is:

$$K = c_p m \Delta t / (A\Delta t_m) \tag{7}$$

In the evaporator, the fluids flow in counter flow, the temperature difference is called the log mean temperature difference.

$$\Delta t_m = \frac{(t_{win} - t_{cout}) - (t_{wout} - t_{cin})}{\ln \dfrac{(t_{win} - t_{cout})}{(t_{wout} - t_{cin})}} \tag{8}$$

where c_p = specific heat at constant pressurer; m = system mass flow rate; Δt = temperature drop of warm surface water through the evaporator; Δt_m = log mean temperature difference of the working fluid in evaporator; K = heat transfer coefficient; and A = heat transfer area.

Calculation equation of heat transfer coefficient of the condenser is:

$$Q = c_p m \Delta t = KA\Delta t_m \tag{9}$$

Thus the heat transfer coefficient of the condenser is:

$$K = c_p m \Delta t / (A\Delta t_m) \tag{10}$$

In the condenser, the working fluid and the cold deep seawater flow in counterflow, the temperature difference is called the log mean temperature difference.

$$\Delta t_m = \frac{(t_{win} - t_{cout}) - (t_{wout} - t_{cin})}{\ln \dfrac{(t_{win} - t_{cout})}{(t_{wout} - t_{cin})}} \tag{11}$$

where c_p = specific heat at constant pressurer; m = system mass flow rate; Δt = temperature rise of cold deep seawater through the condenser; Δt_m = log mean temperature difference of the working fluid in condenser; K = heat transfer coefficient; and A = heat transfer area of the condenser.

4 RESULTS AND DISCUSSION

In the present paper, based on the experimental data, the effect of the major thermodynamic parameter on the system performance for Rankine cycle is analysed. In experiment process get the data by changing the temperature difference between warm and cold seawater. Figure 4 shows the variation of turbine power output versus the temperature difference between warm and cold seawater. It is apparent from Figure 4 that turbine power output

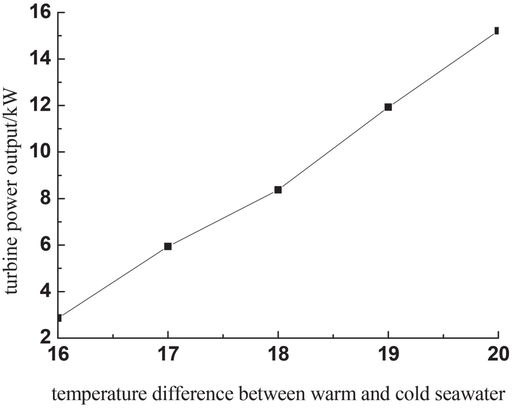

Figure 4. Variation of turbine power output versus the temperature difference between warm and cold seawater.

increase with the increase in temperature difference between warm and cold seawater. The plant achieve the rated power when the temperature difference between warm and cold seawater is 19.7°C.

Figure 5 shows the variation of turbine efficiency versus the temperature difference between warm and cold seawater. It is apparent from Figure 5 that turbine efficiency increase with the increase in temperature difference between warm and cold seawater. Turbine efficiency reaching the maximum, about 73%, when turbine operate under the rated conditions.

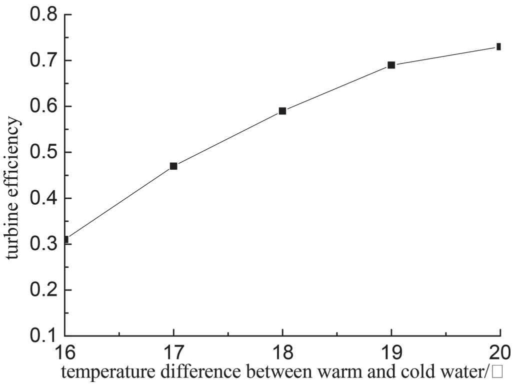

Figure 5. Variation of turbine efficiency versus the temperature difference between warm and cold seawater.

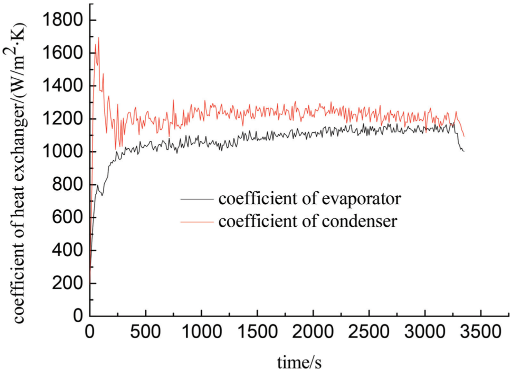

Figure 6. Variation of coefficient of heat exchangers versus over time.

Coefficient of the heat exchanger under different working conditions is obtained and heat transfer performance is tested by experiment. Figure 6 show the variation of coefficient of the heat exchanger versus over time under the conditions: the temperature of cold water is 20°C at inlet, temperature deference is 2.71°C, mass flow-rate of cold water is 129 m^3/h, the temperature of warm water is 40°C at inlet, temperature deference is 2.03°C, mass flow-rate of warm water is 125.3 m^3/h, mass flow-rate of ammonia is 1.27 m^3/h. Coefficient of heat exchanger can be up to about 1700 $W/(m^2 \cdot h)$. When the heat exchanger is normally running, the coefficient of the heat exchangers are between 1200 $W/(m^2 \cdot h)$ and 1300 $W/(m^2 \cdot h)$.

5 CONCLUSION

Through the theoretical analysis and experiment of the 15 kW OTEC plant, the following results are obtained:

1. Turbine efficiency reaching the maximum, about 73%, when the temperature difference between warm and cold seawater is 19.7°C.
2. Coefficient of heat exchanger can be up to about 1700 $W/(m^2 \cdot h)$. When the heat exchanger is normally running coefficient is between 1200 and 1300 $W/(m^2 \cdot h)$.

REFERENCES

Huang Liang Min. The Overview of China's Sustainable Development [M]. Beijing: Science Press, Ocean Development and Management, 2007.

Lavi A. Ocean thermal energy conversion: a general introduction. Energy 1980; 5: 469–480.

Liu Qi. Study on China's New Energy Development [J]. Power System and Clean Energy, 2010, 1, 26(1): 1–2.

Uehara H, Ikegami Y. Optimization of a closed-cycle OTEC system. Trans ASME Journal of Solar Energy Engineering 1990; 112: 112–256.

Wang Chuan Kun. Analysis Methods and Reserves Evaluation of Ocean Energy Resources [M]. Beijing: China Ocean Press, 2009.

Wang Xun. Economic and environmental benefits of ocean thermal energy conversion [J]. Marine Sciences, 2008, 32(11): 84–87.

Advances in Energy, Environment and Materials Science – Wang & Zhao (Eds)
© 2016 Taylor & Francis Group, London, ISBN 978-1-138-02931-6

Construction solutions on data center of PV power systems of Qinghai Province based on big data technologies

Yu Yun
Nanjing College of Information Technology, Nanjing, China

ABSTRACT: With the rapid development of construction of PV plants in Qinghai province, the need for constructing a data center for monitoring and analyzing generation data and environment data of PV plants has become more and more emergent for the sake of the safety and efficiency of PV power generation and dispatching. In this paper, a total solution on constructing a data center of PV Power System in Qinghai province based on Big Data Technologies was put forward by presenting the logical architecture, network topology, physical architecture, and determination of storage configuration. With the support of Big Data technology, the data center can be built as a safe, scalable, efficient, trusted platform for the data and business management of the PV plants. And it will be also profitable for the power grid companies who are responsible for the dispatching and planning of the PV systems within their operation area.

1 INTRODUCTION

By the year 2014, the total installed capacity of PV power systems in Qinghai province of China have reached 4,120 MW. With the rapid development of construction of PV plants in Qinghai province, the need for constructing a data center for monitoring and analyzing generation data and environment data of PV plants has become more and more emergent for the sake of the safety and efficiency of PV power generation and dispatching.

For each PV power system, the measured values, e.g. voltage, current, output power, and so on, we may care can reach up to 20,000 data points. In sum, the designed data capacity for the data center should be set to 2,500,000 data points. To store and handle such large scale of data, the storage capacity for the data center is 100 TB for the first stage. Besides the observed data which can be organized in form of structured data, the non-structured data of design document, monitoring VCR data and so on is also very vital for the efficiency analysis of PV power system for the data center. The data center will be designed providing services for the related system like dispatching system, power trading system, economic analysis system and so on. So, the data with data center should be easy to be accessed for those outside systems.

To meet the needs above, the 'Big Data' technologies (Viktor M. et al. 2013) represented by Hadoop/Spark technology (Srinath P. & Thilina G. 2013, Holden K. et al. 2015) are naturally addressed for providing a safe, efficient, robust solution for the constructing data center of PV systems. According to the heavy job of large scale of observed data collection within PV plants passed on to the site of data center far away, the communication solutions should also be addressed.

2 SYSTEM ARCHITECTURE

2.1 *Logical architecture*

The data flow of the data center can be depicted as the following. The data collection devices installed on-site collecting observed data, which was passed to data center through communication channels. After data analysis, the results will be pushed to display frontend such as desktop PC, smart phone, and display screen. According to the data flow, the data center of PV systems in Qinghai province can be logically divided into 4 layers: infrastructure layer, platform layer, application layer, and display layer, which is depicted as Figure 1.

1. Infrastructure Layer provides basic run-time environment for the business logics of the whole system. Apache Hadoop software library is introduced as the base framework for reliable, scalable, distributed computing. The distributed file system—*HDFS*, the batch processing framework—*Map*/*Reduce* and the coordination service for distributed applications—*Zookeeper* (Flavio J. & Benjamin R. 2013) form the core layer of Hadoop. Above the core layer, *Hbase* (Nick D. & Amandeep K. 2012) designed for structured storage and Hive—a data warehouse infrastructure that provides data summarization

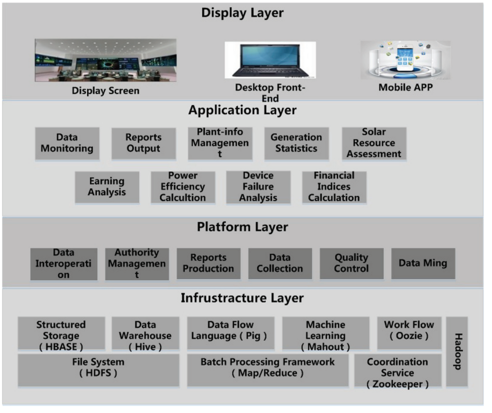

Figure 1. Logical architecture.

and ad hoc querying are based on distributed file system, providing supports for data interoperation mid-ware and data collection mid-ware in the platform layer. The data flow language—*Pig* is an execution framework for parallel computation built upon Map/Reduce and Zookeeper. *Mahout* (Sean O. et al. 2010)—a scalable machine learning and data mining library and *Oozie* (Hortonworks. 2015)—a workflow scheduler system to manage Hadoop jobs provide programming API for the modules of data mining and data quality control in the platform layer.

2. Platform Layer is a collection of business midware providing common use functions for business application modules. The platform layer is running upon the Hadoop services framework. The design objectives are to implement good abstractions for application functions, reduce the dependency between application interfaces and infrastructure layer, and ensure the scalability and reusability. The modules in platform layer includes: 1) Authority Management: a mid-ware which provides a series of management features, such as authority service, log management, and user management. The module provides support for the corresponding UI modules in application layer. 2) Data mining: a mid-ware enables features of data statistics and data mining. One part of the module is designed to be run as backgrounder in the state of batch processing to support off-line tasks. Another part of the module can be run within the application containers, accepting data analysis requests from application layer and returning analysis results. 3) Data interoperation: a mid-ware designed to support on-line data query features. It accepts real-time query requests from application layer then submit to database and return the query results. 4) Report production: a mid-ware for report production by template definition and template replacement. The report system is designed for cross-platform and compatible with excel and xml file formats. 5) Data collection: performing interactions with communication servers to implement persistence operation of on-line monitoring data and statistics data. 6) Data quality control: a module implementing the function of data quality control by filtering and annotation to data based on the domain knowledge and statistic algorithms. It is responsible for the integrity and validity of data.
3. Application Layer contains all of the features shown in UI. Based on BS structure, the application layer is deployed in application container and run in Web browser. The main features include: on-line data monitoring, devices management, reports output, Earnings calculation of generation and generation efficiency analysis.
4. Display Layer renders the application data through display screen, desktop PC and mobile app.

2.2 *Network topology*

Figure 2 depicted the network topology of data center of PV power systems in Qinghai province, which is deployed in 3 security zones: PV Plants, internal zone of master platform, and external zone of master platform.

1. An on-site communication terminal is deployed in PV plant obtaining operation data of the PV system. There are 3 ways for the communication terminal to obtain the operation data from PV system according to different types of data: the device running data are fetched from the existing

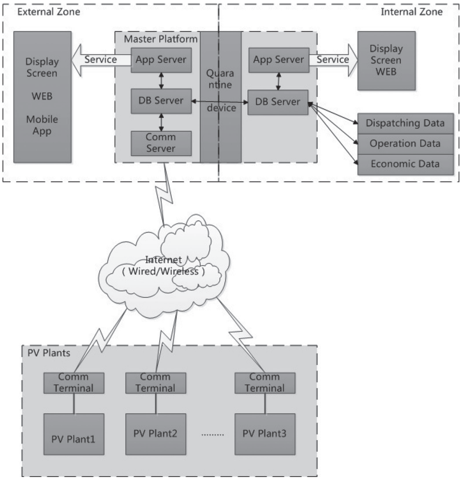

Figure 2. Network topology.

production monitoring system on-site and sent through COM port using the 101 power communication protocol; the climate observation data are directly sent from weather station through Modbus-RTU protocol; the generated energy data are directly sent through DLT645 protocol to the communication terminal. Then, the collected data in the on-site communication terminal are sent through VPN network to the remote master station of data center.

2. The master platform of the data center is deployed in both the external zone and the internal zone. There are quarantine devices for single direction data transport from internal zone to external zone. The devices only support the legal data transport through the TNS protocol, which is used by Oracle. The devices can provide the filtering, analysis and detection services to SQL query, blocking the malice access to platform, guaranteeing the safety of data content and platform. The communication server cluster, the distributed server cluster, Oracle server, and application server cluster are deployed in the external zone. The distributed server cluster supports the large data storage and application server cluster supports the internet information access. Oracle server and application server are also deployed in internal zone. Oracle server provides the storage service for dispatching data, sales data, and economic data. The application server provides the information service for intranet user.

2.3 *Physical architecture*

The physical architecture of data center is depicted in Figure 3. The whole data center platform is divided into external system and internal system by quarantine devices. The external system is the core

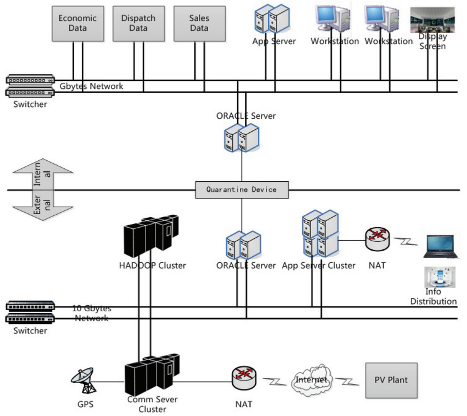

Figure 3. Physical architecture.

part of the whole data center. The communication server cluster, Hadoop cluster, Oracle server, and application server cluster are deployed in it communicating though 10 Gbytes network. The external system is designed to support data processing, core business logic running, and UI service. To obtain the ability of collecting, persisting, and analyzing the TB to PB level data in the near future; Hardtop technologies are introduced in the system. Through Hadoop framework, coordination of distributed applications, distributed file system, distributed database, data warehouse, and data mining service are implemented. To implement real-time duplex communication between remote master platform and on-site communication terminals, communication server cluster are deployed supporting the input of more than 2,500,000 data values. The detail devices of external system are enumerated below:

1. Communication server cluster: PC servers, supporting active standby, providing the data collection service and NTP time service for the system. The communication server cluster should support 150 data channels and 2,500,000 data values.
2. Hadoop cluster: adopting Hadoop framework, to provide distributed business database, data warehouse, and application services.
3. Oracle server: supporting the data transport between external and internal system through quarantine devices using the oracle TNS protocol. It is deployed as the mirror of internal database.
4. Application server cluster: providing frontend services, supporting the interactions through Web browser and mobile terminals.
5. 10 Gbytes network system: providing data communication channels of high efficiency.
6. NAT switcher: providing Network Address Transformation service to support the information distribution and data collection.
7. GPS chronometer: receiving standard time from GPS system and providing time service to the system.

The internal system is designed for internal data (such as energy data) collection, internal web information distribution service which is a supplement for the external system providing some mirror services for the latter. It can also provide data service for other internal business systems. The detail devices configuration is listed below:

1. Oracle server: internal data collection and data analysis.
2. Application server: supporting internal web application service and UI service.
3. Workstations: internal information terminals.
4. Gbytes Network: providing the internal data communications.

3 DETERMINE OF STORAGE CONFIGURATION

To determine the storage configuration of the data center, the data size of collection and analysis jobs should be calculated. The data types been collected and analyzed includes: PV plants production monitoring data, dispatching data, energy production data from sales data, statistics data, testing data, and economic analysis data.

1. PV plants production monitoring data. By 2014, the total installed capacity of Qinghai province is 4120 MW. According to the statistics data, there are 400–600 data values for 1 MW installed capacity. Through comprehensive consideration, in the first phrase, the data center is designed to contain 2,500,000 data values. For each 15 minutes, these data values will be refreshed once. From engineering practice we know that each data values take up room for 128 bytes, that is to say, the growing data size for a year is about 11.21 GB. So the total data size is 56 GB for 5 years.
2. Dispatching data. The dispatching data of PV plants includes running data of inverters, climate data, and output power data with the total of 100 data values for each plant and 15,000 data values for 150 plants. Set the data refreshing frequency to once for 15 minutes. Then the growing data size is 44.85 GB for a year and the total data size is 224.25 GB for 5 years.
3. Energy production from sales data. Relatively smaller size from sales data can be estimated as 3 GB for a year and 15 GB for the total 5 years.
4. Statistics Data. They come from the statistical operation oriented to multi-topics analysis on the detail business data. The number of planned entity tables of statistics data is estimated to 200. Each entity tables contains: time field (8 bytes), unit (16 bytes), 5 business dimensions (5 attributes for each dimensions, 8 bytes for each attribute), 10 data items (10 bytes for each items). So the total data size of each record in each entity table is 164 bytes. The total data size for each entity table is 23.69 GB for 5 years. And the summed data size for all of the entity tables is 4.6 TB.
5. Testing data: 1 GB for each plant and 150 GB for total.
6. Economic analysis data: 200 GB extra data for reserved size.

Table 1 enumerated the whole calculations of storage configuration. The total data size of data center for 5 years is 62 TB. Available storage spaces = (original data size * number of replications + reserved size) * compression ratio * (1+extension rate) * (1+disk redundancy) = 128.7 TB.

Table 1. Calculation of storage configuration.

Item	Unit	Amount
Compression ratio	%	33%
Original size	TB	60
Number of replications		3
Reserved size		1
Extension rate	%	25%
Disk redundancy	%	30%

4 CONCLUSION

With the rapid development of construction of PV plants in Qinghai province, the need for constructing a data center for monitoring and analyzing generation data and environment data of PV plants has become more and more emergent for the sake of the safety and efficiency of PV power generation and dispatching.

In this paper, a total solution on constructing a data center of PV Power System in Qinghai province based on Big Data Technologies was put forward by presenting the logical architecture, network topology, physical architecture, and determination of storage configuration. With the support of Big Data technology, the data center can be built as a safe, scalable, efficient, trusted platform for the data and business management of the PV plants. And it will be also profitable for the power grid companies who are responsible for the dispatching and planning of the PV systems within their operation area.

REFERENCES

Flavio J. & Benjamin R. 2013. *ZooKeeper: Distributed Process Coordination.* Sebastopol: O'Reilly.

Holden K. et al. 2015. *Learning. Spark.* Sebastopol: O'Reilly.

Hortonworks. *Apache Oozie.* 2015. oozie.apache.org.

Nick D. & Amandeep K. 2012. *Hbase in Action.* Shelter Island: Manning Publication.

Sean O. et al. *Mahout in Action.* 2010. Shelter Island: Manning Publication.

Srinath P. & Thilina G. 2013. *Hadoop MapReduce Cookbook.* Birmingham: Packt Publishing Limited.

Viktor M. & Kenneth C. 2013. *Big Data, A Revolution That Will Transform How We Live, Work, and Think.* Boston: Houghton Mifflin Harcourt.

Advances in Energy, Environment and Materials Science – Wang & Zhao (Eds)
© 2016 Taylor & Francis Group, London, ISBN 978-1-138-02931-6

Dynamic simulation on a micro-grid system consisting of photovoltaic power, gas combined heat-and-power and battery

Hideaki Kuronuma & Noriyuki Kobayashi
Department of Chemical Engineering, Nagoya University, Nagoya, Japan

Hongyu Huang
Guangzhou Institute of Energy Conversion, Chinese Academy of Sciences, Guangzhou, China

ABSTRACT: In this study, dynamic analysis of a micro smart grid network system with solar and heat management in a smart grid network system has been investigated. The micro grid network system has been evaluated with considering demanded power changing at different time and weather and the benefits has been estimated.

1 INTRODUCTION

Renewable energy and conservation has become one of the hottest research topics during these days. Researches are looking for ways to increase energy efficiency and ensure a sustainable energy supply that will benefit to realize the energy sustainable society in the future (Meysam, 2012). And now, there is a new way to leverage technology that is generating interest and action—the smart grid. The smart grid is a type of electrical grid, which attempts to predict and intelligently respond to the behavior and actions of all electric power users connected to it—suppliers, consumers and those that do both—in order to efficiently deliver reliable, economic, and sustainable electricity services. The smart grid will help: improve the reliability, capacity and capability of the electricity network; ensure a safe, cost-effective, and environmentally sustainable energy supply; enable faster response and resolution to outages; create a resilient, open and dynamic information network (Colson, 2013; Huang, 2012; Kevin, 2012).

In recent years, a lot of researches relating to the smart grid system with distribution management systems have been carried out (Meysam, 2012; Colson, 2013; Huang, 2012; Kevin, 2012; Feng, 2013; Yun, 2014). Meysam et al (Meysam, 2012) illustrated the smart grid and micro-grid development in the recent decades, and showed that the challenges for the successful realization of smart grid includes the integration of renewable energy resources, real time demand response, and management of intermittent energy sources. Colson et al (Colson, 2013) proposed a comprehensive real-time micro-grid power management and control with distributed agents, and the system and formulations presented demonstrate the viability and capability of decentralized agent based control for micro-grids. Kevin et al (Kevin, 2012) analyzed the cost effective of smart grid network combing power and communication network. Yun et al (Yun, 2014) introduced the development of smart distribution management system for real-time predictive operation in distribution systems, the system consists of device level for the real time data acquisition and the server level for the data related to the voltage, current, faults, power quality, and load profiles of the network.

Each respective element technology in smart grid system (such as solar photovoltaics, gas engine, and various forms of distributed generation, thermal storage, secondary battery, and many more) are being developed. Furthermore, the authors are interested in optimizing the heat and electricity in the smart grid network, it is necessary to investigate the solar and heat management in a micro grid.

In this study, in order to contribute to a green innovation and optimize the heat and electricity in the smart grid network, we tried to develop a simulation model of a micro smart grid system that can predict the needed function of respective element technology according to demand of end user at different weather conditions, it is necessary to investigate the feasibility of this micro smart grid system. We proposed a combined complex smart grid (as shown in Fig. 1) consisting of lots of micro grids including gas engine (heat), solar power plant, thermal storage, end users (such as LED, secondary battery, factory, etc.). The number of installed and the size of each facility of the smart grid and place of installation has been optimized by modeling simulation, and the benefits due to energy balance calculation has been estimated.

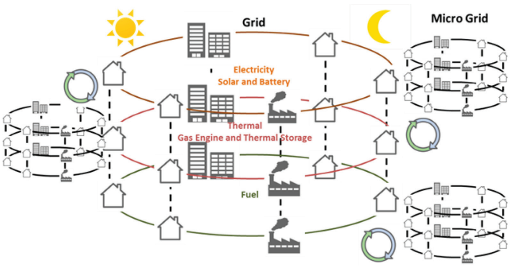

Figure 1. Optimization of heat and electricity supply in a smart grid network.

2 MODELING

At the first stage, model of a micro smart grid system with real time change and management of solar and heat was carried out to establish the evaluation and calculation method of fuel and electricity amount and the benefit effects.

2.1 *Model and approach*

Model of a micro smart grid system is shown in Figure 2, which is consisted of photovoltaics from isolation, a gas engine fueled by methane, and a secondary battery for electricity storage. The image of a micro smart grid model is shown in Figure 2. In the simulation, the following conditions are assumed.

- If solar power is not enough, replenish from the gas engine which has a maximum output of 35 kW grid-power;
- The excess of solar power is stored and used at night;
- If the total power supply is not enough at high consumption, more gas engine is set in parallel;
- The difference of solar radiation in sunny, cloudy day is considered.

$$\begin{aligned}\text{Solar power} &= \text{solar radiation} \times \text{area of solar panels} \times \text{number} \times \text{DC-AC conversion efficiency} \times \text{module conversion efficiency} \\ &\times (1 - \text{temperature correction factor}) \\ &\times (1 - \text{other losses})/3600 \qquad (1)\end{aligned}$$

The approach of the micro smart grid system is illustrated as follows. A non-steady state mode is used by Visual Modeler because insolation for photovoltaics is a non-steady parameter. Units in the micro grid system are added by C program language in the analysis system as show in Figure 2.

All energy forms including electricity from photovoltaics and gas engine, methane fuel, thermal heat from gas engine are all transformed as hydrogen energy as shown in Figure 3.

Table 1. Specifications of equipments.

Solar panel	Product	Sanyo Electric HIT-B200J01
	Module conversion efficiency	17%
	Size	1.319m×0.894m (14kg)
	Numbers	16 pieces (3.2kW total equivalent)
	Temperature correction factor (loss)	12% (June~August)
	Other losses	5%
Power conditioner	Product	Sanyo Electric SSI-TL27A2
	DC-AC conversion efficiency	94.5%
	Power consumption	5% of the solar power consumption
	Standby power at night	3W
Secondary battery	Product	Energy Farm Light EF-2
	Capacity	2500Wh
	Charge efficiency	90%
	Discharge efficiency	90%

Table 2. Specifications of gas engine.

Fuel type	**Methane**
Power output	**35kW**
Power generation efficiency	**34%**
Exhaust heat recycle efficiency	**51%**
Overall thermal efficiency	**85%**

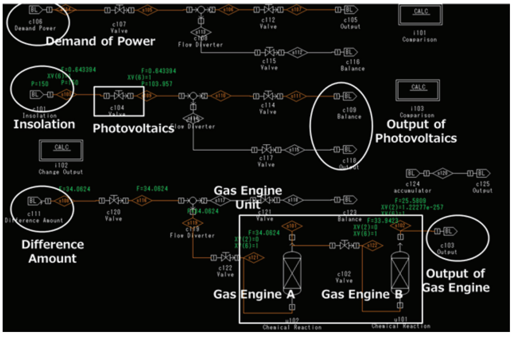

Figure 2. Model of a micro smart grid system.

The calculation flow of the micro smart grid system is shown in Figure 4. The insolation is non-steady and changes with time at every 5 seconds, as the electricity from photovoltaics also changes with time corresponding. If the electricity supply is not enough, the gas engine works and began to supply electricity. If the electricity is in excess, it is stored as electricity or thermal storage.

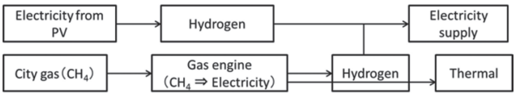

Figure 3. Every energy forms transformed as hydrogen energy.

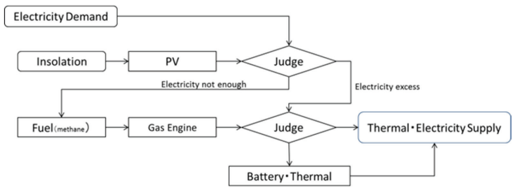

Figure 4. Calculation flow of the micro grid system.

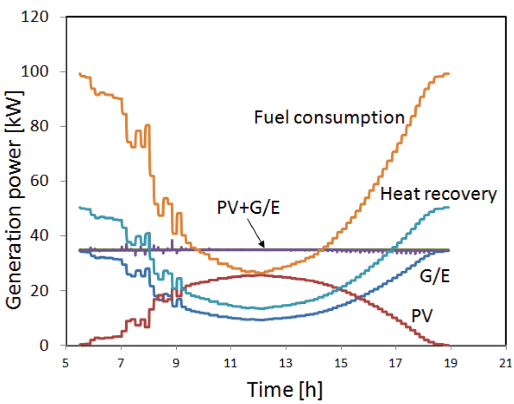

Figure 5. Simulation results (sunny day).

2.2 *Result and discussion*

Based on the above conditions, the thermal or battery recycle effect of the grid power consumption has been calculated. The results of sunny day and cloudy day are shown in Figures 5 and 6.

The horizontal axis of the graph is real time of a day; the vertical axis of the graph is electricity power. The black line is the demanded fuel in the micro smart grid system; the red line is electricity from gas engine; the blue line is the recycled thermal energy; the green line is electricity from solar power; the purple line is the sum electricity amount of solar power and gas engine; the brown line the demanded power. When there is no solar power output from the middle of the night until the morning, replenish from secondary battery or the gas engine. If solar power exceeds the power consumption during the day, the excess is stored with secondary battery and used at night.

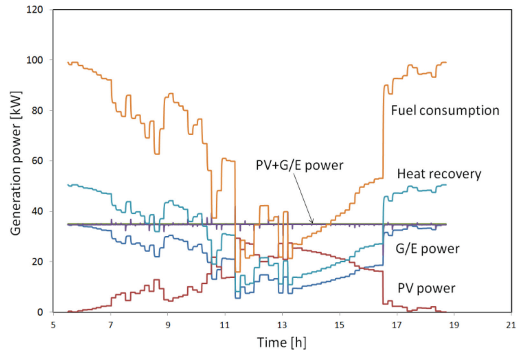

Figure 6. Simulation results (cloudy day).

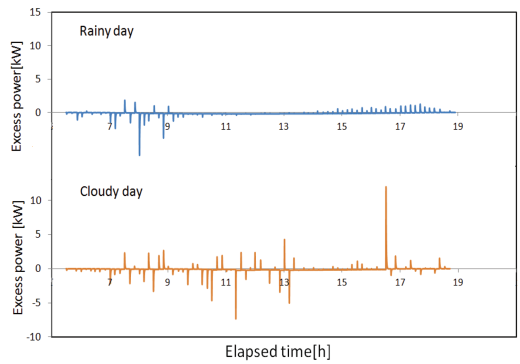

Figure 7. Excess amount of electricity with time.

As shown in Figures 5 and 6, the demanded fuel decreases when the solar power increases because of the higher insolation. It is possible to reduce the fuel consumption with the introduction of solar power and secondary battery. In the case of cloudy, the fuel consumption is changed dramatically because of the non-steady isolation at cloudy day.

From the above results, we estimated the amount of recycled thermal energy. The amount of recycled thermal energy is defined as Equation (2):

$$\text{Recycled thermal energy} = \text{Demanded fuel} \times \text{Heat recycle efficiency} \quad (2)$$

In the sunny day, the amount of recycled thermal energy is about 1.36 GJ during the time period of 5:30 to 19:00, which is averaged about 28 kW. On the other hand, the amount of recycled thermal energy is about 1.56 GJ, corresponding as 32 kW in the cloudy day.

In order to obtain feasibility of the micro smart grid system, it is necessary to know the lacked amount of electricity at these weather conditions

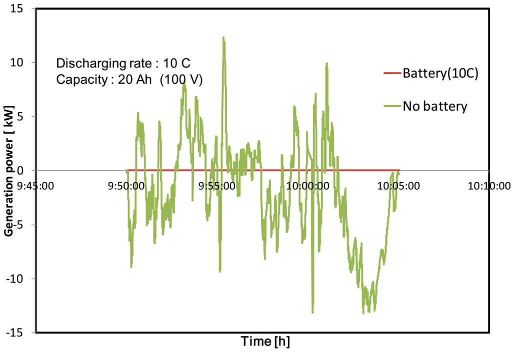

Figure 8. Excess amount of electricity with time (added battery).

which is show in Figure 7. The positive value means the lacked amount of electricity between the demanded electricity and supplied electricity. The negative value means the excess amount of electricity between the supplied electricity and demanded electricity. In case of sunny day, the electricity balance between supplies and demand can be kept, whereas, the lack between supplies and demand at cloudy increases. Figure 8 is the result for added battery. It was possible to supply stability with the electric power by using this battery (discharging rate 10 C, capacity 20 Ah).

3 CONCLUSIONS

In this study, in order to contribute to a green innovation and optimize the heat and electricity in the smart grid network, we tried to develop a simulation model of a micro smart grid system that can predict the needed function of respective element technology according to demand of end user at different weather conditions. A combined complex smart grid was proposed, at the first stage, model of a micro smart grid system with real time change was carried out to establish the evaluation and calculation method of complex smart grid and estimate the benefits effect.

It was able to model the case of a micro smart grid system introducing the equipments of solar power generation and gas engine power generation with thermal storage and secondary battery for electricity storage. The simulation was carried out to estimate the energy consumption and recycled thermal energy by the balance calculation. The benefit effects of sunny day, cloudy day are 1.36 GJ and 1.56 GJ, equal as 28 kW and 32 kW respectively.

In case of sunny day, the electricity balance between supplies and demand can be kept. Whereas, the lack between supplies and demand at cloudy increases. The lacked amount of electricity between supplies and demand is maximum at 12 kW at cloudy, in order to solve this shortfall, a maximum battery at 20 Ah is needed.

REFERENCES

Colson C.M., Nehrir M.H. Comprehensive real-time microgrid power management and control with distributed agents. IEEE Transitions on Smart Grid, March, 2013.

Feng G., Luis H., Robert M. Comprehensive real-time simulation of the smart grid. IEEE Transactions on Industry Applications, March/April 2013.

Huang H.Y., Kobayashi N.Y., Yukita K.Z., Cheng Y., Guo F.H., He Z.H., Yuan H.R. Predictive Simulation of Smart Grid Network System. Soft Computing and Intelligent Systems (SCIS) and 13th International Symposium on Advanced Intelligent System (ISIS), 20–24 Nov, 2012.

Kevin M., Juan A.O., Chris D. Combining power communication network simulation for cost-effective smart grid analysis.

Meysam S., Chin K.G., Chee W.T. A review of recent development in smart grid and micro-grid laboratories. IEEE International Power Engineering and Optimization Conference, 6–7 June 2012.

Yun S.Y., Choo C.M., Kwon S.C., Song K. Development of smart distribution management system for predictive operation of power distribution systems. 21st International Conference on Electricity Distribution, 6–9 June 2014.

Advances in Energy, Environment and Materials Science – Wang & Zhao (Eds)

Numerical simulation analysis on the tower foundation deformation of the high voltage transmission line caused by iron ore mining and filling

Bangshu Xu, Cheng Chen & Qin Yan
School of Civil Engineering, Shandong University, Jinan, China

Shan Dong
Limited by Share Ltd., Metallurgical Design Institute of Shandong Province, Jinan, China

Shiwu Liu
Fujian Yongfu Engineering Consultants Ltd., Fujian, China

ABSTRACT: ±800 kv high voltage transmission line project from Shanghai temple to Shandong province needs to cross the Shenghong iron ore mining area. Shenghong iron mine has not yet been constructed. It has yet to determine the distribution of underground iron roughly depending on the survey report. In order to analyze the tower foundation deformation of the high voltage transmission line caused by iron goaf, the paper adopts Flac3D software to simulate the process of iron ore mining and filling. The main conclusions are: (1) Excavation of the sloping iron mine causes the surface final vertical displacement a "parabolic" distribution and the horizontal displacement curve a "horizontal s" distribution. (2) During the excavation, the maximum subsidence offsets to the goaf slowly. In the influence range of the excavation, the trend of the parabolic in the incremental interval is almost consistent with the trend of the iron. The shallower depth of the iron, the smaller depth of the surface it could cause. The horizontal displacement shows symmetrical distribution on both sides of the iron. The horizontal displacement curve changes from "straight line" distribution to "parabolic" distribution slowly, and finally shows in "horizontal s" distribution. (3) The surface vertical displacement and the horizontal displacement at the location of the tower foundation are very small, the maximum different vertical displacement and different horizontal displacement satisfy the requirement of the standard.

1 INTRODUCTION

So far, study on the surface buildings caused by iron ore mining and filling was quite mature. Zhang et al. studied the home buildings caused by mining and filling by utilizing numerical simulation method (Zhang et al. 2005). Wang et al. analyzed surface subsidence caused by ore mining through three-dimensional finite element method of porous media solid-liquid coupling (Wang et al. 2010). Wang et al. had a research on the impact of the key isolation layer under the filling shaft to the surface subsidence by using numerical simulation method (Wang et al. 2010). But there was little research on the surface subsidence caused by sloping ore. It is hard to express clearly about the surface deformation rule through the mechanics-physics model as the complexity of the ore geological conditions. However, the simulation method can make the flaw up. On the basis of the seniors' research, the surface and surface buildings deformation rule during the sloping ore mining and filling are studied with Flac3D, with the Shenghong iron ore as the background.

2 ENGINEERING BACKGROUND

The project of ±800 kv high voltage transmission line is between the Shanghai temple and the Shandong province. The line begins at the junction of the Liangshan and Dongping, and the terminal is located at the south of the Yuning, by way of Dongping, Wenshang, Ningyang. The line has to cross the Yangdian iron and Shenghong iron goaf as the path corridor restriction in the churchyard of Weishang. The mining area is alluvial plain geomorphology; ground elevation is about 50 m; the ore shows in monocline or stratiform distribution. The trend of the ore is nearly perpendicular to the line path. The overall occurrence is 256° ∠45~55°. The occurrence is relatively stable and buried under 44.3 m. Ore output level is 4.30 ~ –610.70 m and the design mining elevation is –40 m ~ –400 m.

The ore above –40 m is reserved as protecting pillar. The design of the underground ore adopts the shaft development scheme and shallow-hole shrinkage stoping method. The middle design height is 60 m and the iron ore is divided into 7 middle levels includes –40 m, –100 m, –160 m, –220 m, –280 m, –340 m, and –400 m. On the basis of characteristics of mineral geology, mining method, mining scheme and so on, adopting the method of numerical simulation, analyzing the deformation and movement rules of the surface, solving the deformation characteristic value, making a judge whether the ore area could be used as the architectural place and the degree of harm to the tower foundation.

3 NUMERICAL SIMULATION

3.1 *Modeling*

The quasi-three dimensional geologic model is established according to geological section map of the geological prospecting line in the geologic report. When establishing the model, the iron mine is simplified that nonuniform thickness ore is equivalent to equal thick iron ore, so equivalent thickness of iron ore I-3 is 2.5 m; equivalent thickness of iron ore I-5 is 4.0 m; equivalent thickness of iron ore I-6 is 3.5 m. In order to consider the boundary effect of the model, left and right boundary of the model are taken 200 m that the influence range of ore, and the surface is taken as upper boundary, lower boundary is 597 m, and width is 826 m. The mesh model is established through Abaqus software, and then imported to the Flac3D software. The model is shown in Figure 1.

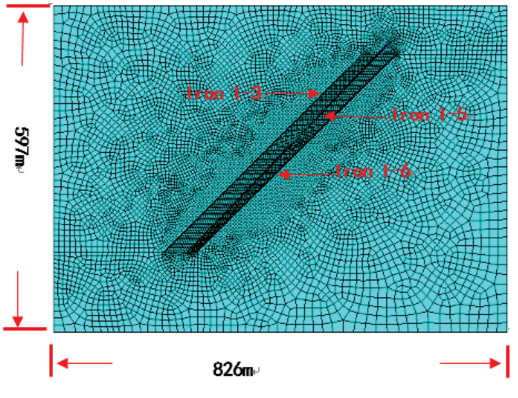

Figure 1. Numerical mesh model.

3.2 *Physical and mechanical parameters*

According to the geological prospecting report, 70 m under the surface is quaternary loose rock, and the other is basement. Backfill parameters refer to Zhang et al., and iron mine parameters refer to the geological prospecting report (Zhang et al. 2009). The physical and mechanical parameters are shown in Table 1.

3.3 *Process of mining and filling*

The first phase section height of the ore is 60 m and is divided into seven middles that include –40 m, –100 m, –160 m, –220 m, –280 m, –340 m, and –400 m. Among them, –100 m middle is the level of return air and the other is the mining level. Generally, iron ore is mined from –400 m level to –340 m, –280 m, –220 m, –160 m, –100 m level upwardly. Accordingly, the ore is divided into six mining levels including diagram 1, diagram 2, diagram 3, diagram 4, diagram 5, diagram 6 and are shown in Figure 2.

3.4 *Result and analysis*

3.4.1 *Analysis of surface displacement*

In the Figure 3, iron mine is mined into six levels, and every level acts as a construction step. Analyzing the result of the six construction steps, it could be seen from the Figure 3 (a) to Figure 3 (b) that the settlement first occurs in roof position as the mining and filling of the ore, then gradually spreads to the surface. Surface vertical displacement increases gradually during the constructions, and maximum surface subsidence offsets to the goaf slowly. After the mining, vertical displacement reaches to the maximum value. Due to the

Table 1. Physical and mechanical parameters.

Stratum	Density (Kg/m^3)	Elastic modulus (GPa)	Poisson ratio	Cohesion (MPa)	Internal friction angle (°)	Strength tension (MPa)
Quaternary	1960	0.05	0.32	0.05	28	0.02
Basement	2650	1.6	0.22	1.25	35	1.28
Ore	3460	12	0.26	14.9	37.9	12.2
Backfill	2000	0.6	0.3	0.75	30	1.20

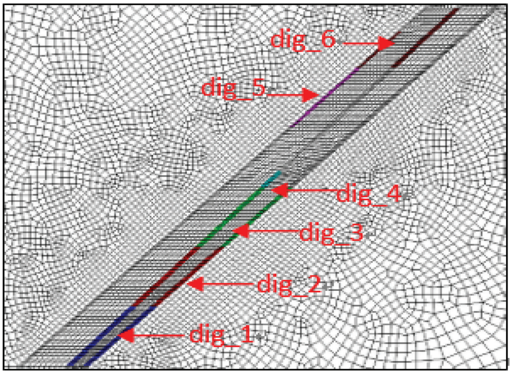

Figure 2. Mining and filling sequences.

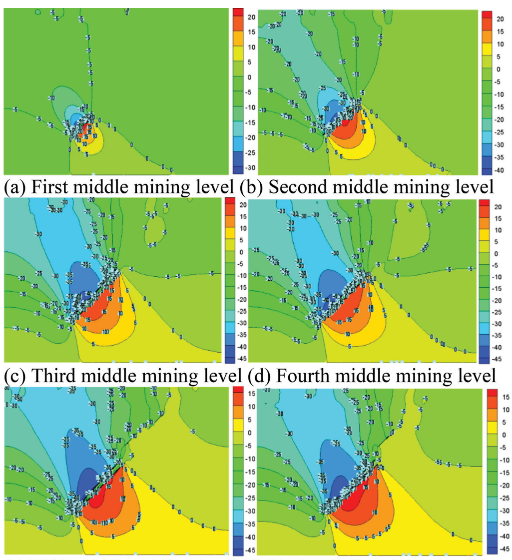

(a) First middle mining level (b) Second middle mining level
(c) Third middle mining level (d) Fourth middle mining level
(e) Fifth middle mining level (f) Sixth middle mining level

Figure 3. Vertical displacement isoline map of different middle mining levels (unit mm).

action of overlying rock gravity, the goaf deforms, moves and breaks gradually during the mining. The goaf area increases, and settlement spreads to the surface. At the same time, a moving belt forms in a certain range of the surface. The buildings in the moving belt may be influenced by the mining.

It could be seen in the Figure 4, the horizontal displacement of soil caused by different mining levels shown in symmetrical distribution. Above the ore, horizontal displacement turns to right. Under the mine, horizontal displacement turns to left, because rock is disturbed and rock stress releases after the mining. However, the strength of the filling cannot reach the rock strength,

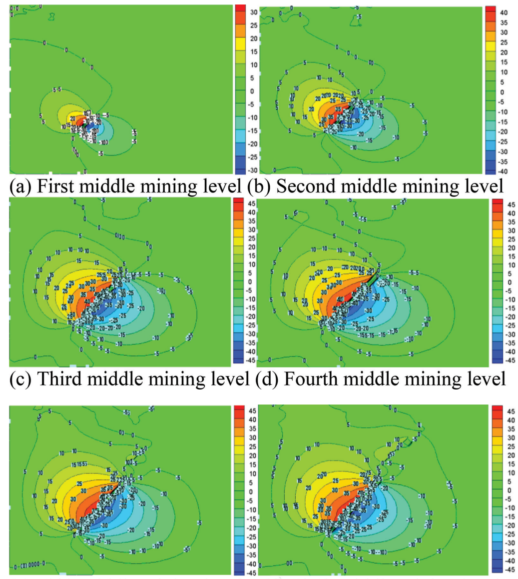

(a) First middle mining level (b) Second middle mining level
(c) Third middle mining level (d) Fourth middle mining level
(e) Fifth middle mining level (f) Sixth middle mining level

Figure 4. Horizontal displacement isoline map of different middle mining levels (unit mm).

under the action of active earth pressure, rock moves to the goaf, causing the rock above the ore moved to the bottom right corner and the mine under the mine moved to the top left corner. The horizontal displacement spreads to the surface with the goaf increasing. As the dip angle of the mine, the horizontal displacement above the ore spreads faster than the horizontal displacement under the ore. So it could be seen in the Figure 4 (f), after the construction, the surface horizontal displacement basically shows the trend that moves to the right.

It could be seen in Figure 5 (a) that the vertical displacement shows in "Parabolic" distribution, parabola apex gradually moves downward and shifts to the goaf with the area of the goaf increasing, and the trend of the settlement curve is almost consistent with the trend of ore in the parabolic incremental interval. The maximum displacement occurs at the surface where X equals to 250 m, while the surface projection interval corresponds to the range of the mine distributed between X equals to 240 m to X equals to 320 m. So, in the process of the sloping ore mining and filling, the deepest depth of the ore corresponds to the range of the surface that has the largest settlement. It could be seen in the Figure 5 (b), the surface horizontal displacement changes from the "Straight line" distribution to "Parabolic" distribution. After analysis, in the beginning of the mining, ore hanging wall declines, footwall raises, making footwall soil moves negatively, and horizontal displacement

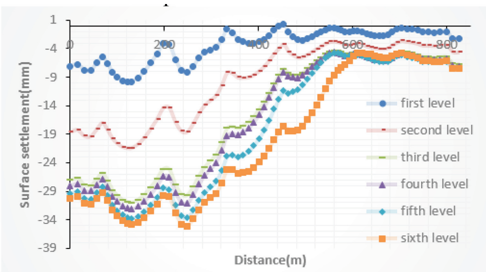

(a) Surface vertical displacement curve

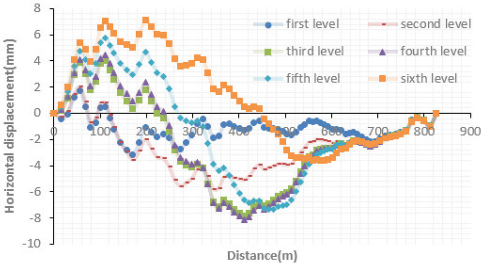

(b) Surface horizontal displacement curve

Figure 5. Surface displacement curve changes during the construction steps.

is both negative. It could be seen in the Figure 4, positive horizontal displacement caused by the hanging wall spreads to surface faster than foot-wall, making the surface of the projection interval corresponding to the hanging wall moving positively and "Parabolic" distribution converts to "Horizontal S" distribution. So, the trend and angle of the sloping mine have a great impact on the surface displacement.

3.4.2 *Tower foundation displacement analysis*

The tower foundation is located at the surface where X equals to 370 m. It could be figured out in the Figure 6 that (a) the vertical displacement increases with the area of the goaf increasing. Diagram 1 and diagram 2 construction steps have great impact on the displacement of tower foundation. The slope of the curve changes fastest, because the quantities of the ore in the diagram 1 and diagram 2 are the most, and the other four construction steps are less than them. Accordingly, it has little disturbance to the surrounding rock, and surface settlement correspondingly reduces. The final settlement reaches 25.8 mm. The trend of horizontal displacement at the location of the tower foundation is equal to the surface. In the previous five constructions steps, the location of the tower foundation moves negatively of x-axis and the displacement increases firstly and then decreases. In the construction of step 6, the horizontal displacement at the location of the tower foundation moves to the positive direction

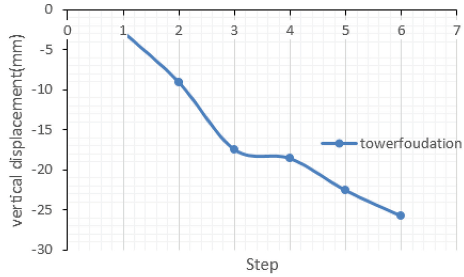

(a) Vertical displacement curve of tower foundation changes during the construction steps

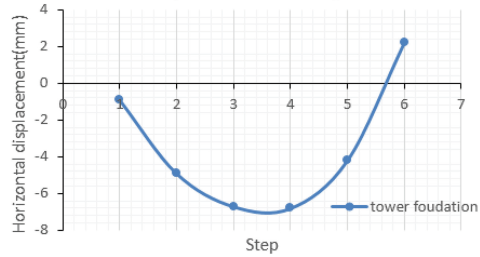

(b) Horizontal displacement curve of tower foundation changes during the construction steps

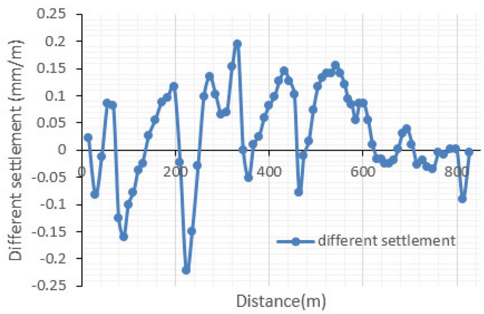

(c) Different value of vertical displacement curve

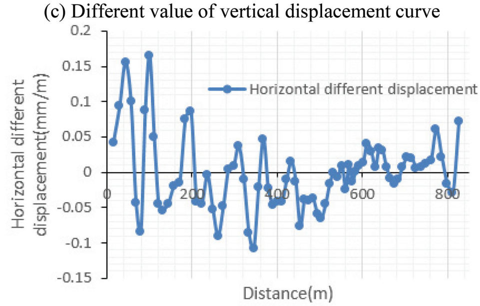

(d) Different value of horizontal displacement curve

Figure 6. Displacement curve of tower foundation.

of x-axis. The final horizontal displacement value reaches 25.8 mm positively of x-axis. According to the provision of "coal mining regulation under buildings, railways and water-bodies" published by Coal Industry Press, the allowed deformation values of building are got (Coal Industry Press, 2000):

Slope: $i = \pm 3$ mm/m
Curvature: $k = \pm 0.2 \times 10^{-3}$
Horizontal displacement: $\varepsilon = \pm 2$ mm/m

It could be seen in the Figure 6 (c) and Figure 6 (d) the maximum different value of vertical displacement reaches 0.25 mm/m, which is less than the specified value 3 mm/m. The maximum different value of horizontal displacement reaches 0.15 mm/m, which is less than the code value 2 mm/m. In conclusion, iron ore mining has little impact on the tower foundation deformation of the high voltage transmission line.

4 CONCLUSION

The paper describes the studies of the surface deformation rules caused by iron ore mining and filling. The main conclusions are:

1. The surface vertical displacement caused by sloping ore mining and filling shows in “Parabolic” distribution. During the mining, parabola vertex displacement increases gradually and offsets to the goaf with the goaf area increasing. The trend of the parabola is almost the same with the trend of the ore.
2. The surface horizontal displacement increases firstly and then decreases with the goaf area increasing, which shows in “Straight line” distribution and then to “Parabolic” distribution, finally changing into a “Horizontal S” distribution. Different angles and angle of the ore lead to different horizontal displacement of the ore.
3. The maximum vertical displacement of the tower foundation reaches 25.8 mm, and the final horizontal displacement reaches 2.2 mm. The maximum different horizontal displacement reaches 0.15 mm/m, and the maximum different vertical displacement reaches 0.25 mm/m. According to coal mining regulation under buildings, railways, and water-bodies, tower foundation deformation is in the range of specified requirement. In conclusion, ore mining and filling has little impact on the deformation of tower foundation of the high voltage transmission line.

ACKNOWLEDGMENTS

Financial supports for this paper provided by National Science Foundation of China (No. 50909056) and Provincial Science Foundation of Shandong Province (No. ZR2014EEM014, ZR2014EEM029), and Science and Technology Project Plan in 2015, Ministry of Housing and Urban-Rural Development of China (No. 2015-K5-004) are gratefully acknowledged.

REFERENCES

Coal Mining Regulation under Buildings, Railways and Water-bodies, Coal Industry Press, 2000.06.

Wang P., Xu M.G., Li H.Q. Numerical simulation analysis on surface caused by mining in filling mining method and caving method [J]. Industrial Safety and Environmental Protection. 2010(10):50–52.

Wang X.J., Fang S.Y., Liu J.X. Numerical simulation analysis on surface subsidence controlled by key isolation layer in filling shift [J]. Metal Mine. 2010(10):13–16.

Zhang M.H., Gao Q., Zhai S.X. Design optimization and numerical simulation analysis on mining and filling of Jinchuan second ore [J]. Metal Mine. 2009(11):28–31.

Zhang T., Xu M.G., Ouyang Z.H. Numerical simulation analysis on a black iron ore mining and filling [J]. Gold. 2005(11):24–27.

This page intentionally left blank

Advances in Energy, Environment and Materials Science – Wang & Zhao (Eds)
© 2016 Taylor & Francis Group, London, ISBN 978-1-138-02931-6

Application on the some nuclear power engineering of the hydro-fracturing technique

Xianbin Wang & Ming Zhang
National Nuclear Power Planning Design and Research Institute, Beijing, China

ABSTRACT: Initial earth stress condition is the important parameter used in the nuclear engineering design of the outlet tunnel, and the hydro-fracturing technical is the ideal method on measuring the earth stress. Based on the practical engineering, this paper introduces the principles and methods of the hydro-fracturing method, the results show that: the maximum horizontal principle stress is 3.92–6.07 MPa, and the lateral principle stress is 2.75–4.92 MPa. The direction of maximum horizontal principle stress is NE33°, and the structural stress is main. Earth stress has some benefits on the stability of the tunnel, which cannot produce the rock burst phenomenon, and it can propose the important information for the design of tunnel.

1 INTRODUCTION

Now in China, water supply and drainage tunnel is the most applied scheme in the nuclear power plants. The arrangement of the grotto principal axis is influenced by the condition of original crustal stress. And for the spatial arrangement of tunnel, the forecast of adjoining rock stability, and design of lining, the results of crustal stress test is very significant. According to the in-situ stress test method issued by International Society for Rock Mechanics, there are many in-situ stress test methods, including the drill hole diameter changing measurement, strain measurement, stress recover measurement, and hydro-fracturing technique. Comparing with the other three measuring methods, hydro-fracturing technique has many advantages, like simplicity of operator, short test period, and so on. So the limitation of the point stress state and the nonuniformity of the geological conditions could be avoided. And the error caused by the choice of rock elastic parameter can be also avoided (Li, 2006). So in the rock mass stress measurement, hydro-fracturing technique cannot be matched by other kinds of the measurements.

2 THE FUNDAMENTAL PRINCIPLE HYDRAULIC FRACTURING TECHNIQUE

Hydraulic fracturing technique is a kind of in-situ stress test methods, which the crustal stress is calculated according to the pressure of the fracture conditional curve. And the fundamental principle is based on these three hypotheses as follows: (1) the surrounding rock is isotropous and elastic; (2) the fluid in the rock is under the Darcy law; (3) one of the principal divection is the vertical direction which is according to the gaging hole in the vertical direction (Peng, 2006 & Liu, 1999).

3 PROJECT EXAMPLE

3.1 *Project profile*

There is one nuclear power plant planning and constructing two 1000 MW pressurized water reactor nuclear power unit. The water intake system is gravity type water supply tunnel. Each unit has one water supply tunnel, which the diameter and length of the tunnel is 4.8 m and 1200 m, the space between the two tunnels is 36 m, and the elevation of the tunnel bottom is −15 m. The rock which the tunnels went across is ignimbrite, and hydraulicfracturing technique is applied to measure the crustal stress parameter.

3.2 *Measuring method of the hydraulic fracturing technique*

3.2.1 *Measuring equipment*

There are three parts for the measuring equipment: (1) Packer system of the drilling and pressure-bearing section, which is constituted by two parkers. And between these two parkers, there is a space for pressure-bearing section; (2) compression system which is included in heavy pressure fluid pump with mass flow and push-pull valve; (3) record system which is included in functions recorder, pressure transducer, pressure gage, and so on.

In the Figure 1, the length of the low-duty packer is 3.4 m with 1.2 m rubber sleeve. And the length of the hydraumatic section is 1.0 m.

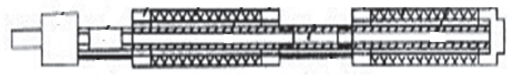

Figure 1. The low-duty packer.

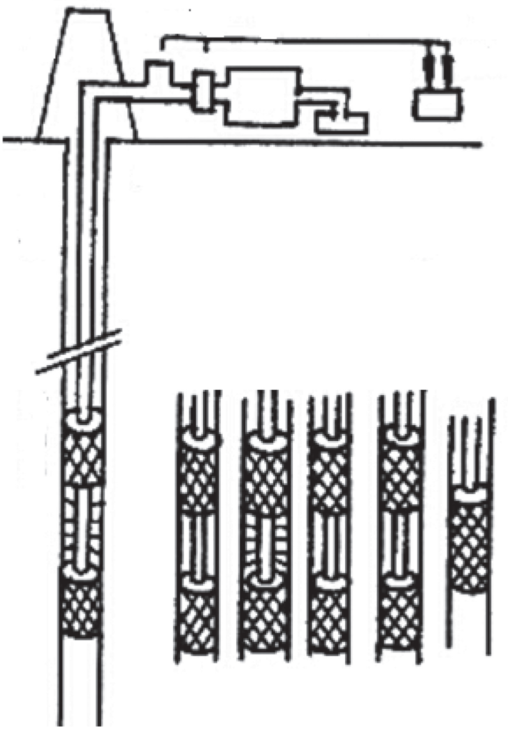

Figure 2. The geo-stress measurement routine of hydraulic fracturing.

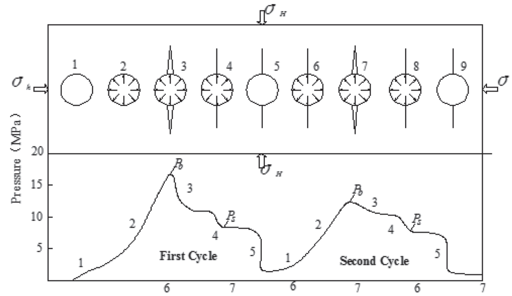

Figure 3. The conditional curve of hydraulic fracturing.

3.2.2 *Measurement procedure*

The single tube compression system is applied in this test. The push-pull value on the orifices is applied to control the flow direction of the liquid, and load to the packer. The measurement procedure is showed in the Figure 2, and the fracturing conditional curve is depicted in Figure 3.

Before the hydraulic fracturing test, the permeable rate and the gradient of the drill hole must be checked. The leakproofness of the drill pipe is also checked and the measurement procedure is as follows:

1. Down and seal the packer: Two packers are arranged in the selected section, and let the packers expand for the space of the compression (the pressure of the down and seal the packer in this test is 4 MPa);
2. Water injection and inflating: After driving the change-over valve by drill pipe, inflating to the fracturing section by water injection, so the pressure on the wall of hole increases gradually.
3. Fracturing palisades: Under enough pressure, the cracks occur in the direction of the least resistance on the wall of hole and expand in the direction which is perpendicular to minimum principal stress direction. Accordingly, the pressure decreases fast due to the fracture of the rock, when the pumping pressure gets the critical bursting pressure.
4. Turn off the pump: after the pressure pump is turned off, the pumping pressure decreases fast. When the pressure decreases to the pressure of critical closure state, it is called closing pressure P_s;
5. Pressure relief: open the pressure value and release the pressure for letting the cracks closed.
6. Re-open: repeat the steps from 2) to 5) until getting the reasonable parameters.
7. Blocking: after the test, the liquid in the packer is expelled and the packer is shrunk to the original state.
8. Recording the direction of cracks: Applying the directional impression device, the length and the direction are recorded.

3.2.3 *Parameters of the pressure*

Pressure parameters P_b, P_s, P_r, and P_0 are the basis for calculating the crustal stress of the hydraulic fracturing, which is confirmed by the fracturing conditional. Averagely, the peak value of the first circulation pressurization curve is selected as the bursting pressure P_b. And the inflection point of the rising section of circulation pressurization curve is selected as reopening pressure P_r. Due to the rising section of circulation pressurization curve is steep. So the point where is the departure from the straight as the reopening pressure, which is depicted in the Figure 4. For the instantaneous shutoff pressure, it is selected from the inflection point of the declining part of fracturing cyclic curve. To the cases whose inflection point is not clear, the tangent method and double tangent method could be applied, which is depicted in the Figure 5. The pore water pressure P_0 of the rock mass could be got from the pore water pressure gauge. When the testing depth is very little, the hydrostatic pressure could be regarded as pore water pressure. And in this test, the hydrostatic pressures of different sections are regarded as the pore water pressure, which the formula is $P_0 = \gamma_{water} H$: where the γ_{water} is the volume-weight of water, and the H is the depth of the rock (Chen. 2004; An, 2004).

The formula for calculating the principal stress of the vertical direction is $\sigma_v = \gamma H$, where the γ is the unit weight which is 27, and H is the height.

3.2.4 *Analysis of the test results*

The depth of the testing drill hole is 84 m, and the diameter is 75 mm. In the range from 29.7 m to 79.3 m, 7 crustal stress trial curves were got, which the testing results are showed in the Table 1. And the representative records of the geostress survey are depicted in the Figure 6.

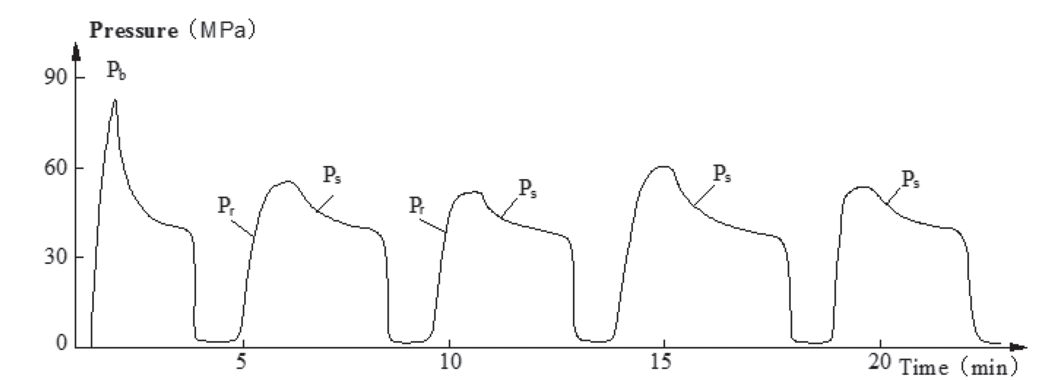

Figure 4. Confirm P_s and P_r according to cyclic curve of pressure.

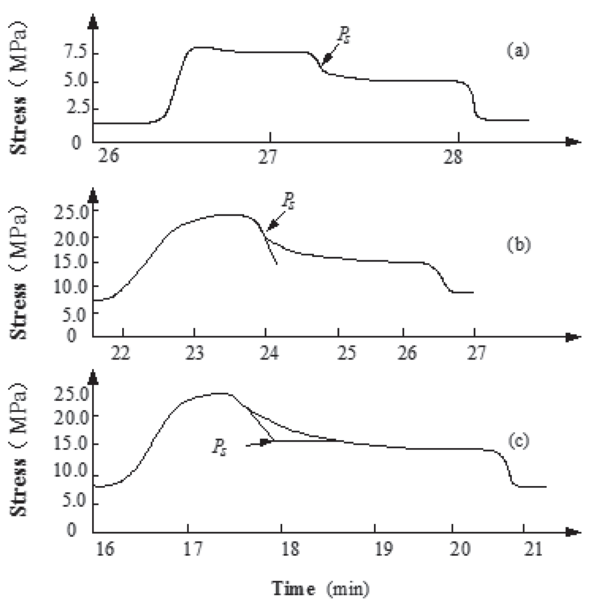

Figure 5. Confirm P_s according to bathmometry, tangent method and bitangent method.